A Numerical Analysis of Groundwater Abstraction on Aquifer-River Interactions

by

Garth Cooper

Submitted in fulfilment of the thesis requirement for the Degree of

Bachelor of Engineering (Civil) Honours

School of Civil Engineering

University of New South Wales

3rd of June, 2011

Thesis Supervisor: Dr Martin Søgaard Andersen

Co-supervisor: Andrew McCallum

Originality Statement

'I hereby declare that this submission is my own work and to the best of my knowledge it contains no materials previously published or written by another person, or substantial proportions of material which have been accepted for the award of any other degree or diploma at UNSW or any other educational institution, except where due acknowledgement is made in the thesis. Any contribution made to the research by others, with whom I have worked at UNSW or elsewhere, is explicitly acknowledged in the thesis. I also declare that the intellectual content of this thesis is the product of my own work, except to the extent that assistance from others in the project's design and conception or in style, presentation and linguistic expression is acknowledged.'

Signed .....

Date .....

Acknowledgements

Much thanks goes to my thesis supervisor Martin Andersen who through his patience, expertise and kindness has found the time in his busy schedule to assisted me greatly in not only producing a thesis but teaching me the concepts of hydrogeology. A special mention goes to Andrew McCallum who has been patient with my numerous trivial modeling questions as well as providing me extensive literature. One more mention goes to Gabriel Rau who allowed me to go on one of his many field trips to the Maules Creek.

I would like to acknowledge the Cotton Catchment Communities CRC that has provided me a scholarship to provide financial assistance to conduct this experiment. Without these funds travel between home and WRL would have become difficult. Another acknowledgement is the staff at the Water Research Laboratory in Manly Vale who provided me with a computer and desk space that allowed a place of study for the summer period.

My colleges who have taken time to read and edit my thesis also deserve special thanks; specifically Irene Chong, Ishan Shrestha, Gitendra Pradhanaga and Yasadi Peiris who have taken time from their busy work schedules. Lastly, my father Brian who has provided me constant support and my mother Sui-Pat, who has let me off housework in the assumption that I was working on my thesis. Oh and I suppose my girlfriend Julie.

Abstract

With an increase in world population and recent global climate changes causing increasingly unpredictable and extreme weather patterns, the reliance on groundwater is and will continue to be increasing. As a result, there has been an increase in research efforts to better understand groundwater processes, in particular how these interact with surface water systems and how groundwater abstraction affects this interaction. The aim of this thesis is to create an understanding of these processes through the use of a generic numerical model of river, aquifer and abstraction bore.

A numerical model domain was defined for an aquifer-river system based on the general aquifer geometry and aquifer parameters at Elfin Crossing in Maules Creek. Model parameters such as hydraulic conductivity and gradient, distance of pumping bore from the river, pumping rate and a streambed clogging layer were varied within reasonable bounds for the field site. The aim was to quantify the influence each parameter has in terms of stream depletion and the time for the river water to reach the pumping bore. From these parameters values were selected to create a base case model. In addition realistic upper and lower values of each parameter were combined to make worst and best case scenarios. Then through a sensitivity analysis these scenarios were compared to observe the combined effects of these parameters on the system response and the stream flow depletion.

Results of the sensitivity analysis found that the greatest effect was the distance that the abstraction bore was placed from the river followed by the pumping rate, then the hydraulic conductivity and the streambed clogging layer. It was also found that pumping induced by parameters when applied to historical flow data from Maules Creek caused extremely low flow values which could decrease water quality and deny downstream users of valuable irrigation water.

Table of Contents

List of figures

List of Tables

1 Introduction

The sustainable management and use of groundwater resources as a source of drinking water, irrigation and for other consumptive uses as well as a supplementary source for surface river flows and of wetlands and wildlife habitats calls for increasing attention to two major and interdependent sources of concern, namely, stream depletion and pollution (Burchi 1999).

An assessment on the current global groundwater situation by the United Nations Environmental Program (Morris et al. 2003) states that fresh water use continues to rise at the expense of environmental requirements of minimal water levels for the maintenance of ecological diversity. In particular, page 6 of this report states that there was a six-fold rise in the total global groundwater use between 1900 and 2000, which was not only related to the increase in global population per capita but also to the amount of groundwater withdrawals.

There is a global dependence on groundwater resources. Cities in many arid and semi-arid regions worldwide are dependent on a constant groundwater supply for drinking water and irrigation needs, causing a decline in baseflow over time. One of many examples is highlighted in Kim 2010 where a numerical study of 20 years worth of data of Gapcheon watershed in South Korea showed a decline of 53% decrease in groundwater levels. As demands on groundwater resources increase, so must our understanding and adaptation to develop and to deliver necessary groundwater management (Sinclair et al. 2005).

This thesis focuses on river-aquifer interactions through a numerical investigation and the effect of groundwater abstraction on stream depletion, a topic which has many environmental implications in the management of groundwater resources.

A product of this thesis is a generic numerical model that examines and quantifies the effects of groundwater abstraction near a river.

1.1 Background

As part of a larger research project in the Maules Creek catchment area (Rau et al. 2010), a pumping bore will be installed in Elfin Crossing to investigate surface-groundwater interactions in the aquifer in the area.

To justify the placement of the pumping bore, a modeling study must be undertaken to aid in deciding the position that will optimise the effects observed in the river and hence the research of the project. In particular, a focus of this study is to investigate the impacts that nearby groundwater has on the stream flow and hyporheic zone flow process using numerical modelling.

The main purpose of this thesis is creating a generic numerical model that can be applied to other areas in need of investigation and carrying out a sensitivity analysis to determine numerically the effects certain parameters have on this generic model.

1.2 Thesis Structure Overview

Chapter 1 contains Introduction and motivation to for the thesis and Chapter 2 contains the ultimate Objectives of this thesis

Chapter 3 contains a broad Literature Review of relevant past works, background reading and techniques to quantifying the effects of groundwater abstraction on river-aquifer interactions.

Chapter 4 contains the Methodology of the thesis which describes the model configuration and forms of comparison of parameters to quantify the effects of groundwater abstraction on river-aquifer interactions

Chapter 5 contains the Results. Observations and brief explanations of the results were given. Detailed explanations were reserved for the discussion

Chapter 6 contains the Discussion. Explanations and implications of the results in Chapter 5 are given in detail.

Chapter 7 contains the Conclusion. Evaluates the key findings of thesis.

2 Objective of this study

This thesis aims to provide an understanding of how groundwater abstraction affects an aquifer- river system. As such, the main objective is:

- To create a generic numerical model to analyse the properties and physics of river-aquifer interactions influenced by groundwater pumping.

In more detail, the objectives of this study are:

- To investigate the effect that parameters such as hydraulic conductivity, position of pumping bore, rate of pumping and clogging layer have on water being abstracted from a near-by stream by conducting a sensitivity analysis
- To be able to quantify the physical effects that abstraction near a river will have on the aquifer-river system

3 Literature Review

Stream depletion is a major hydrological concept developed to quantify the effects of groundwater abstraction for water resources management. Recent droughts, and the over provision of large yield wells for irrigation, has led to focused research and increased interest in developing the concept of stream depletion (Zlotnik 2004).

The basic of mechanics of stream-aquifer interactions have existed in the literature for an established amount of time with Theis 1941 proposing the first model analytical model of stream-aquifer interactions and the effects that a pumping bore placed near a river has on stream depletion. Independent of Theis's work, Walton 1970 proposed a simple linear relationship based on Darcy's law which assumes leakage as the controlling mechanism through semi-pervious stratum. Eight years later, Rushton et al. 1979 expanded on Walton 1970 to expand this theory to provide a more description model of aquifer leakage. These two concepts were important for the development of the concept of stream depletion as they explained the connectivity of groundwater and surface water.

More recently, with an increase in computational power and more robust analytical techniques, there has been an explosion in the literature on specific analytical and numerical methods relating to the quantification of the effects of well pumping near a river. Hunt 1999 suggests that analytical solutions exist only for specific scenarios, based on certain assumptions, such as the aquifer being of infinite length as well as being homogenous and isotropic.

Often these unrealistic assumptions can undermine the accuracy of analytical methods but the use of numerical modeling can overcome these limitations (Parkin et al. 2007). Numerical modeling is advantageous as it is a more general approach for modeling the aquifer. Rigid assumptions that analytical solutions require can be relaxed in numerical models such that the parameters which take into account the vertical component of flow near the streambed as stated in Chen et al. 2001 can be employed. However Hunt 1999 cautiously points out there are still issues with numerical models.

The assumptions of isotropy and anisotropy effect modeling of stream-aquifer interactions. These effects are investigated through a study on the effects of anisotropy and heterogeneity on groundwater flow and the effects of these parameters on current analytical and numerical methods for modelling groundwater flow are compared.

Another topic central to surface-groundwater interactions specific to pumping is the effect of clogging layers on the river infiltration. Bouwer 2002 is a key paper in the science of clogging layers and a brief summary is given on the effects of clogging layers in modeling stream depletion.

Finally, case studies conducted on stream depletion are included to review the current literature on modeling the interactions between groundwater and surface water and their effects on stream depletion. A few key papers such as Chen et al. 2001 and Sophocleous et al. 1995 have compared numerical and analytical solutions have drawn conclusions to their effectiveness in quantifying stream depletion. Comparison of results of these case studies has been placed in Figure 12.

3.1 Basic mechanics of stream-aquifer interactions

Groundwater and surface water resources shouldn't be studied as separate parts of the hydrological system, but rather as a single entity that interact within the environment that they are both exist in. This concept implies that the development or depletion of either resource has an effect on the other. Thus, in order to manage each resource effectively, an understanding of the basic science of interactions between groundwater and surface water is required (Sophocleous 2002).

The interaction with how the surface water body is connected to the groundwater component is called the stream-aquifer system. A system that contains a connection between the surface water and groundwater is called a hydraulically connected system. In this system, the flow is determined as a function of the difference in head of the river and aquifer. This flow can be determined by a simplistic model which considers the flow between the aquifer and the river to

be governed by the same controlling mechanism as leakage through a semi-impervious rock layer in one dimension. This mechanism is based on Darcy's law:

$$q = k\Delta h \tag{3.1}$$

Where:

$$\Delta h = h_a - h_r \tag{3.2}$$

h_a Aquifer head in meters;

h_r River head in meters;

q Flow (leakage) between the river and aquifer in m^3/day;

k Constant representing streambed leakage coefficient in m/day.

Equation 3.1 is based on Darcy's law, where the flow is a direct function of hydraulic conductivity and head difference. This equation can be used to represent both base flow and river recharge, depending on the sign of Δh (Sophocleous 2002).

This linear assumption describing the relationship between q and Δh is too simplistic for predicting field values. Rushton et al. 1979 conducted a numerical study on the linear nature of this mechanism and found that a weakness of the linear assumption is that at times of high recharge, excess leakage occurs. This excess leakage is much higher than observed in practice and takes no account of the increased resistance to the passage of water as the volume increases. A non-linear relationship was proposed, which gave a better description of the flows:

$$q = k_1[1 - \exp(k_2\Delta h)] \tag{3.3}$$

Where k_1 and k_2 are constants. The equation above allows for a large increase in flow for a small value of change in head, but doesn't allow for large values for change in hydraulic head, thus a combined equation of both linear and non-linear relationships was proposed:

$$q = k_1\Delta h + k_2[1 - \exp(k_3\Delta h)] \tag{3.4}$$

This equation allows for both a change both small and large magnitudes of change in head, as the linear part of equation 3.4 takes into account large changes of head while the non-linear component takes into account small changes in head.

The equations above describe flow as leakage between the river and aquifer in simplistic terms. These equations are fundamental in defining the concept of stream depletion. Under certain circumstances, water abstraction from wells near a stream can reduce the natural flow in the stream called baseflow. For smaller streams, the reduction of baseflow can be significant enough to cause harm to aquatic life in the stream (Hunt 1999).

In most cases a stream is either *gaining* or *loosing*. A stream is considered gaining if there is a constant source of baseflow from an adjacent source of water such as groundwater from an aquifer. This concept is illustrated in Figure 1. On the other hand, Figure 2 illustrates the concept of a losing stream; that is water being drained from the stream to an adjacent source of water. These processes happen naturally over the course of many years, but these processes can be greatly exaggerated by artificial processes involving pumping. When a pumping well is placed in an aquifer that is hydraulically connected to an adjacent stream, the groundwater table will fall and a cone of depression will form between the stream and pumping well. During this time, a reversal of hydraulic gradient occurs and flow from the stream will be diverted into the pumping well (Chen et al. 2001). Figure 3 illustrates this case.

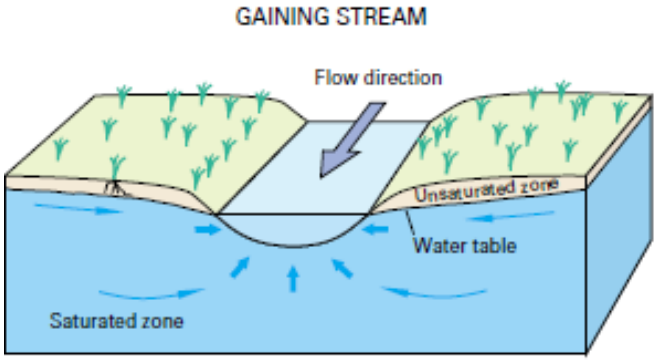

Figure 1: Illustration of a gaining stream (Alley 1999)

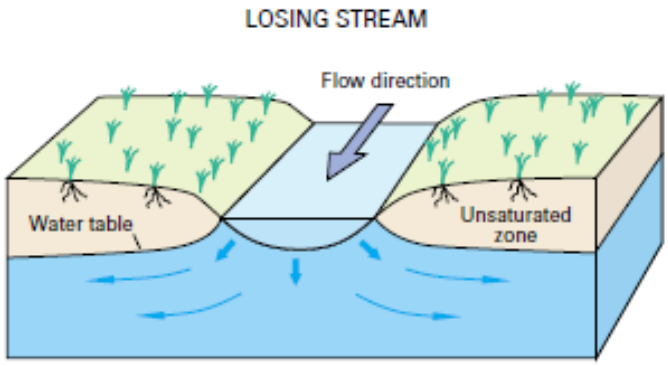

Figure 2: Illustration of a losing stream (Alley 1999)

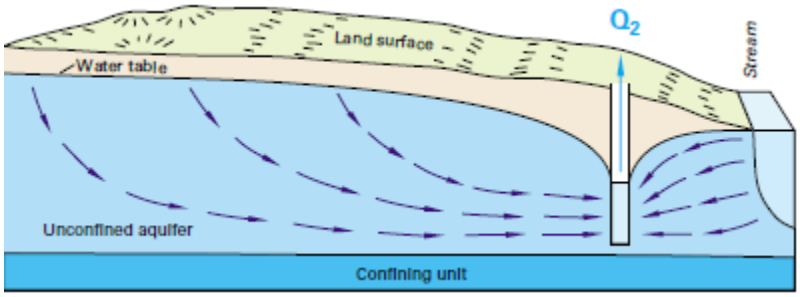

Figure 3: Illustration of the change of baseflow due to pumping (Alley 1999)

3.1.1 Analytical Solutions

Analytical solutions for modeling stream depletion have been in scientific literature for over 70 years. This section of the literature review contains a brief review of the key papers on stream depletion based on the paper published by Bruce Hunt in 1999 entitled "Unsteady Stream Depletion from Ground Water Pumping". These referenced papers include; Theis 1941, the first paper published on stream depletion which describes a solution to modeling the water being abstracted from a river due to pumping; Glover 1954, the paper that builds on Theis 1941 solution by reformulating this solution to include a more elegant mathematical form; Hantush 1965, adding more complexity to Theis solution by considering a less permeable material between the river and the pump.

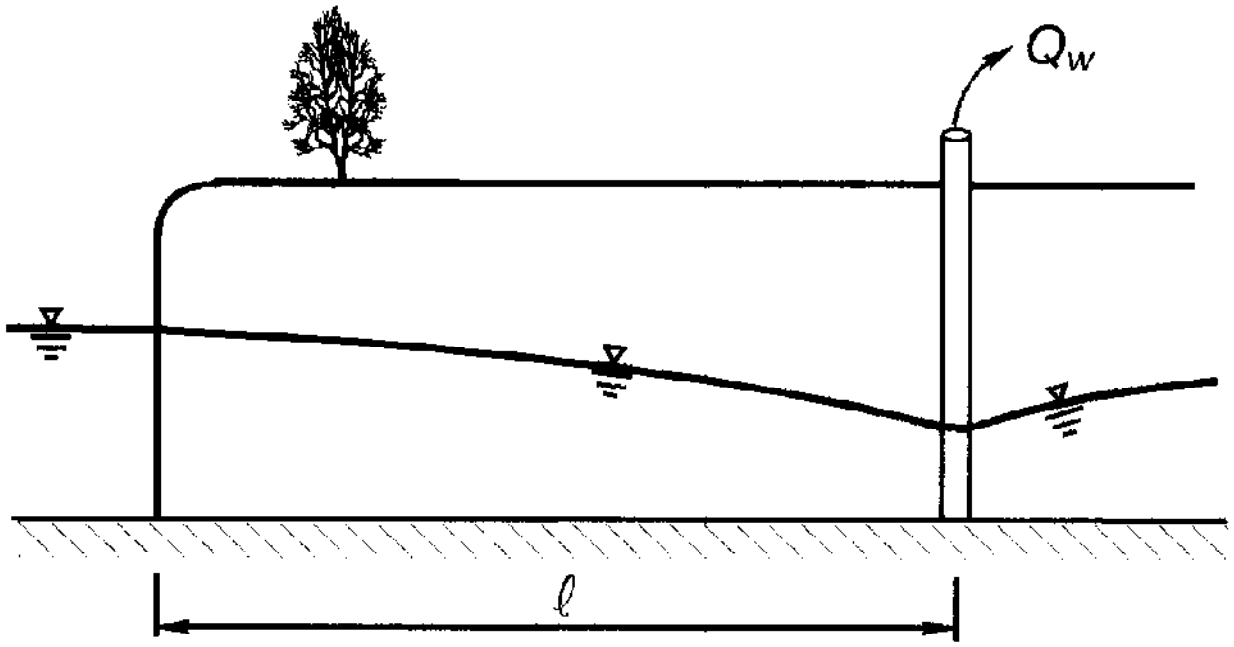

Figure 4: Illustration of the Theis 1941 model domain. (Hunt 1999)

Figure 4 shows the simple case of a river hydraulically connected to an aquifer with a pumping bore positioned *l* meters away. This case is considered simple because there is a fully permeable barrier between the river and aquifer, so there is a direct hydraulic connection between the river and pumping bore. Theis developed a solution to model this solution. Thirteen years later Glover 1954 rewrote the solution in terms of the complimentary error function:

$$\frac{\Delta Q}{Q_w} = \operatorname{erfc}\left(\sqrt{\frac{s\ell^2}{4Tt}}\right) \qquad 3.5$$

Where:

ΔQ Stream depletion flow rate in m^3/day;

Q_w Constant flow rate abstracted at the well from t = 0 to t = ∞ in m^3/day;

S Aquifer storage coefficient (dimensionless), specific yield or effective porosity;

T Aquifer transmissisity in m^2/day;

t Time in days;

ℓ Shortest distance between the well and stream edge in meters.

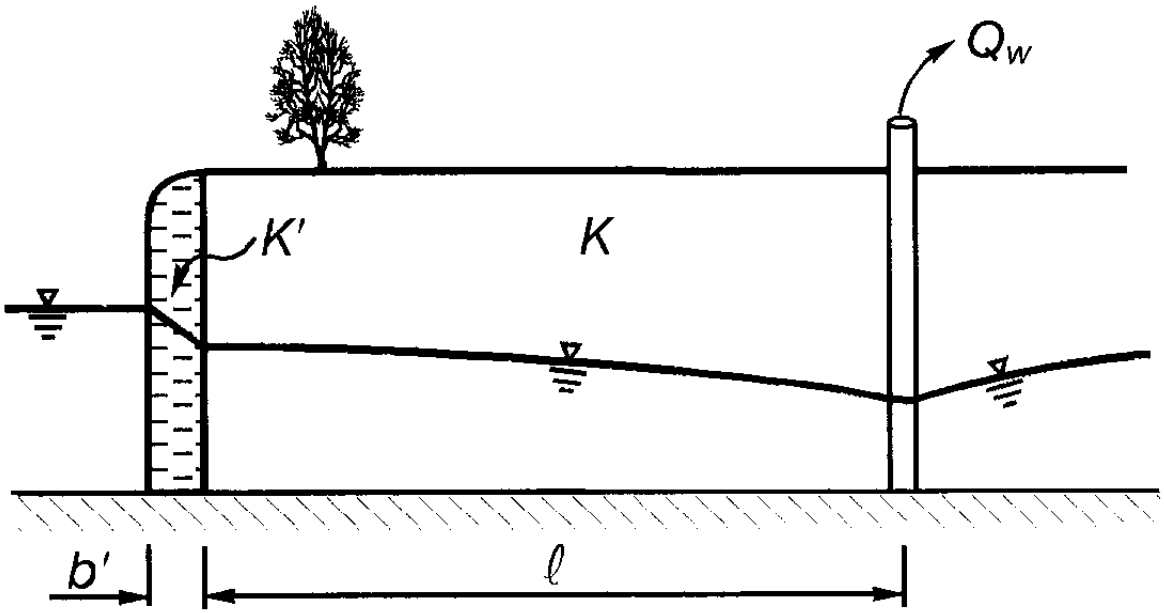

Figure 5: Illustration of the Hantush 1965 model domain. (Hunt 1999)

Hantush 1965 considered the case when there is a semi-permeable barrier between the aquifer and the adjacent river as shown in Figure 5. The expression developed by Hantush 1965:

$$\frac{\Delta Q}{Q_w} = \operatorname{erfc}\left(\sqrt{\frac{s\ell^2}{4Tt}}\right) - \exp\left(\frac{Tt}{SL^2} + \frac{\ell}{L}\right)\operatorname{erfc}\left(\sqrt{\frac{Tt}{SL^2}} + \sqrt{\frac{s\ell^2}{4Tt}}\right) \qquad 3.6$$

Where L is stream leakage that is defined as:

$$L = \frac{K}{K'}b' \qquad 3.7$$

Where:

L Stream leakage that has dimensions of length;

K Aquifer permeability in m/day;

K' Permeability m/day;

b' of the semi pervious layer in m.

Note that this expression reduces to equation 3.5 when L → 0.

Hunt 1999 went on to develop an expression for drawdown based on the expressions developed by Hantush 1965 and Theis 1941. Given the model domain set up in Figure 6, Hunt developed the equation:

$$\Phi(x,y,t) = \frac{Q_w}{4\pi T}\left\{E_1\left[\frac{(\ell - \mathrm{x})^2 + y^2}{4Tt/S}\right] - \int_0^{\infty} e^{-\theta} E_1\left[\frac{(\ell + |\mathrm{x}| + 2\mathrm{T}\theta/\lambda)^2 + y^2}{4Tt/S}\right] d\theta\right\} \qquad 3.8$$

Where:

E_1 The exponential integral that is often called the well function;

x Distance from the stream (positive toward the pumped well) in meters;

y Distance along the stream in meters;

t Time;

θ Dummy integration variable which is used to evaluate the integral in equation 3.7;

λ Streambed leakage parameter which has the same units as velocity (m/s).

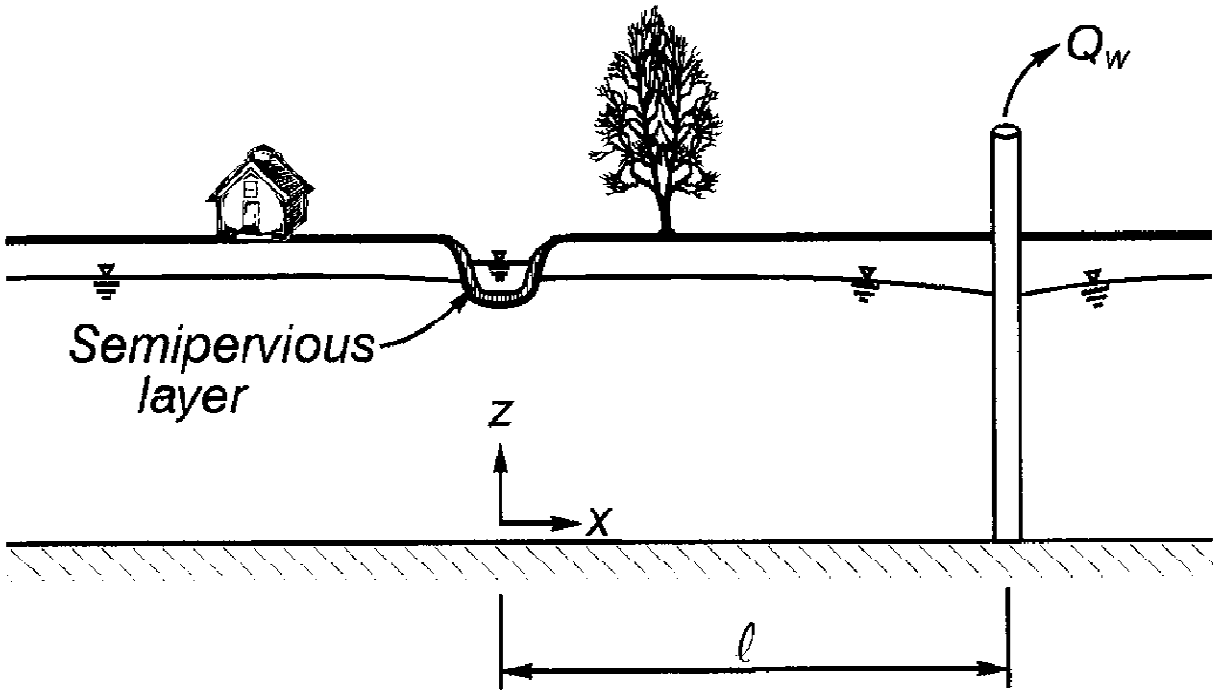

Figure 6: Illustration of the Hunt 1999 model domain. (Hunt 1999)

Hunt 1999 mentions a few assumptions that underpin Equation 3.5, Equation 3.6 and Equation 3.8, these assumptions are:

- The ratio of vertical to horizontal velocity components is small (the Dupuit approximation)
- The aquifer is of infinite extent and is homogenous and isotropic in all horizontal directions
- Drawdowns are small enough compared with saturated aquifer thickness to allow the governing equations to linearized.
- The streambed cross section has horizontal and vertical dimensions that are small compared to the saturated aquifer thickness, and the stream extends from y = -∞ to y = ∞ along x = 0
- The flow rate, Q_W, is constant for 0 < t <∞
- Changes in water surface elevation in the river created by pumping are small compared to the changes crated in the water table elevation on the aquifer side of the semipervious layer
- Seepage flow rates from the river into the aquifer are linearly proportional to the change in piezometric head across the semipervious layer.

3.1.2 Numerical Solutions

In recent years, there has been a shift to the use of numerical models for modeling groundwater with the increase in computing power and the demand for more computational solutions. The advantage that numerical methods have over analytical solutions is the ability to relax the rigid assumptions of analytical solutions. If a numerical model is correctly understood and configured, a reasonably accurate description of the groundwater process can be simulated. Anderson et al. 1992 give a good description of the mathematical set up of numerical modeling software. Mathematically, groundwater flow has the same properties as heat flow and naturally the *diffusion equation* used in heat problems can be applied as a governing equation for groundwater:

$$\frac{d}{dx}\left(T_x\frac{dh}{dx}\right)+\frac{d}{dy}\left(T_x\frac{dh}{dy}\right)=S\frac{dh}{dx}-R+L \qquad 3.9$$

Where:

h Units of head in meters;

T_x,T_y Components of transissivity in m^2/day;

x ,y Coordinate of flow across a unit mesh in meters;

S storage coefficient (dimensionless);

R since source in meters;

L leakage in meters.

It is observed that when using the above equation it is standard practice to assume that $T_x = k_x h$ and $T_y = k_y h$(k being the hydraulic conductivity in m/s in respective directions) and when these parameters are substituted into the Equation 3.9 the non-linear Boussinesq equation is formed:

$$\frac{d}{dx}\left(k_x h \frac{dh}{dx}\right) + \frac{d}{dy}\left(k_y h \frac{dh}{dy}\right) = S_y \frac{dh}{dx} - R \qquad 3.10$$

Where L in the equation above is equal to zero and the storage coefficient (S) is equal to specific yield (S_y). By realising that:

$$\frac{dh^2}{dx} = 2h\frac{dh}{dx} \qquad 3.11$$

$$\frac{dh^2}{dy} = 2h\frac{dh}{dy} \qquad 3.12$$

The equation 3.10 can be re-written:

$$\frac{d}{dx}\left(k_x \frac{dh^2}{dx}\right) + \frac{d}{dy}\left(k_y \frac{dh^2}{dy}\right) = 2S_y \frac{dh}{dx} - R \qquad 3.13$$

By using current values of saturated thickness, the above equation can be effectively linearized in a numerical model using finite element or finite difference techniques.

After this equation is derived, certain conditions must be imposed on the model domain; these conditions are known as *boundary conditions*. In groundwater models there are four types of boundary conditions imposed: Fixed hydraulic head boundary condition, fluid-flux boundary condition, fluid transfer boundary condition and well boundary condition.

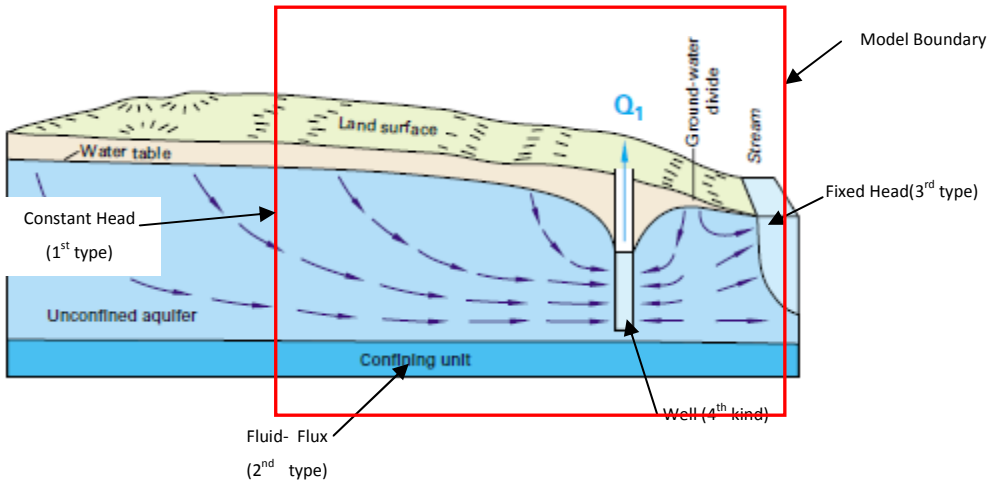

Figure 7: Diagram of boundary conditions

Figure 7 shows the four types of flow boundary conditions. The following section describes the various boundary conditions have been adapted from "Feflow online help".

The constant head boundary condition, also known as 1st kind/Dirichlet boundary condition, is used to represent a pre-defined hydraulic head. The areas that are assigned to these boundary conditions have a constant value of head and remain that value for the simulation run. This boundary condition simulates a constant source of water entering the model domain such as a river leaking into an aquifer and the model domain has no influence on this river, or the situation shown in Figure 7, were a constant source of groundwater is entering the boundary. Head boundaries are applied to where the hydraulic potential is known in advance. This boundary condition has units of head in meters.

The fluid-flux boundary condition, also known as 2nd kind/Neumann boundary condition, is used to represent a "no flow" condition. This condition indicates that there will be no flow across the boundary or where the gradient of the flow *flux* is known in advance. This can be the case where there are inflows into the aquifer in a valley from steep slopes or for the connection to a neighbouring aquifer where the flux can be assumed to be constant. This boundary condition has units of m^2/s if applied in a 2D model and m/s if applied in a 3D model.

The fluid transfer boundary, also known as 3rd kind/Cauchy boundary condition, is used to represent a combination of Dirichlet and Cauchy boundary conditions. This condition is used to

represent an area such as a river where a clogging layer is present or a partially clogged layer, where there is material in a normally constant condition that can change through the model simulation. For example, a lake with a river bed of smooth large cobble stones with constant flow would have a constant head boundary, but given the same lake but with a river bed filled with silts and smaller grainy material a fluid transfer boundary condition would be more appropriate. To account for the extra variability, a constant called a transfer rate is incorporated into the boundary condition and mathematically:

$$\phi = \frac{K}{d} \qquad 3.14$$

Where:

K Hydraulic Conductivity of the clogging layer (m/s)

d Thickness of the clogging layer (m)

ϕ Transfer rate (m)

The well boundary condition is used for a fix abstraction or infiltration rate in a point on the model domain. It can also be used if flow at a certain point is known. This boundary condition has units of m^3/s or l/s.

The last section of the model domain consists of an area to conduct the model simulation on. This area is known as a *mesh* which breaks the model domain into smaller areas known as *nodes*. There are two methods to create a mesh; finite element and finite different methods. Finite difference methods discretize the model domain into smaller rectangles as defined and the governing equation is solved across the discretized surface. Finite element methods discretize the model domain in terms of triangles and numerically integrate to solve the governing equation over the smaller triangles. Finite difference and finite element methods have their particular advantages and disadvantages.

On the topic of stream depletion there are several ways of calculating this. Sophocleous et. al. 1995 suggests finding the difference between the original stream flow and the stream flow after pumping, and dividing it by the pumping rate:

$$\text{Leakage due to well as a percentage of pumping} = \frac{q - q_o}{Q} \qquad 3.15$$

Where:

q Current leakage after pumping (m^3/s)

q_o Initial Leakage (m^3/s)

Q Current pumping rate (m^3/s)

Equation 3.15 is plotted against time so that the leakage due to pumping a stream can be illustrated. This approach has also been used in Chen et al. 2001 and Chen et al. 2002 to calculate the leakage due to pumping.

Zume et al. 2008 exemplifies how numerical modeling can be used to model stream depletion. Numerical modelling software, MODFLOW (McDonald et al. 1988), evaluates the impacts of groundwater exploitation on stream flow depletion. MODFLOW uses finite difference techniques to evaluate the governing equations to provide a model of the physical process that occur during groundwater abstraction. In this study, MODFLOW was used to investigate the impacts of groundwater pumping from an alluvial aquifer on stream-aquifer interactions, specifically, streamflow depletion, in a semi-arid but agricultural important area of north western Oklahoma.

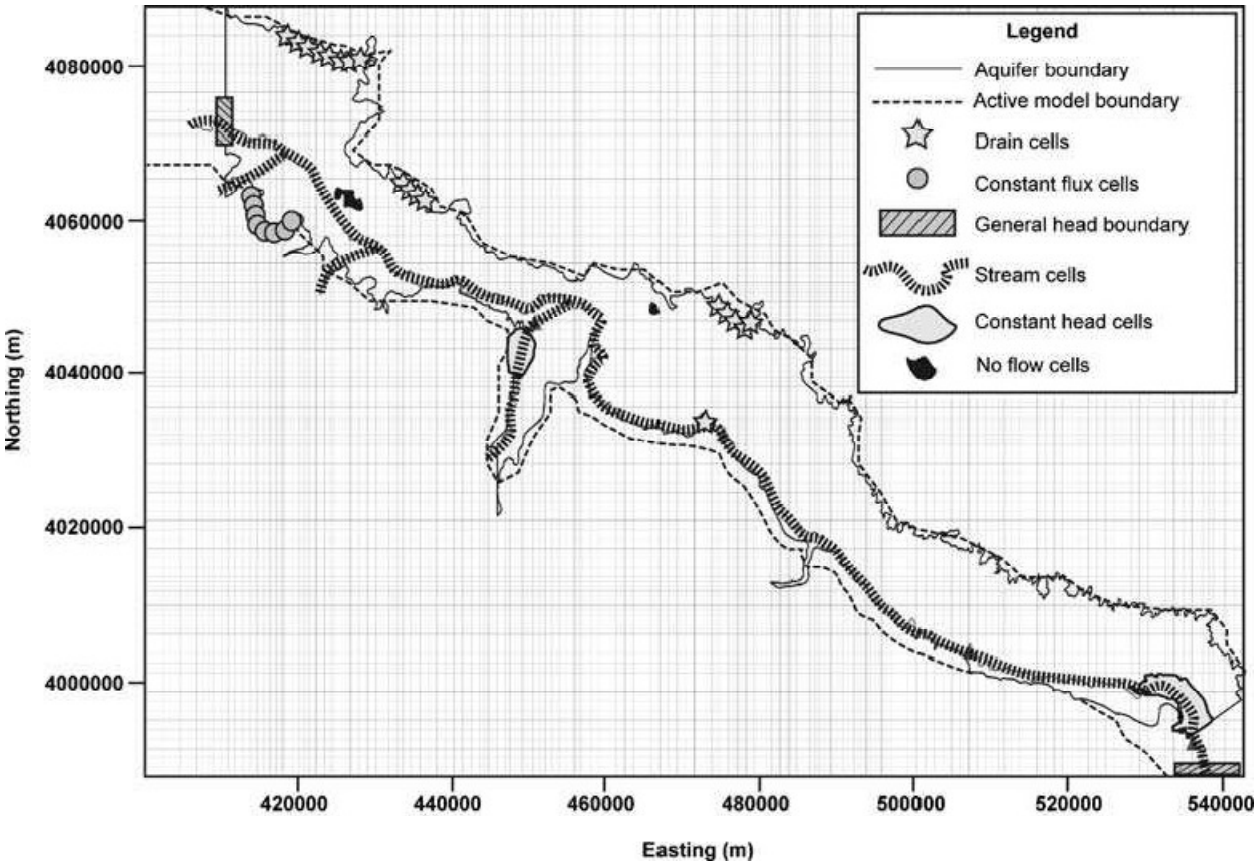

Figure 8: Zumeet. al. 2007. Map of numerical experiment configuration

A 2D model of the area of importance in Northwest Oklahoma, shown in Figure 8, was created with a square mesh consisting of cells, with certain cells containing boundaries conditions simulating certain conditions and features of the agricultural area, such as stream cells representing rivers and constant head cells representing areas of recharge. The stream routing packing in MODFLOW was used to calculate the flow between each stream cell and corresponding aquifer flow using:

$$Q_L = C_s(h_s - h_a) \qquad 3.16$$

Where:

Q_L Flow between the stream and aquifer (m^3/d);

C_s Streambed hydraulic conductance (m^2/d);

h_s Hydraulic head in the stream cell (m);

h_a Hydraulic head in the aquifer side of the stream bed (m).

Whether the water discharges to the stream, or vice versa, depends on the direction of the slope between the hydraulic head. The C_s term is calculates as:

$$C_s = \frac{KwL}{M} \quad 3.17$$

Where:

K Hydraulic conductivity of the streambed material in the reach (m/s);

w Width of the stream (m);

L Length of the stream (m);

M Thickness of the streambed material (m).

Equation 3.17 holds for fully saturated hydraulic connections between the stream and the aquifer. For the disconnected case; i.e. when the head in the aquifer falls below the streambed bottom elevation (h_{bot}), the head gradient in Equation 3.17 is accessed between the stream stage and $h_{bot} \times Q_L$ is calculated as:

$$Q_L = C_s(h_s - h_{bot}) \quad 3.18$$

The model was then calibrated using various historical data of groundwater elevations using data recorded between 1978 and 1979 to obtain initial values of the flow and head values. This calibrated model was then used to estimate pumping-induced stream flow depletion, resulting from reduced base flow and stream leakage. To determine the changes in base flow and stream leakage, a transient model was run with the pumping wells switched off. Then the same model with the pumping wells turned on was simulated, and stream-aquifer fluxes were compared in both model runs. The resulting difference was used as the stream depletion rates.

The results from MODFLOW confirmed that pumping from wells decreased the baseflow the river systems in the North Canadian River. Results showed that before pumping, 56% of baseflow contribution went to streams while stream leakage provided 30% of total aquifer recharge. When pumping was turned on after 1, 5 and 15 years of pumping, baseflow contribution to rivers was reduced to 47%, 35% and 27% respectively and stream leakage increased by 35%, 44% and 48% respectively.

This paper showed how inducing pumping on an irrigation system can be used to quantify stream depletion using a numerical model. By creating a mesh with boundary conditions attached to certain areas to represent physical attributes in the system.

3.1.3 Numerical and analytical comparisons

Analytical and numerical solutions provide a wealth of insight into the process and mechanics of groundwater processes. Both types of solutions have their various advantages and disadvantages in their accuracy and limitations. Parkin et al. 2007 mentions that analytical methods provide simplified representations of river-aquifer processes and interactions which lead to significant errors in representing fully penetrating rivers and lack of representation of river sediments and aquifer storage beyond the stream. Sophocleous et al. 1995 compared the predictive accuracy of Glover 1974 analytical solutions to stream depletion which were used to administer water rights in Kansas, America. The study found that analytical solutions over estimate stream leakage and stream depletion when compared against numerical studies.

These results confirmed by Spalding et al. 1991 that analytical solutions over estimate stream depletion rates. Analytical solutions mentioned in Theis 1941; Jacob 1950; Glover 1954; Hantush 1965 were compared against a numerical model AQUIFEM. The effects of various assumptions on stream depletion were considered. It was found that neglecting the combined effects of partial penetration and clogging layer resistance can cause errors in calculated stream depletions. Figure 9 shows the over estimates as shown in Spalding et al. 1991.

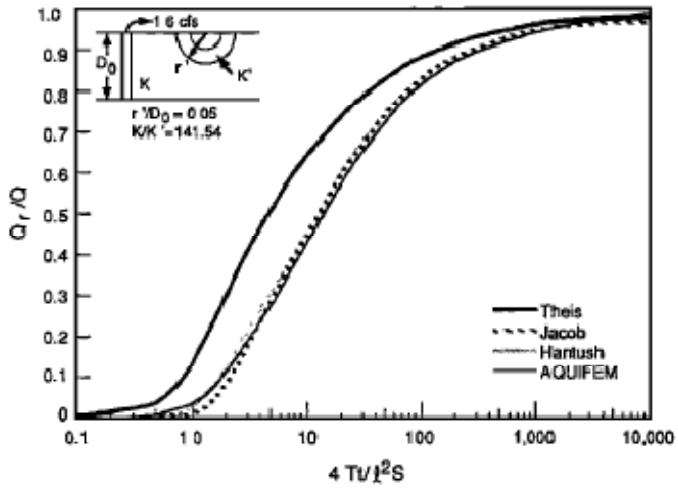

Figure 9: Ratio of stream depletion to well discharge as a function of dimensionless time for Theis, Jacob, Hantush and AQUIFEM

Numerical models have the advantage that they are more robust to their analytical counterparts and can be generalized more easily than analytical solutions often handing hydraulic complexity much more efficiently (Sophocleous et al. 1995). However numerical methods are still subjected to error. Konikow et al. 1992 lists three possible sources of error that could occur in groundwater models; conceptual errors about the basic process incorporated in the model, numerical errors arising in the equation-solving algorithm and uncertainties and inadequacies in the input data. In most cases conceptual problems and uncertainty concerning the data are the most common sources of error. Hunt 1999 also gives caution to the use of numerical models stating that while numerical models can lead to a generality in stream flow depletion models, accurate results can only be obtained if large amounts of good field data are available for use by a skilled numerical modeller.

3.2 Isotropy and Anisotropy

If the hydraulic conductivity is independent of the direction of measurement at a point in a geologic formation, the formation is *isotropic* at that point. On the other hand, if the hydraulic conductivity varies with the direction of measurement at a point in geologic formation, the formation is *anisotropic* at that point. Homogeneity and heterogeneity have similar definitions respectively; *homogenous* meaning the hydraulic conductivity is *independent of position* within

a geological formation and *heterogeneous* being hydraulic conductivity is *dependant of position* within a geological formation (Acworth 2010). These concepts have important implications in modeling because incorrect assumptions of isotropy and anisotropy of the model can lead to incorrect or inaccurate results.

Knochenmus 1996 conducted a study on the effects of anisotropy and heterogeneity on modelling groundwater flow in the Upper Floridan Aquifer in Florida America. The study focused on the use of numerical and analytical solutions to model the effects of anisotropy and heterogeneity in a typical karst carbonate aquifer system. While this study has no direct relation to stream depletion, the implications of aquifer anisotropy and heterogeneity in groundwater modelling still has its implications on groundwater models as these properties has effects on the direction and velocity of groundwater flow.

Field data was collected from well in the area of focus and these values were used to determine values of transmissivity. These values were then input into different analytical and numerical models with similar geological modeling domains, but with different configurations such as single layer anisotropic and multilayer setup. Various models were compared using a self defined term *area of contribution*- a term that quantifies areas of influence that an abstraction bore has on a certain area.

The study concluded that the distribution and nature of aquifer heterogeneities will affect the size, shape and orientation of *areas of contribution* in a karst carbonate aquifer system. Model parameters such as simulated withdrawal rates, effective porosity of the geology and transmisivity have a big influence on the area of contribution with effective porosity being the governing factor. Also, results of simulations incorporating aquifer heterogeneity indicated that the oversimplification of the flow system may result in the incorrect definition of flow fields.

3.3 Effect of a clogging layer in the stream channel

A clogging layer reduces the hydraulic conductivity of the streambed sediments, slowing the transmission of water from the stream to the underlying aquifer (Treese et al. 2009). The clogging layer has implications on pumping as it reduces the rate of infiltration as it disrupts the

stream-aquifer interactions. As mentioned in Section 3.1.2, the clogging layer is represented through Cauchy boundary conditions as a transfer rate, so a section on clogging layers and its effects on stream-aquifer interactions is included.

Bouwer 2002 gives a detailed overview on clogging layers and its effects on infiltration rates. Clogging in a river system is caused by physical, biological and chemical processes. Physical processes that cause clogging are the accumulation of inorganic and organic suspended solids in the recharge water, such as clay silt particles and biological agents such as algae and microorganism cells and sludge flocs in sewage effluent. Another physical process that contributes to clogging layers is the movement of fine particles in the soil or surface water where there is accumulation of fine particles where the soil is denser or finer. The depth of this clogging layer can range from a few mm to a few cm or more.

Biological causes of clogging layers include the build-up of algae and bacterial flocs in the water on the infiltration; and development of micro-organisms on and in the soil to form biofilms and biomass that block pores and/or reduces block size.

Chemical processes that produce clogging layers incorporate precipitation of calcium carbonate, gypsum, phosphate and other chemicals in the soil. Occasionally, during photosynthesis caused by algae, these precipitations are induced as they eliminate the CO_2 from water. Bacteria also produces gases such as nitrogen and methane that block pores and accumulate below clogging layer to create vapour barriers to infiltration.

In relation to groundwater-surface water interaction they reduce infiltration rates and become the controlling factor bottlenecking the stream leakage into the aquifer (Figure 10). When the clogging layer hydraulic conductivity becomes less than the hydraulic conductivity of the soil below the clogging layer, this soil becomes unsaturated to a water content and the whereby the corresponding unsaturated hydraulic conductivity is equal to the infiltration rate. The clogging layer can also cause the river to disconnect from the aquifer due to pumping.

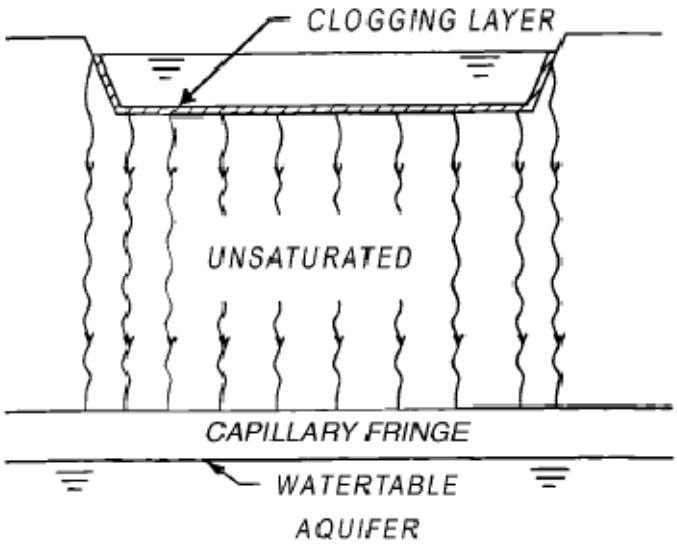

Figure 10: Bouwer 2002. Basic diagram of a generic clogging layer

In numerical modeling the clogging layer is generally represented by factoring the hydraulic conductivity of the surrounding aquifer by considering a separate hydraulic conductivity of the aquifer and multiplying this conductivity by a ratio of the estimated depth of the clogging layer. As previously mentioned in Section 3.1.2 the clogging layer can be factored into the numerical model by using Equation 3.14 or Equation 3.17.

Brunner et al. 2009 considers the following equation as a condition to determine if a river will ever disconnect due to a clogging layer in a two dimensional model:

$$\frac{k_c}{k_a} \leq \frac{h_c}{d + h_c} \qquad 3.19$$

Where:

k_c Hydraulic conductivity of the clogging layer (m/s)

k_a Hydraulic conductivity of the aquifer (m/s)

h_c Thickness of the clogging layer (m)

d Depth of ponded water

3.4 Case Studies

Numerous publications exist for numerical and analytical models for river-aquifer interactions on the subject of stream depletion. Various case studies are presented where numerical models have attempted to simulate stream depletion. Methods of each study and their results have been presented and comparisons between each study will be presented in Figure 12.

Numerical modeling has been used to quantify the effects of pumping on river-aquifer interactions. Chen et al. 2001 numerically models the interaction between a hypothetical river and aquifer during seasonal pumping. Chen et al. 2002 focused more on the stream bed properties of river-aquifer interactions and focused the study on one cycle of seasonal pumping. Sophocleous et al. 1995 used a hypothetical stream-aquifer system to compare the numerical modelling with its analytical counterparts.

Chen et al. 2001 undertook a numerical study of the effects of seasonal abstraction has on the baseflow of a river after seasonal pumping. This study calculated the stream depletion in two separate terms; one term consisting of the leakage of the river to the aquifer from pumping as indicated in equation 3.15, the other term being the baseflow that is reduced after pumping:

$$D_b = \frac{R_o - R}{Q} \qquad 3.20$$

Where:

R_o Baseflow if the well is not pumped (m^3/s)

R Baseflow is the well is being pumped (m^3/s)

Q Pumping rate of the well (m^3/s)

D_b Reduced baseflow

The domain of the model is presented in Figure 11. The model parameters that varied were the distance between the river and the pumping bore and the hydraulic conductivity. Values which remained constant were the pumping rate of 2727 m^3/d and the well screen of 9.1m. The model was also run for two years, which consisted of two seasonal pumping cycles.

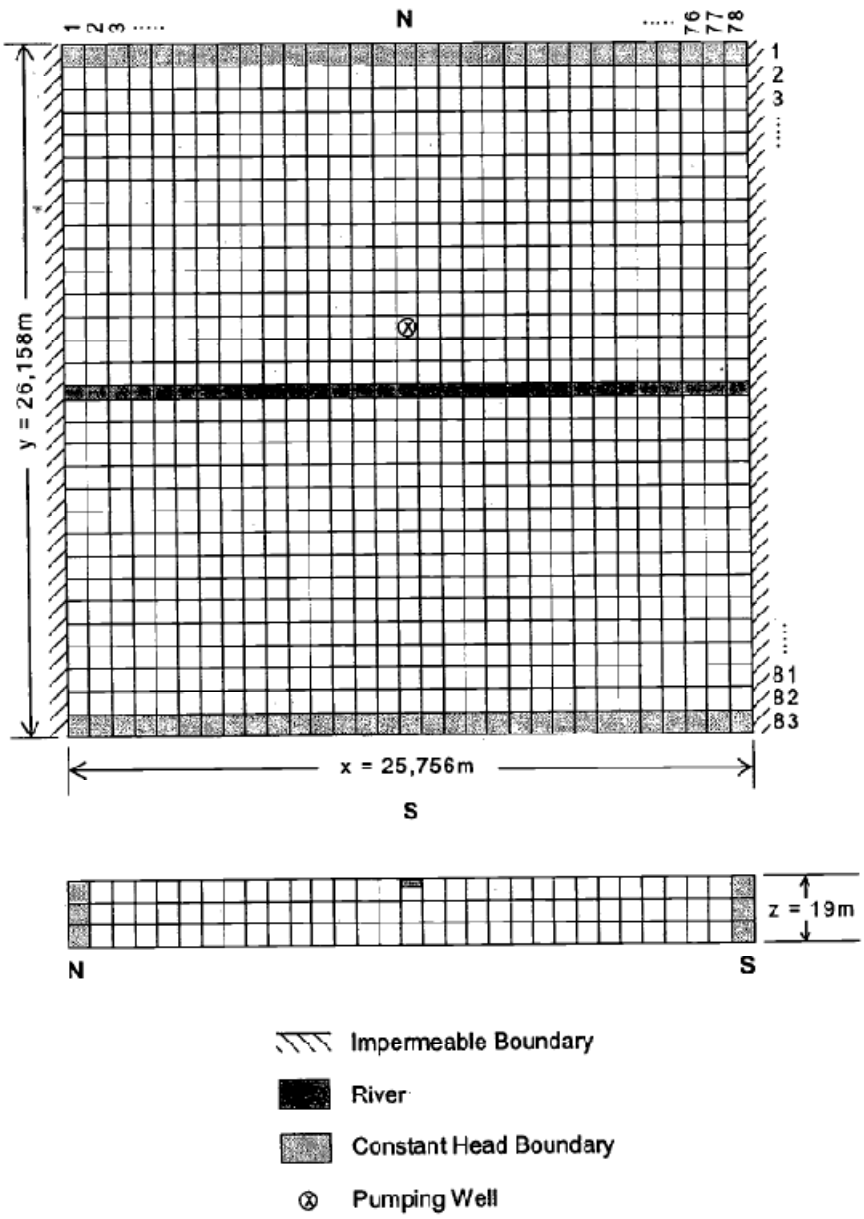

Figure 11: Chen 2001. Map of numerical experiment setup

The study concluded that the total stream depletion was dependant on the hydraulic gradient as the value of baseflow is governed by the difference in head. In the case where there was no hydraulic gradient between the aquifer and river, the stream depletion was entirely governed by induced infiltration. Baseflow reduction occurs almost immediately for distances close to the river (305m and 710m), but for longer distances such as 1524m a lag of four days was observed. However, the induced stream infiltration was not observed immediately with pumping.

The stream depletion in this case occurred as a function of distance from the river. The total depletion was smaller for a larger distance to the river during each pumping period. This infiltration occurred after the pumping was stopped; the total depletion during the non-pumping period was larger for a pumping well located further from the river. This result is in agreement in Sophocleous et al. 1995 where stream flow depletion is inherently time dependant. As the pumping well was placed a long distance from the river, the time taken for this stream to recover to its initial baseflow is extended. If more time was allocated between periods of pumping, similar stream depletion rates might be observed between distances closer to the river.

A later study by conducted by one of the same authors, Chen et al. 2002 used the same method of analysis as the previous paper, but focused on two stream depletion parameters; stream conductance and areal recharge. Stream conductance was defined as:

$$C^* = \frac{k_s W}{M} \qquad 3.21$$

Where

k_s Vertical hydraulic conductivity;

W Stream width (m);

M Thickness of the stream bed (m)

Stream infiltration was calculated using a similar method in Chen et al. 2001. The model domain was 10,000 m by 10,000 m with a river of depth of 1.7m. A constant pumping rate of 4,000 m^3 per day was applied to all the model runs, which were of duration of 90 days with periods of no pumping lasting 275 days.

This paper came to the same conclusions as Chen et al. 2001, but added that as pumping stoped, the total pumped volume was equal to the volume of storage depletion, stream infiltration and base-flow reduced. Also, a higher streambed conductance will result from a either a wider stream, a thinner streambed, a more permeable stream sediment or a combinational of the three resulted in a higher hydraulic conductivity producing rates of higher stream depletion. The hydraulic conductivity had strong effect on the stream depletion rates.

The hydraulic conductivity acted as a clogging layer to bottle neck the flow of the water and having a higher hydraulic conductivity increased the rate of stream depletion. Lastly, the paper came to the conclusion that while the stream conductance has a high hydraulic connection to the aquifer, there is no linear correlation between stream conductance and stream depletion.

In another study, Chen et al. 2004 compared semi-analytical solutions to results from MODFLOW. The model domain consisted of a square area of 20,000m by 20,000m with an aquifer thickness of 25m divided evenly by three layers. The model had similar boundaries to previous studies mentioned. Yet again a period of 90 days of pumping with 275 days of non-pumping was applied with a pumping rate of 4500 m^3/day. It was concluded from this study that the simulations run showed a good correlation between semi-analytical solutions and numerical simulations, which verified the numerical solutions.

In a key paper, Sophocleous et al. 1995 evaluated analytical solutions of stream water depletion that were commonly used to administer water rights in America. Sophocleous et al. 1995 used MODFLOW to simulate a boundary area of 3,800m by 1,980m with a pump situated 80m from the river with a pumping rate of 5 m^3/day (Figure 12). Sophocleous concluded that stream-aquifer analytical solutions will often overestimate stream depletion. The reason for the over estimation is discussed in Section 3.1.2 and the over estimation was due to the conservative nature underpinning the assumptions of made in analytical solutions.

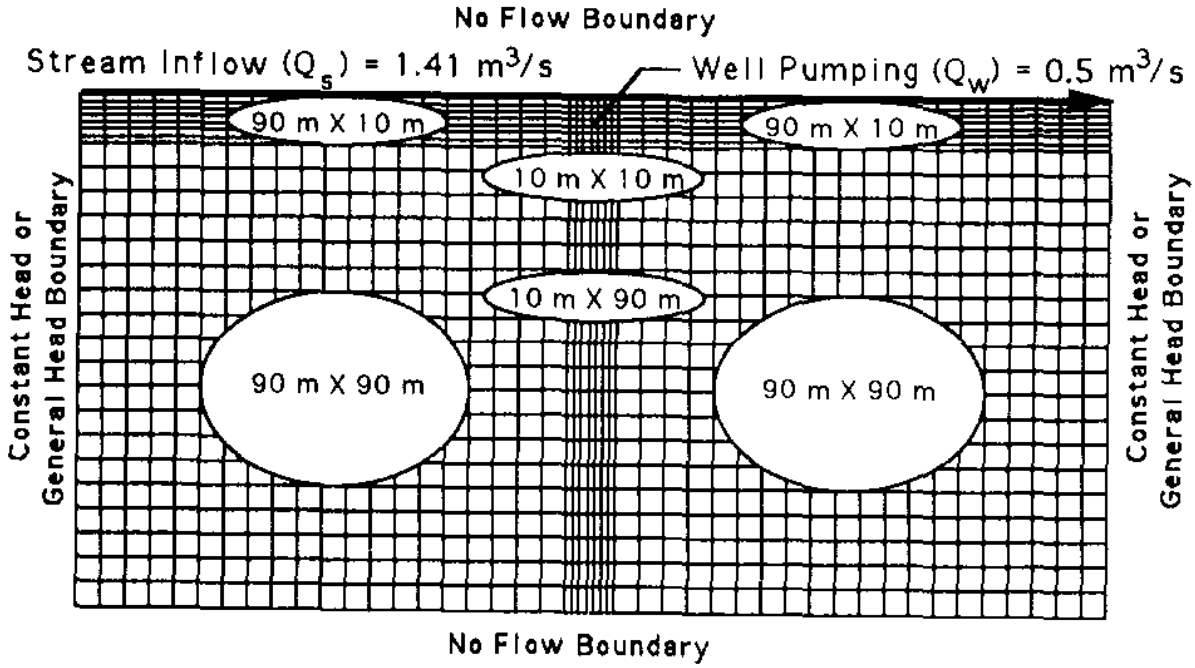

Figure 12: Model domain for Sophocleous et. al. 1995

Table 11 in Appendix A provides a numerical comparison of the results in the papers mention in the beginning of Section 3.4.1. The variables in the table are identified from the collection of papers as factors that influence the rate of depletion; Distance of pumping bore from river – X (m), Rate of pumping – Q (l/s), vertical hydraulic conductivity - k_v (m/s), ratio of vertical to horizontal hydraulic conductivity - k_v/ k_h, hydraulic gradient – i, transfer rate – ϕ (m/s), peak of stream depletion as calculated in equation 3.15 (Percentage).

To find any relationship between variables, a regression analysis was done using Minitab. A *Best Subsets Regression* was preformed the variables in Table 11 to determine which variables had the most influence on the peak. The motivation for the best subsets procedure searches through all the possible models and reports for each subset size the values of the R^2, $\overline{R}^2$ and C_p. C_p is a measurement of goodness of fit, that is minimising C_p is a form of managing the correlation of variables/complexity trade off (Sisson 2008). Figure 58 shows the Best Subset Regression output from Minitab.

There is strong evidence relating the distance of the pumping bore from river (X) with stream depletion, as out of all the possible model combinations that is the most frequent variable to be chosen in the model as well as having the lowest C_p value when used in a linear regression as the only variable. The next common variable is transfer rate (ϕ), but this value is absent in 10 out of the 23 values and most probably has little effect on the parameters. The transfer rate is tied for rank with hydraulic gradient and followed by pumping rate and then hydraulic conductivity.

Hypothesis testing was performed on various combinations of variables based on Figure 58. The rejection criteria was set to a 95% confidence criteria, that is P-Values greater than 0.05 are rejected based not enough evidence to accept the hypothesis that there is a relationship between the variables to predict values of peak stream depletion values. Table 1 summarises the values of the hypothesis testing.

Variables	P- Value
All	0.174
X, Q, ϕ	0.049
X, i, Q	0.063

Table 1: Results of Hypothesis Testing

Figure 59 contains a regression of all variables and a P-Value of 0.174 was produced; this was expected as there would be little correlation between many variables with limited data. Figure 60 contained a regression of X, Q, ϕ and gave a P-value of 0.049; there was evidence to accept the hypothesis testing. Interestingly, the variables X, i, Q had a P-value of 0.063 which were rejected based on the confidence interval of 95%; this was despite having a C_p value of 2.2 which was lower than X, Q, ϕ with a C_p value of 2.3. This was because of a combination of the values of ϕ absent for a majority of the data or the results of Sophocleous et al. 1995 containing high values of "i" creating outliers in the data.

It should be noted that this linear regression was biased against a certain type of methodology; most of the results in Table 13 were based on studies conducted by the same author (Chen 2001,2002,2004) and these papers have referenced to Sophocleous et al. 1995.

4 Methodology

This thesis examines the effects that certain parameters have on a numerical model depicting the physical interactions between a river and an aquifer induced due to a pumping bore placed near the river. The parameters of interest are; hydraulic conductivity, distance from river, pumping rate and effect of clogging layers. A numerical sensitivity analysis will be performed to determine the effect that these parameters have on the numerical model and stream depletion through the use of a finite element package FeFlow (Trefry et al. 2007).

4.1 Study Area

The geography, geology and numerical parameters for this numerical experiment originate from research currently being conducted in Maules Creek sub-catchment located in the Namoi River. For more specific information on the general area and research in the area refer to Andersen et al. 2009.

Figure 13: Drilling at Elfin's Crossing

The geology of this generic model is based on geology found at Elfin's Crossing shown in Figure 13. The creek extends several kilometres.

4.2 Finite Element Mesh and Boundary Conditions

The model domain for the generic three dimensional numerical models is illustrated in Figure 14 and Figure 15.

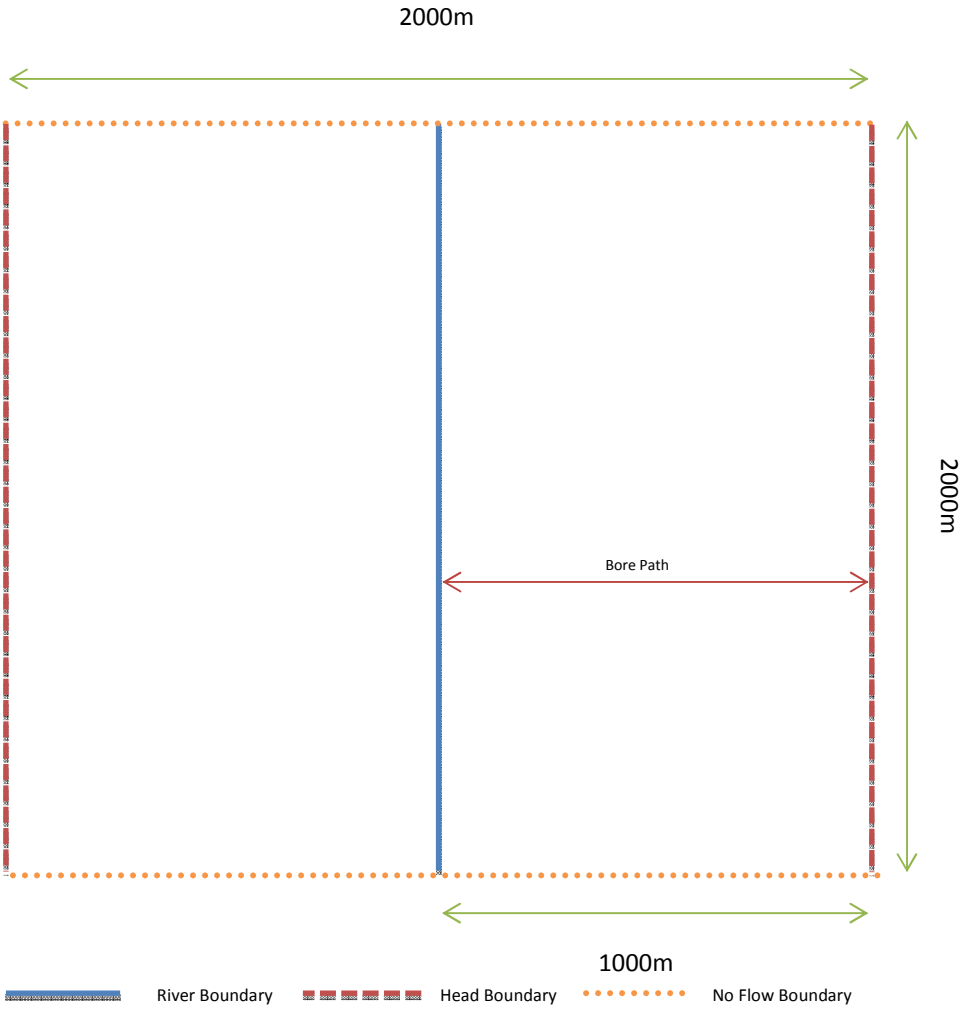

Figure 14: Over View of the proposed model boundaries

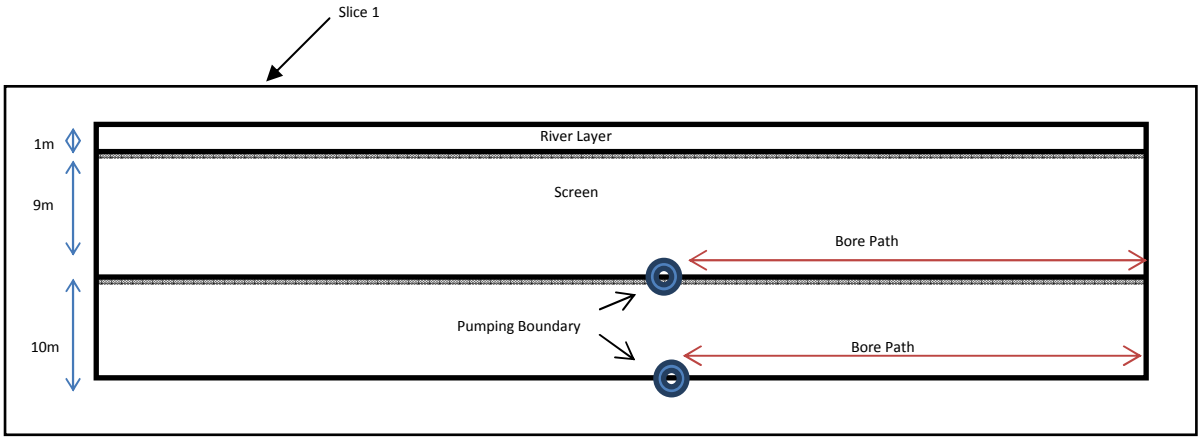

Figure 15: Cross Section of boundary conditions and aquifer

In this model, the outer boundaries were chosen to be 2000m by 2000m to allow the domain to be sufficiently large so as to not affect the pumping modelling boundary conditions. The river boundary condition was placed directly in the middle of the domain from North to South to represent the river at Elfin Crossing. A no-flow boundary condition was set on the North and South boundaries and Head Boundaries were set up on the East and West boundaries. This was placed to represent groundwater flow entering the river from the East-West direction. The pumping boundary location varied in the model and this was positioned on defined locations on a path as indicated by *bore path* in Figure 14.

Figure 15 shows the cross section of the model domain. Four slices resulting in three layers were implemented in this model. The first layer represented the river and had a depth of 1m due to the clogging layer, as defined in Equation 3.14. This allowed the clogging layer to be determined by changing values for the transfer rate. The second layer was set to be 9m thick so that a screen length of 10m can be modelled. The last slice was placed 20m below the top creating a bottom layer of 10m thickness and allowing the model domain to reach a depth of 20m. The top slice was set to phreatic, the two corresponding layers were set to unspecified and the last later was set to fixed. A phreatic surface allowed for elements to be partially saturated as the water table would vary in the model.

The model mesh was refined around the bore path and river nodes. The element size was reduced in these areas to increase accuracy in the model. As the pumping location varied in each model run it was more economical to mesh all the elements around the bore path and use the mesh for all model runs. The pumping boundary condition was positioned vertically at 10m and at 20m. This simulated the screen length of 10m and the value of each pumping node summed up to the total rate of pumping. The hydraulic gradient was set to 0; there was no change from the river boundary condition to the east and west boundary conditions.

The time step was set to one day. The total time length of each model run varied depending on the model run. For example a model with a high hydraulic conductivity could take two weeks to obtain results. On the other extreme a model with a low hydraulic conductivity would take several months to obtain results. As the model was run in time steps, all the simulations were

run in transient mode as opposed to steady state mode. The difference between the two modes was that time steps are governed by the numerical software package and is run until certain conditions are met as opposed to transient mode were the time steps are manually inputted.

Table 2: Summary of model properties

Component	Location	Values
Model Boundaries	Edge of model domain	2000m x 2000m
Constant Head Boundary	East and West Boarders	0m
No Flow Boundary	North and South Boarders	0 m
River Boundary	Runs from North to South	0m
Number of slices	Below the surface	4 units
Surface	-	Phreatic
Bore Depth	Varies along bore path	20 m
Screen Length	Varies along bore path	10 m
Time Step	-	10 days to 120 days
Porosity	Assumed saturated throughout model	0.2

4.3 Governing Parameters of the sensitivity analysis

Section 3.4 highlighted a few parameters of interest that were investigated in a sensitivity analysis. A sensitivity analysis involves the study of how the variation in the output of a mathematical model can be apportioned, qualitatively or quantitatively, to different source of variation in the input of the model (Saltelli A. et. al. 2008). The parameters chosen were:

- Distance of pumping location from the river (m) – X
- Pumping Rate (l/s) – Q
- Effect of hydraulic Conductivity (m/s) – K
- Effect of clogging layers (m/s) – Φ

A table of parameters used for the sensitivity analysis is presented in Table 3.

Table 3: Table of parameters

Parameter	Favorable	Base	Unfavorable
Q (l/s)	2.5	5	10
K (m/s)	5.00E-05	5.00E-04	5.00E-03
Φ (m/s)	5.00E-04	5.00E-05	5.00E-06
X (m)	20	30	50

To be able to determine impact that each parameter had on the river, two of the parameters were kept constant while one parameter changed. Figure 16 shows the directional diagram of how the analysis was conducted.

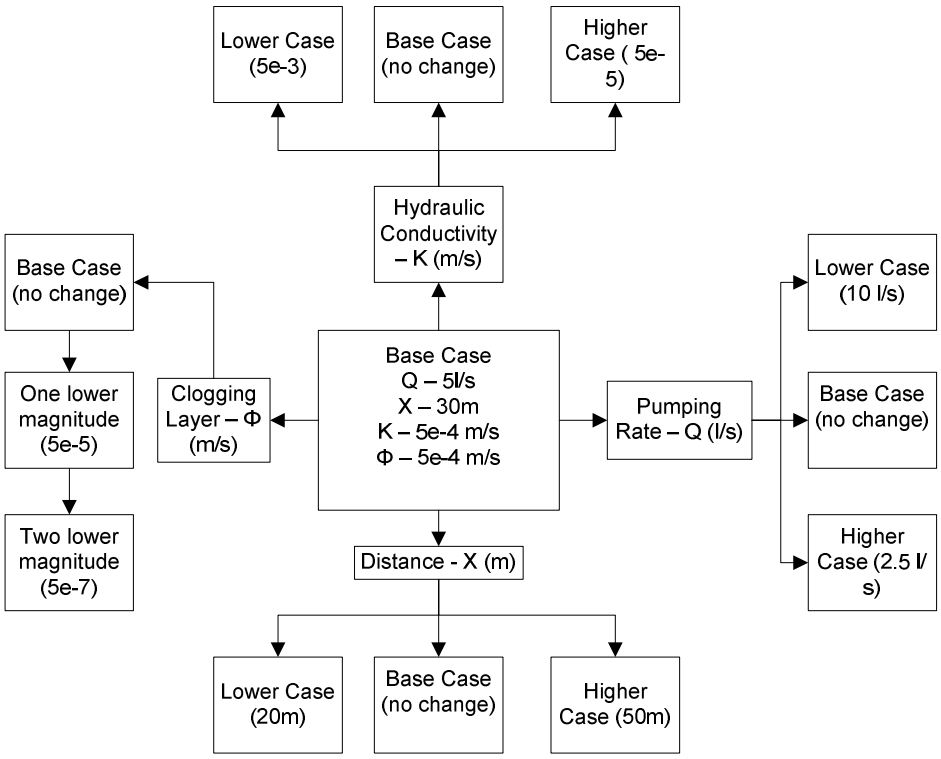

Figure 16: Directional diagram for sensitivity analysis

The physical constraints of where the model could be placed was the most important parameter in this problem; the location of the pump could be placed at most 50m from the river and closest was 20m before borehole drilling was considered too close to the river. The values chosen for the sensitivity analysis was 20m, 30m, and 50m; 20m and 50m were the two

extremes of constraint and 30m was used as a intermediately point. The pump was placed on the perpendicular “bore path” in Figure 15.

The pumping rate was also identified as having an impact on stream depletion rates. The pump’s physical capacity was a limiting factor in the sensitivity analysis with the maximum pumping rate being 10 l/s.

Hydraulic conductivity at the field site during field work fluctuated in values. On reviewing results from a slug test (Figure 62) conducted at Eflin Crossing the average hydraulic conductivity was determined to be $5x10^{-4}$ m/s. Orders of magnitude lower and higher ($5x10^{-5}$ m/s and $5x10^{-3}$ m/s) were chosen in the sensitivity analysis representing a wide range of hydraulic conductivities.

Parameters for the clogging layer differed from the other parameters, as there was no physical situation identified in the experiment; where the hydraulic conductivity of the clogging layer was considered higher than the hydraulic conductivity of the aquifer. In this run of models, two magnitudes of lower hydraulic conductivities of the clogging layer were considered. The clogging layer hydraulic conductivities were respectively $5x10^{-4}$ m/s, $5x10^{-5}$ m/s and $5x10^{-6}$ m/s.

Two extreme runs were added to the sensitivity analysis as an indication of the worst and best scenario runs. One extreme had the optimum conditions excluding the clogging layers; the pumping bore location was placed 20m from the river, pumping rate was 10 l/s, hydraulic conductivity was $5x10^{-3}$ m/s. The inverse situation had the worst condition; pumping bore location was placed 50m from the river, pumping rate was 2.5 l/s and hydraulic conductivity was $5x10^{-5}$ m/s.

4.4 Methods of comparisons

4.4.1 Head verse time data

Observational points were placed in positions shown in Figure 17 to determine the behaviour of the river boundary conditions. Four observation points were setup on either sides of the river bank, in the middle of the river and near the river. These points were then placed on the first

and third slice leaving a total of eight observational points. Then at each time step the value of head was recorded and plotted against time. These observational wells correspond to the drawdown or the *cone of depression* that is caused by pumping.

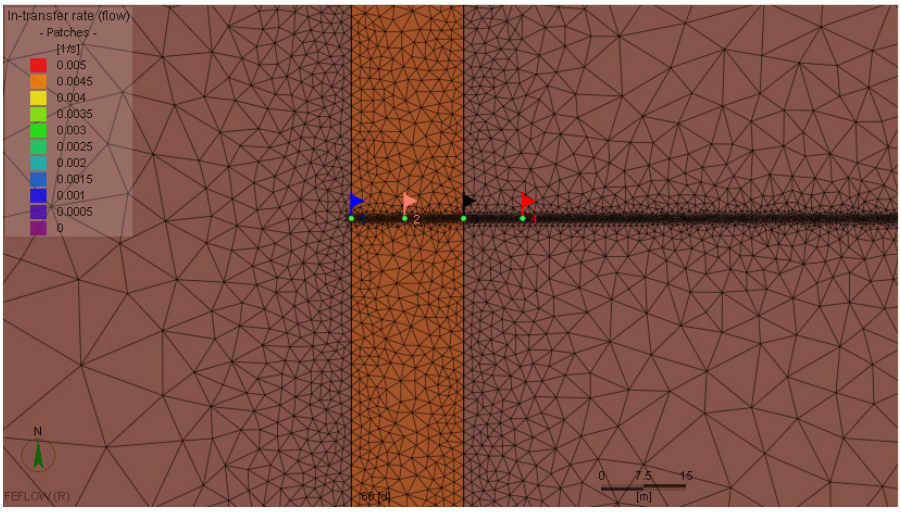

Figure 17: Location of observation wells

The vertical hydraulic gradient was calculated between Slices 1 and Slices 3 which had a distance of 10m between them. The following equation was used:

$$i_v = \frac{h_2 - h_1}{s_2 - s_1} = \frac{h_2 - h_1}{10} \qquad 4.1$$

Where:

h_i Value of head at point i (m)

s_i Distance from surface at point i (m)

The hydraulic gradient was calculated to determine if there was any significant difference in pressure between the two slices. As this model was configured with a screen of 10m there is a possibility under certain conditions that the pressure heads could differ between each slice.

4.4.2 Forward Particle Tracing

In a similar way a radioactive tracer can be placed in a river to trace the path of the water through groundwater. Particle tracing techniques can be applied numerically; i.e. particles can be placed at certain points on the numerical mesh and the path and velocity the particle can be

tracked. A particle was placed on the river bank perpendicular to the pumping bore and its perpendicular distance was recorded.

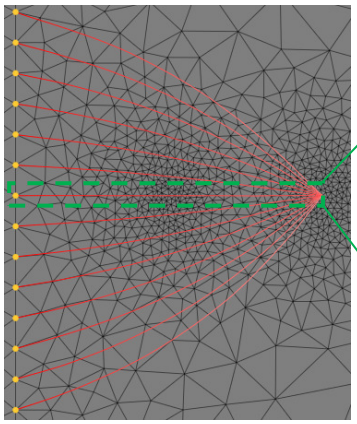

Figure 19: Bank of River Nodes

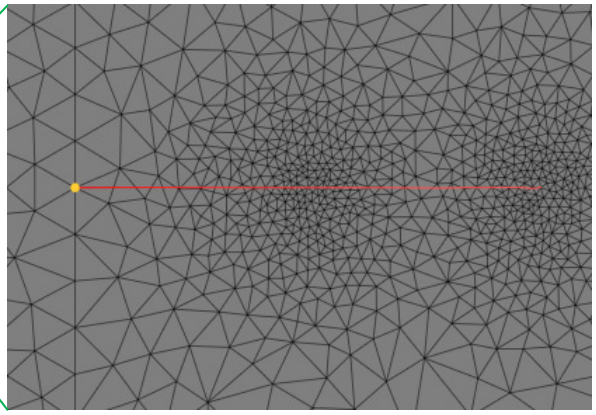

Figure 18: Path of a Perpendicular Particle

A series of tracers were placed on the bank in Figure 19 to illustrate the tracer technique. In this section the particle perpendicular to the pumping bore was used as illustrated in Figure 18. For each of the graphs there was a flattening of the graph were the particle has terminated in the x-direction and for the purpose of this section the particle should be considered terminated in the x-direction.

4.4.3 Plume Evolution

In this section, particle tracers were placed across the river similar to a river transect. The purpose of this was to gain an insight into the evolution of particles in terms of days. Figure 20 illustrates the path of the river transect as exported from Feflow.

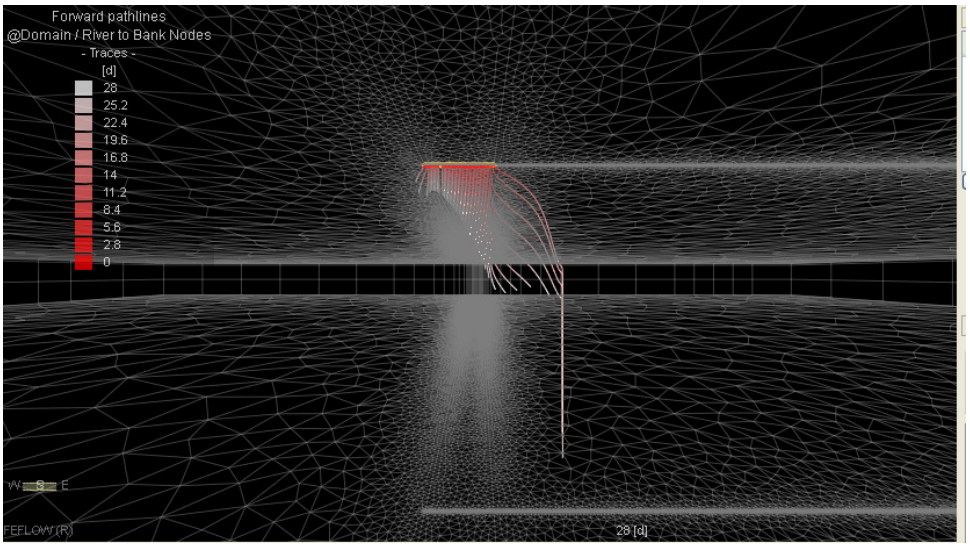

Figure 20: Particle Transect in terms of mesh

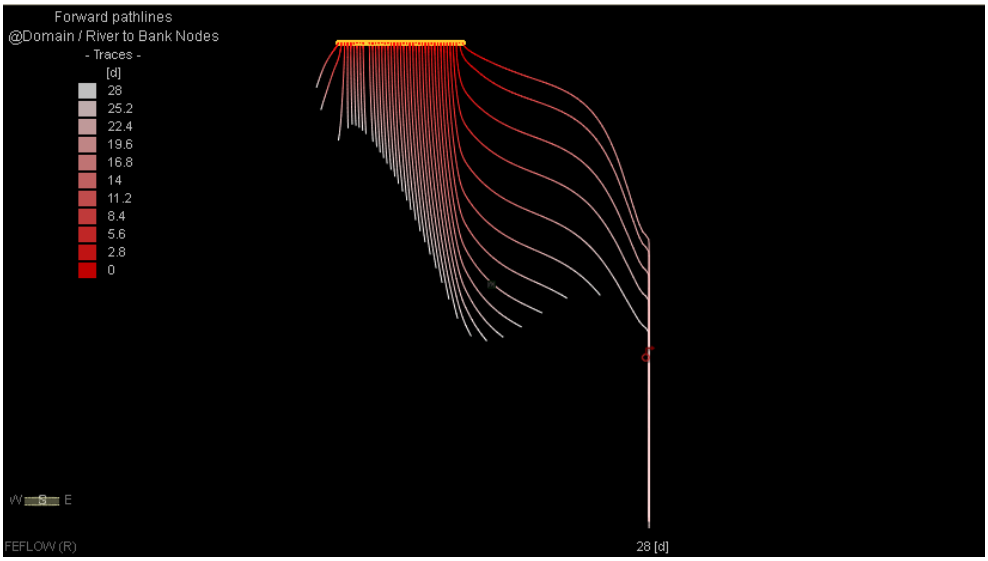

Figure 21: Base Case particle transect

The coordinates and time steps of the particle transect were placed into Surfer (Madison 2011) and a contour plot was created to represent layers of day similar to the concept of a plume. The *Time of Impact* is the time when the lowest layer hits the pumping bore; the *bandwidth* is the lowest point of the layer that first hits the pumping bore. These terms are shown on the first figure in Figure 43. The bandwidth is a rough measure of the height of the plume as the particles all had the same initial location.

4.4.4 Percent sourced from river

The water being sourced from the river rather than the groundwater can be quantified using the boundary conditions of the pump and the river boundary conditions. The flux across the river boundary conditions (Cauchy boundary condition) divided by the pumping rate of the pump boundary condition determines the percentage of water being drained from the river:

$$\text{Percent from river} = \varpi = \frac{\phi_+ + \phi_-}{Q} \qquad 4.2$$

Where:

ϕ_+ Flux inflowing from river (m^3/day)

ϕ_- Flux out flowing from river (m^3/day)

Q Pumping rate (m^3/day)

Equation 4.2 was applied at every time step. The data was then plotted against time to produce a Percent from river verses time graph. To be able to apply a comparison between each change in variable, the time the model run took to reach 90% was recorded.

4.4.5 Stream Depletion

A rate period between January and August 2010 was chosen to demonstrate the effects that pumping near a river have on the flow of a river with low flow rate. Recent historical data[1] (Information 2011) was chosen as it was assumed that the conditions during low flow will have much variation from the planned experiment.

[1] Data was obtained from http://waterinfo.nsw.gov.au/ from the java application on Real Time data in the Maules Ck@ Avoca East recording station

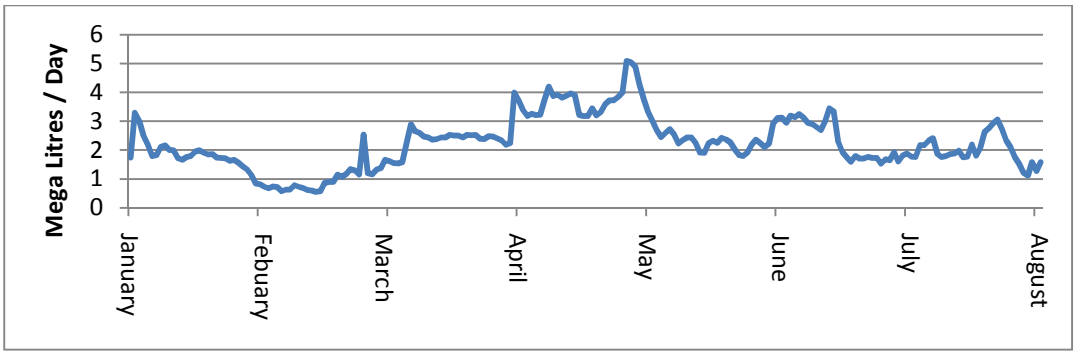

Figure 22: Daily flow rate for between January and August 2010

The Percent Sourced from river was multiplied by the current flow rate to determine the amount of water being taken from the river:

$$\text{Water Taken from River} = \varpi \times \text{flow at stream} \tag{4.3}$$

Then to calculate the flow in the river:

$$\text{Flow in river} = \text{Water Taken from River} - \text{Flow at Stream} \tag{4.4}$$

It was assumed that flow rate in the river was not influenced by any other effects apart from the stream depletion due to pumping.

5 Results

This section contains the results of the implementation of the methodology. All sections apart from Section 0 are structured in such a way that results of each form of comparison as mentioned in Section 4.4 are presented in a graphical from. A summary and brief explanation to the findings of the results is placed in the last subsection, however a full explanation to the results are reserved for the discussion.

5.1 Drawdown verse time data

This section contains the drawdown verses time for Observational Well 4 located on the first slice, approximately 10m from the river as shown in Figure 17. The drawdown verses time graphs for Observational Well 8 have been placed in the Appendix C - Drawdown.

5.1.1 Comparison of Hydraulic Conductivity

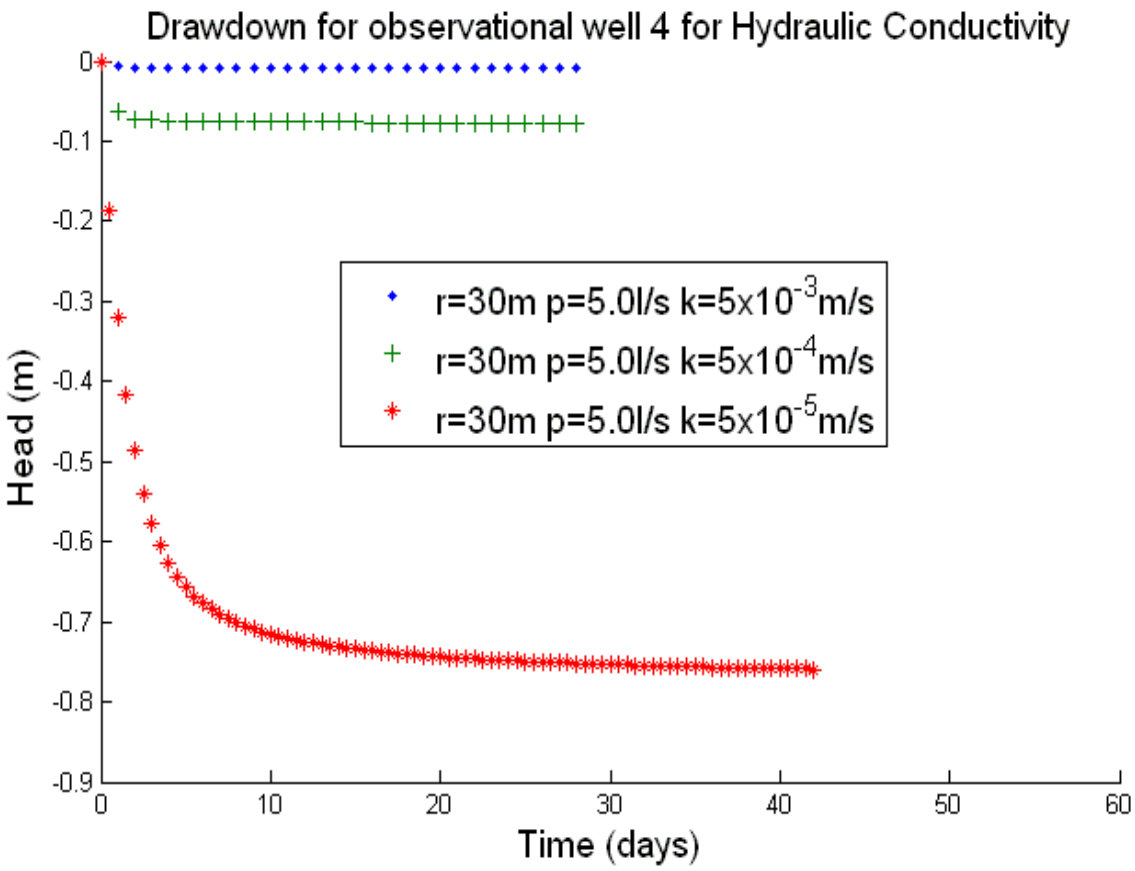

Figure 23: Drawdown verse time – Comparison of Hydraulic Conductivity Observation Well 4

Figure 23 shows the head data at observation wells 4 as detailed in Section 4.4.1. Both observation wells had a large increase drawdown as the hydraulic conductivity decreased. In the unfavourable case ($k = 5x10^{-5}$ m/s) there was a negative vertical hydraulic gradient of 0.01m (Equation 4.1 was used to calculate the vertical hydraulic gradient as shown in **Error! Not a valid bookmark self-reference.**. The vertical hydraulic gradient was ranked in the same manner as in Table 4.

Table 6). It should also be noted that the observational points 4 and 8 are placed less than 10m away from the river; the low hydraulic conductivity has a significant impact on hydraulic head levels. On the other hand, a high hydraulic conductivity ($k = 5x10^{-3}$ m/s) caused less of a vertical hydraulic gradient.

5.1.2 Comparison of Pumping Rate

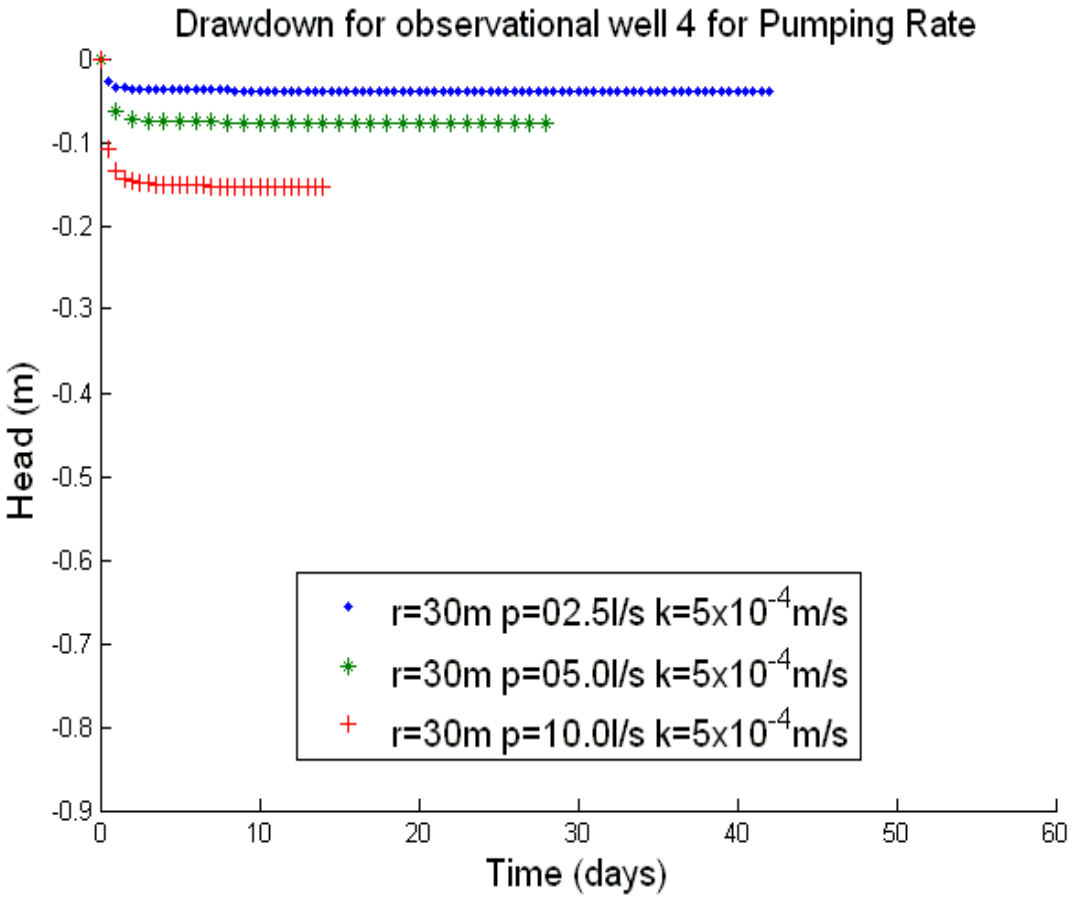

Figure 24: Drawdown verse time - Comparison of pumping rate Observation Well 4

The pumping rate has an impact on cone of depression; a low pumping rate (Q = 2.5 l/s) causes less drawdown than that of a high pumping rate (Q = 10 l/s). This results was expected, pumping at a higher rate in the same conditions will cause the water levels near the river to drop. There was also a slight increase in hydraulic gradient (Equation 4.1 was used to calculate the vertical hydraulic gradient as shown in **Error! Not a valid bookmark self-reference.**. The vertical hydraulic gradient was ranked in the same manner as in Table 4.

Table 6) indicating a widening of the cone of depression.

5.1.3 Comparison of Pumping Location

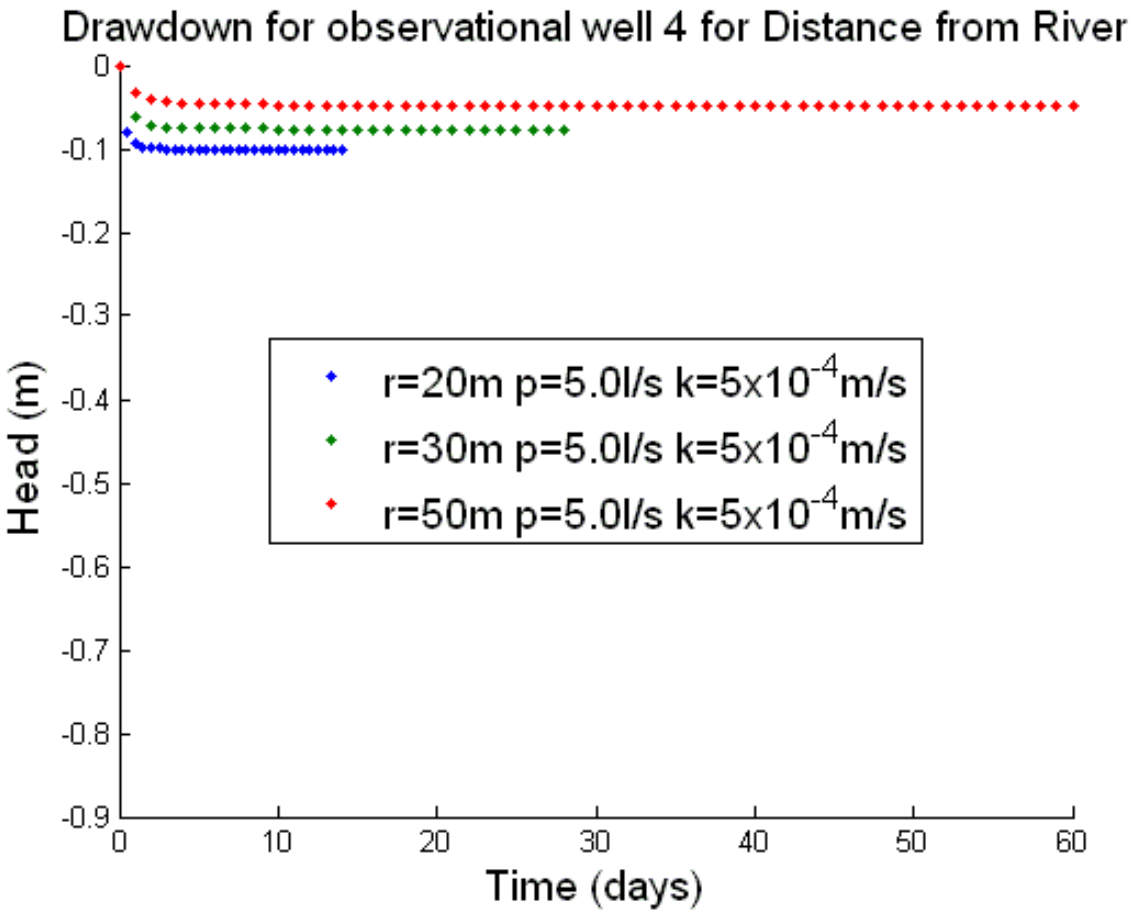

Figure 25: Drawdown verse time - Comparison of pumping location Observation well 4

The closer the bore was placed to the river, the lower the drawdown. As all the other conditions remained the same the geometry of the drawdown cone near the river was essentially stretched. This was also reflected in the hydraulic gradient (Equation 4.1 was used to calculate the vertical hydraulic gradient as shown in **Error! Not a valid bookmark self-reference.**. The vertical hydraulic gradient was ranked in the same manner as in Table 4.

Table 6); the gradient decreased as the distance from the river increased.

5.1.4 Comparison of Clogging Layers

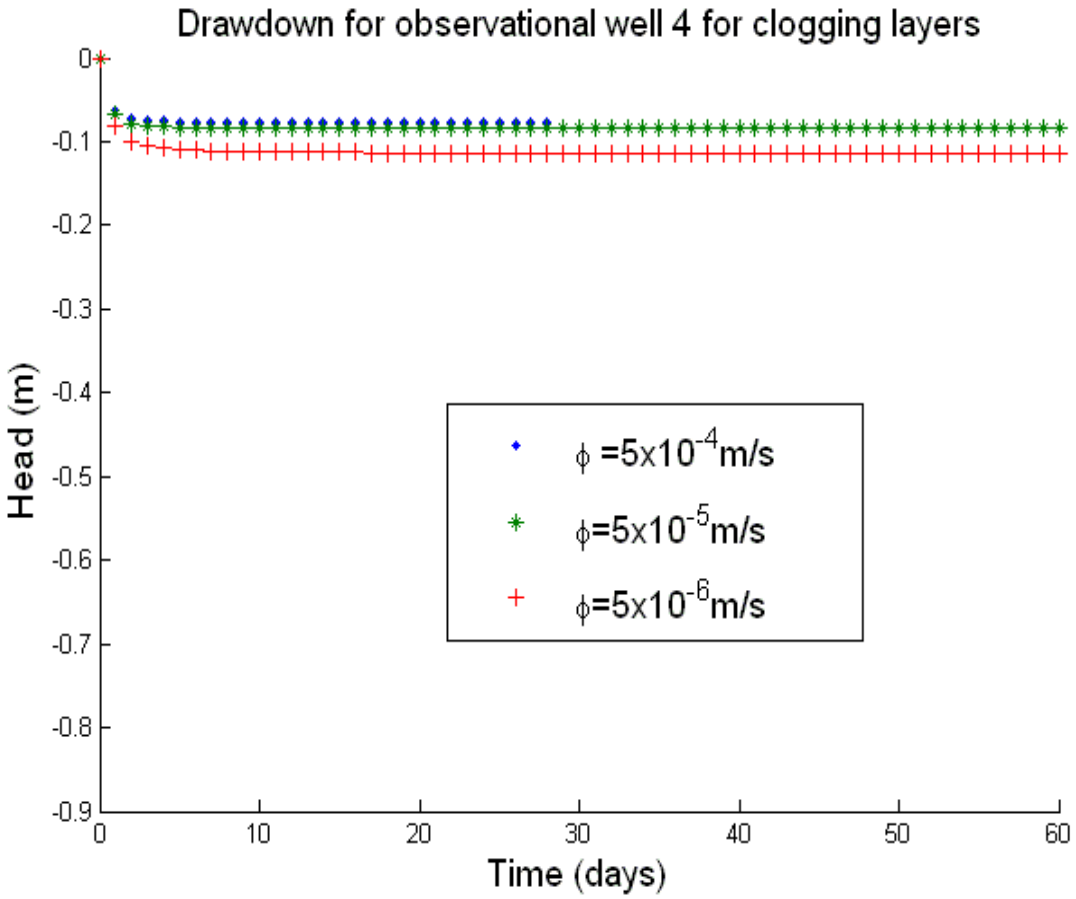

Figure 26: Drawdown verse time - Comparison of clogging layer Observation Well 4

The clogging layers caused a slight increase in drawdown of water levels in the aquifer. Despite the change in magnitudes (from $\phi = 5x10^{-4}$ m/s to $\phi = 5x10^{-6}$ m/s) the water levels did not change significantly.

5.1.5 Comparison of Extreme Cases

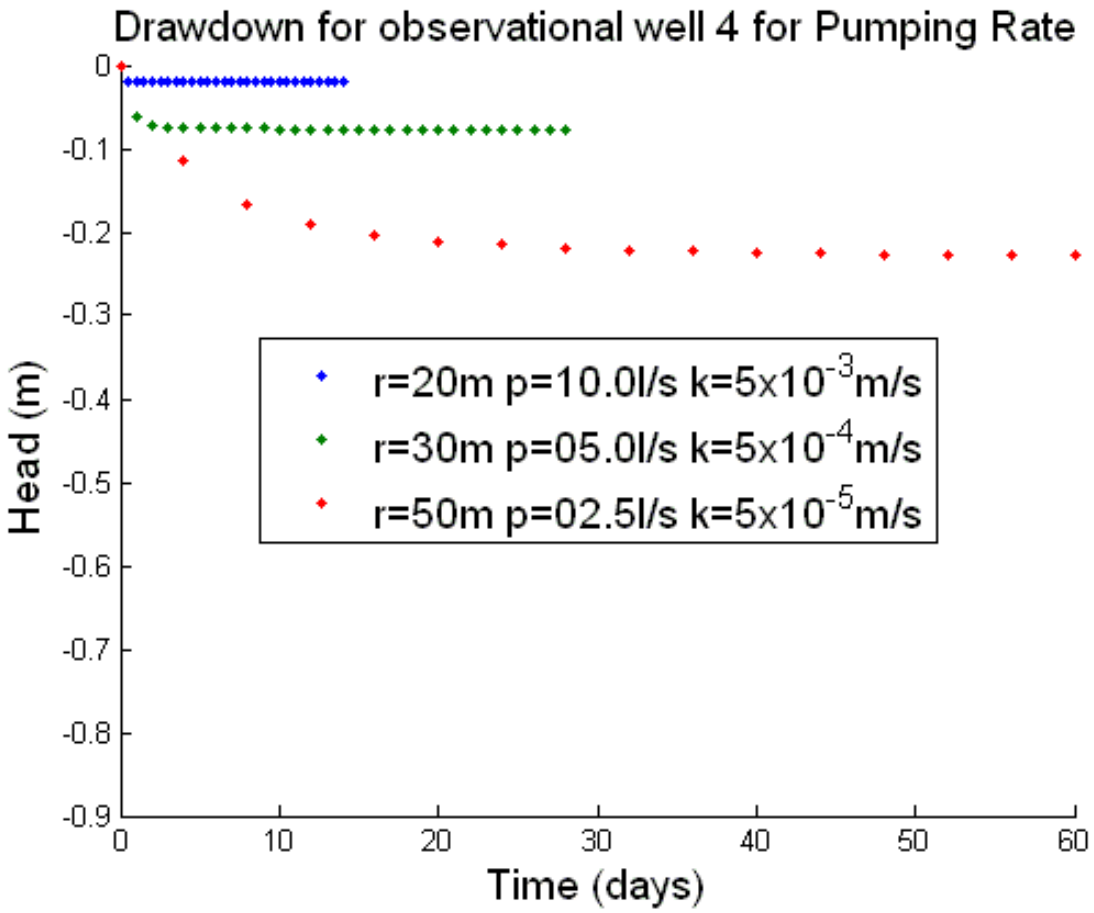

Figure 27: Drawdown verse time - Comparison of pumping location Observation well 4

For the scenario with the favourable parameters, the water levels near the aquifer had very small drawdown of several millimetres. In the case with the unfavourable parameters the drawdown reached more than 0.2m which contained the largest drawdown.

5.1.6 Table of results

Table 4 and Table 5 contains the values of drawdown at 10 days as mentioned in previous sections. A ranking was placed on the difference between the favourable and unfavourable cases for each model scenario (Figure 7), the parameter with the largest variation in the results had the highest rank and the parameter with the lowest rank had the smallest variation in results.

Table 4: Comparison of observation well 4 drawdown values

Parameter Change	Favourable (m)	Base (m)	Unfavourable (m)	Rank
Hydraulic Conductivity	-0.008	-0.077	-0.759	1
Pumping Rate	-0.038	-0.077	-0.153	2
Distance	-0.102	-0.077	-0.048	3
Clogging Layer	-0.077	-0.085	-0.114	4
Extreme	-0.020	-0.077	-0.180	-

The hydraulic conductivity seemed to have a large amount of spread especially in the unfavourable case of k = 5 x 10^{-5} m/s where the drawdown was -0.759m. The inverse situation was also applied for the favourable case of k = 5 x 10^{-3} m/s, where a drawdown of 8mm was recorded. Overall the hydraulic conductivity has the greatest variation from the base case as indicated by the rank. As the range of hydraulic conductivities was spread over several magnitudes, the drawdown would have also contained a large range. The low hydraulic conductivity of k = 5x10^{-5} m/s appears to have forced more water to be sourced from a larger drawdown geometry but this is discussed later in Section 6.1. As the pumping rate increased, so did the drawdown; to compensate for a larger volume of water, the area of water being sourced from the river increased. For the distance from the river, a larger distance from the river caused a smaller drawdown; the volume of water required remained the same so the geometry of the drawdown cone was essentially stretched. As for the clogging layer, the greater the clogging layer the larger the drawdown however as indicated by the rank this drawdown didn't have as large a variation as the other parameters. This was a function of the clogging layer; the lower streambed hydraulic conductivity of the river forced water to be sourced from other areas in the aquifer rather than near the river. Table 5 mirrors similar conclusions to Table 4.

Table 5: Comparison of observation well 8 drawdown values

Parameter Change	Favourable (m)	Base (m)	Unfavourable (m)	Rank
Hydraulic Conductivity	-0.008	-0.083	-0.832	1
Pumping Rate	-0.041	-0.083	-0.165	2
Distance	-0.126	-0.083	-0.051	3
Clogging Layer	-0.083	-0.090	-0.118	4
Extreme	-0.025	-0.083	-0.250	-

Equation 4.1 was used to calculate the vertical hydraulic gradient as shown in **Error! Not a valid bookmark self-reference.**. The vertical hydraulic gradient was ranked in the same manner as in Table 4.

Table 6: Comparison of hydraulic Gradient between Slice 1 and Slice 3

Vertical Gradient	Favourable	Base	Unfavourable	rank
Hydraulic Conductivity	5.85E-05	5.92E-04	7.34E-03	1
Pumping Rate	2.96E-04	5.92E-04	1.20E-03	3
Distance	2.43E-03	5.92E-04	2.43E-04	2
Clogging Layer	5.92E-04	5.10E-04	3.88E-04	4
Extreme	4.89E-04	5.92E-04	1.47E-03	-

The vertical hydraulic gradient mirrored similar results to Table 4 and Table 5. The vertical hydraulic gradient was steeper for the hydraulic conductivity; this makes the pressure difference between the slices greater. The pumping rate and distance had different conclusions to Table 4. This can be explained by the drawdown cone being exaggerated over a longer distance, causing the pressure difference between the slices to be greater. As for the clogging layer, there was little difference in the pressure.

5.2 Drawdown Cone Visualisation

Drawdown data from each node on the slice of interest was exported and plotted in two and three dimensional plots. For the two dimensional plots, the head data was plotted against the

x-axis and y-axis. It should be noted that all images depicted in the next sections are off the base case scenario as stated in Section 4.3 and the data was all taken at the last time step of the model run (40 days).

5.2.1 Y-axis slice

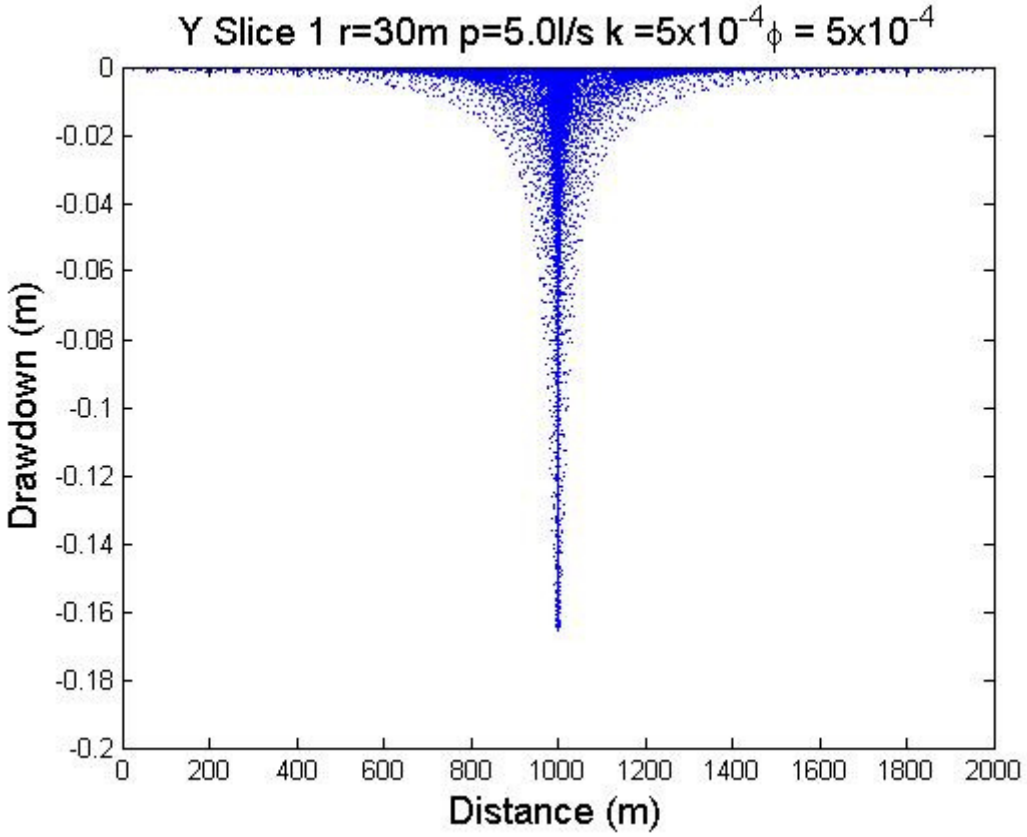

Figure 28: Drawdown cone for the Y-axis for the Base Case

The base case of the drawdown cone in the Y-axis was shown (Figure 9) as there was little variation in the geometry apart from the depth of the drawdown. The density of the drawdown cone as indicated by the lack of white space in the cone is focused mainly around the top and bottom of the pumping bore. The density is also focused on either side of the drawdown cone forming a distorted v shape as indicated by Figure 68 in Appendix C. Also as the conditions in the Y-axis had no variation there was a symmetric distribution relative to this axis.

5.2.2 X-axis slice

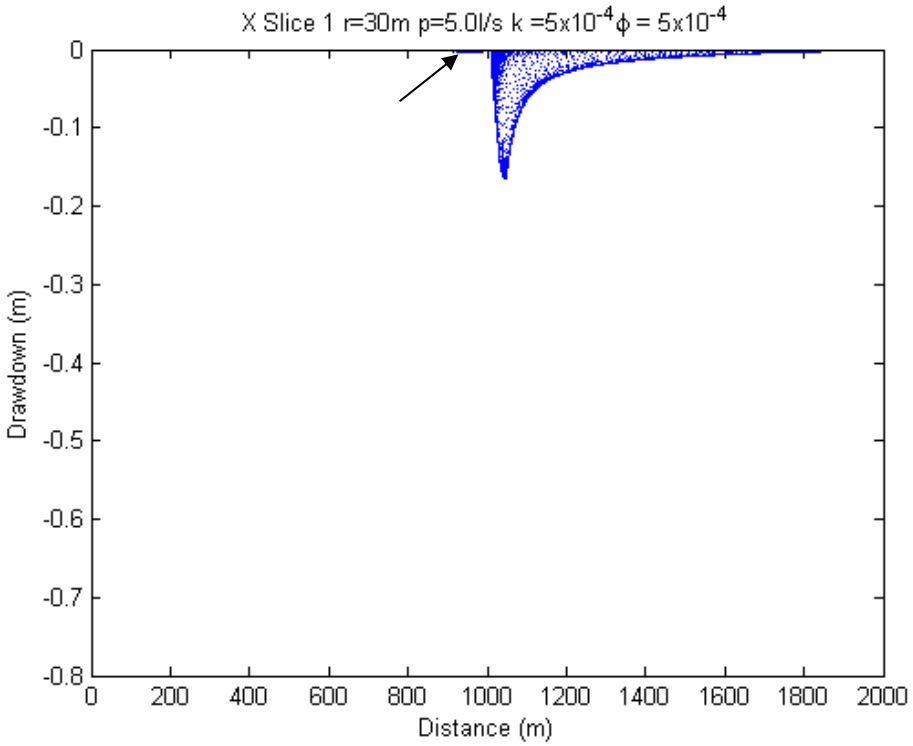

Figure 29: Base Case – Drawdown cone for the X axis, first slice

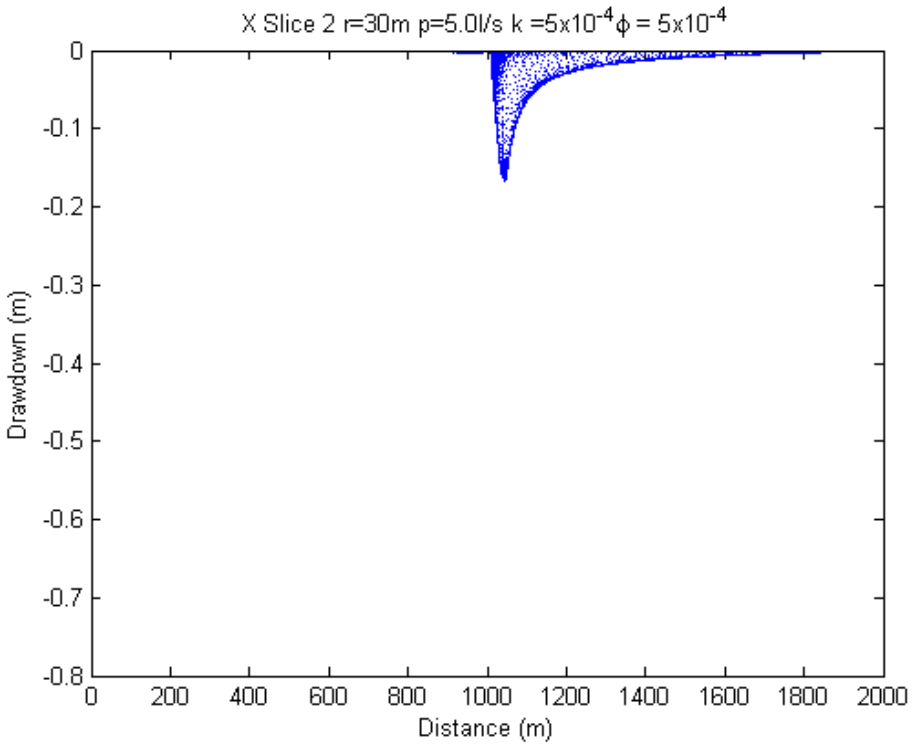

Figure 30: Base Case – Drawdown cone for the X axis, second slice

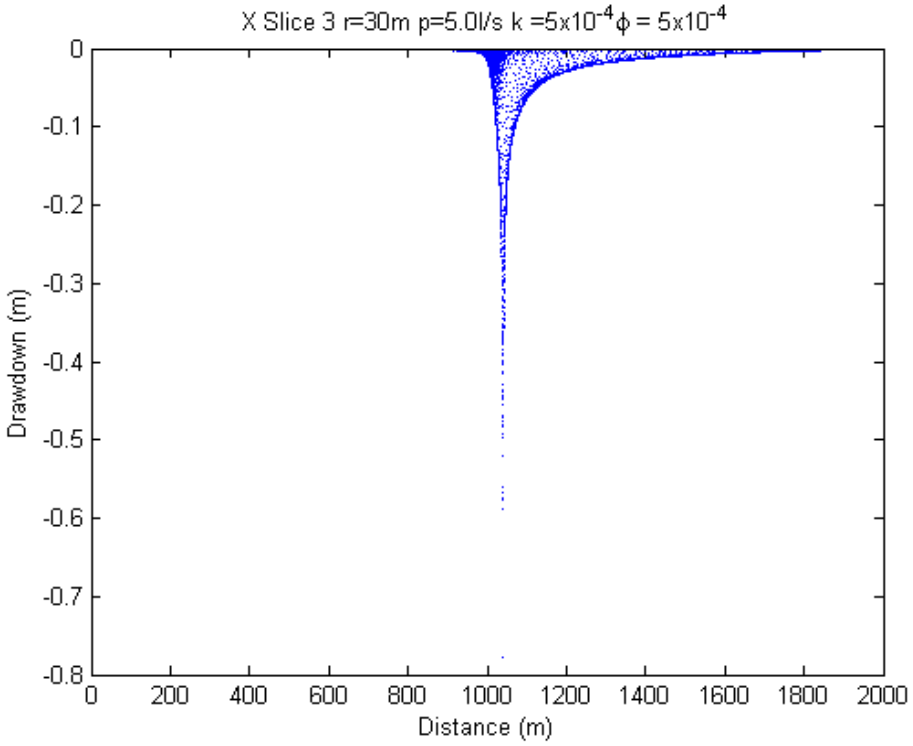

Figure 31: Base Case – Drawdown cone for the X axis, third slice

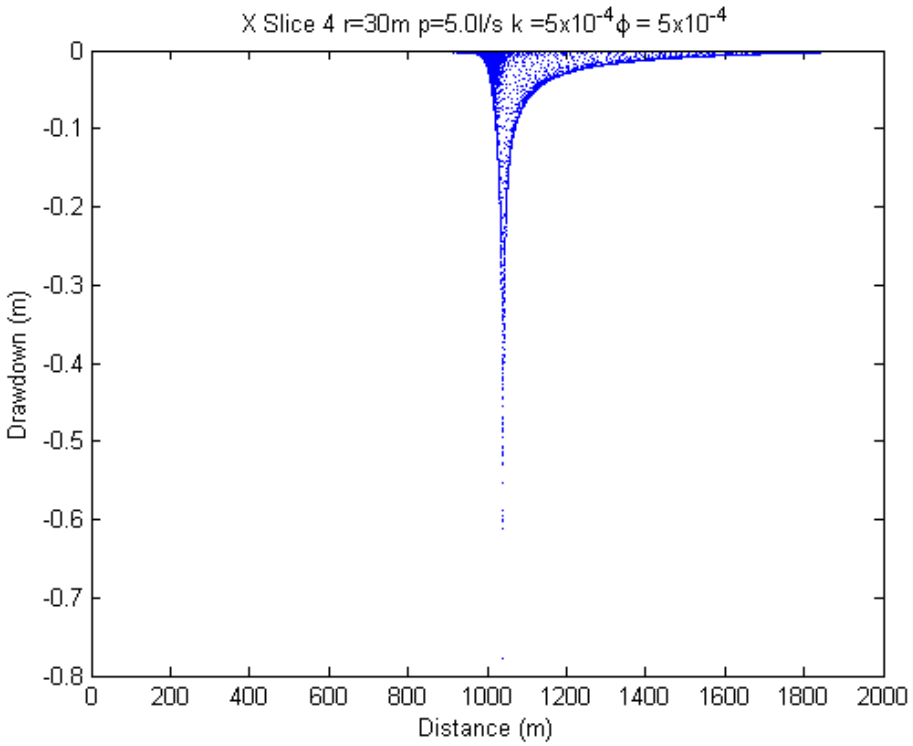

Figure 32: Base Case – Drawdown cone for the X axis, fourth slice

The drawdown cone for each slice was plotted because the screen length of the pumping bore was installed at a depth of 10m, causing a pressure difference that varied between each slice of the model domain. The drawdown cone in the X-axis had a non-symmetric distribution for two reasons; firstly the river boundary conditions limited the drawdown cone restricting it to remain on the pumping side of the river and secondly, the placement of the borehole was on one side of the river. As a result, the normally expected circular distribution of the drawdown cone deformed along the edge of the river. The density of the cone was focused directly beneath the river and towards the edge of the cone. Another feature of interest was the appearance of water being sourced from the opposite side of the river as indicated by the arrow in Figure 29. This is described in more detail in Section 5.2.5.

5.2.3 Contour view

Figure 33 shows the contour graph of the drawdown cone for the first slice. As mentioned in the previous section, the drawdown cone in the X-axis is non-symmetric and resulted in an oval shaped contour.

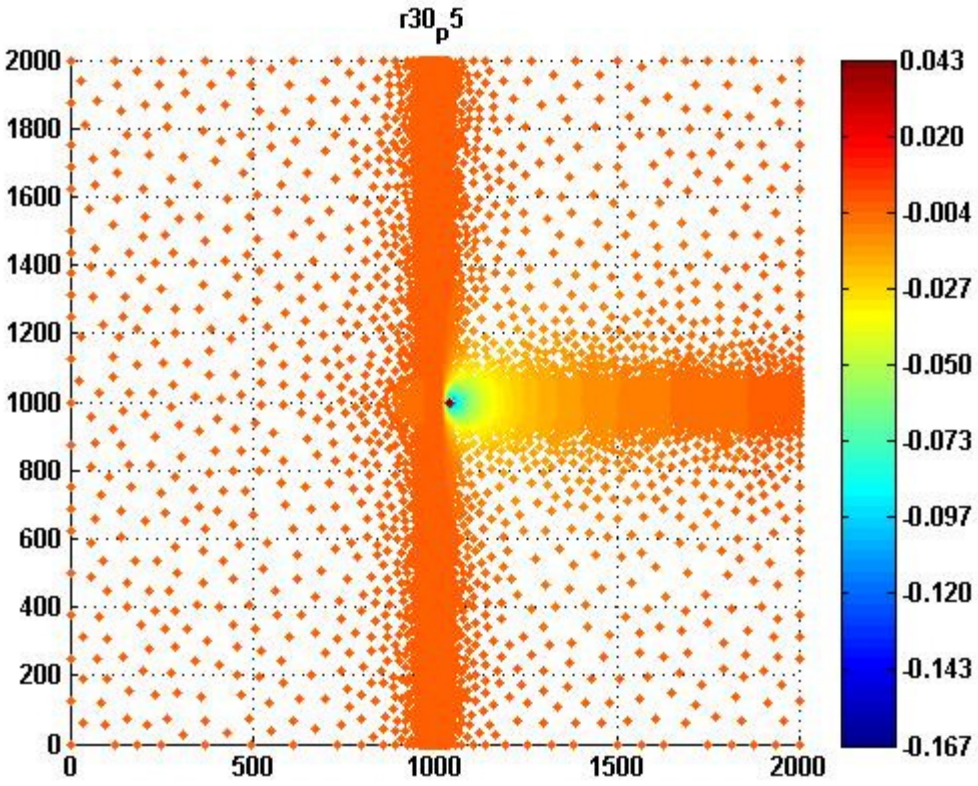

Figure 33: Base Case – Contoured map of drawdown. All units are in meters.

5.2.4 3d view

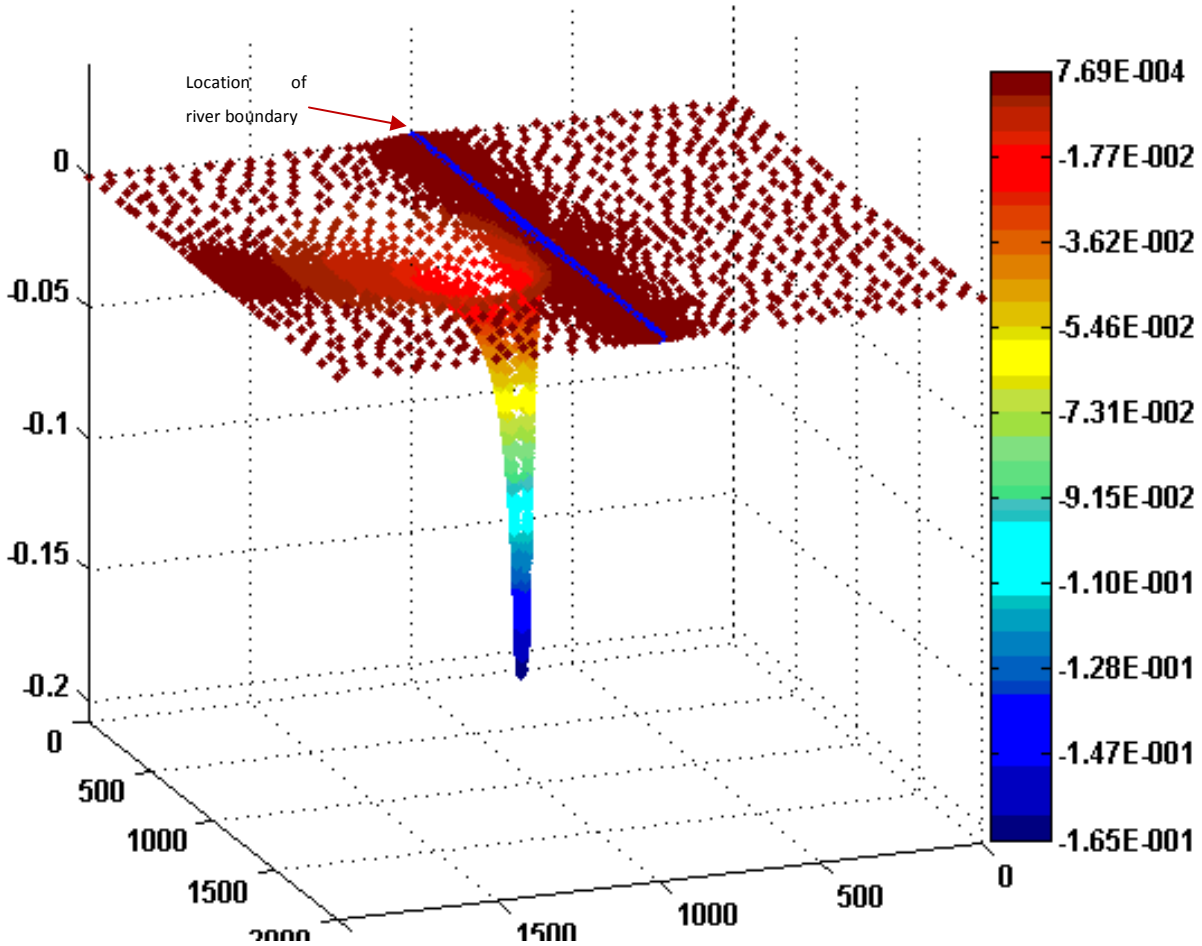

Figure 34: Three Dimensional View of the drawdown cone. All units are in meters.

Figure 34 shows a three dimensional view of the drawdown cone with coloured contours. A blue line has been placed to represent the location of the river. This is a combined implementation of the previous sections; the drawdown cone can be viewed in different angles.

5.2.5 Clogging Layer X-axis slice

Figure 35 shows the combination of the three cases of the clogging layer. Separate drawdown cones of individual clogging layers are given in Appendix C in Figure 69 to Figure 71. The clogging layers enlarge the drawdown cone, and cause water to become sourced from the opposite side of the river. As the clogging layers are increased, a more symmetric distribution appears to have formed. This indicates a violation of the assumptions as the river boundary condition was ignored.

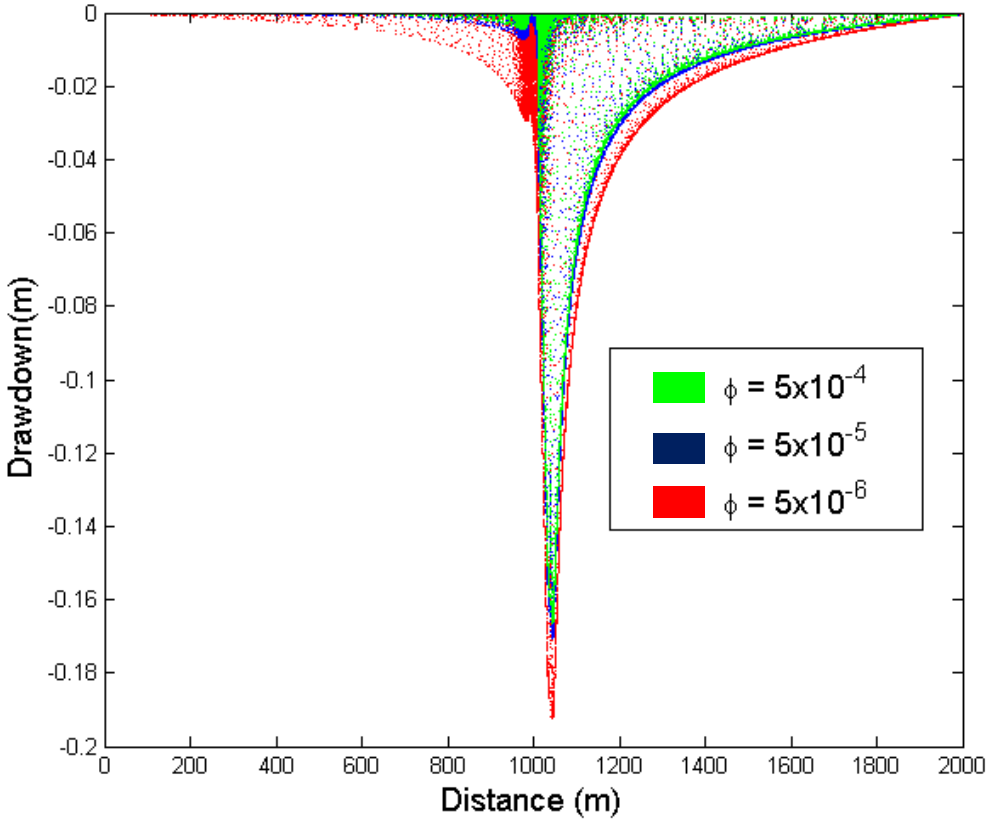

Figure 35: Combination of all three clogging layers

Figure 36 and Figure 37 provide a different perspective of Figure 35 for the worst case clogging layer (ϕ=5x10^{-6} m/s). Figure 37 shows the head values underneath the river boundary conditions. This implies that the boundary river condition has been inappropriately applied for a clogging layer of this large a magnitude.

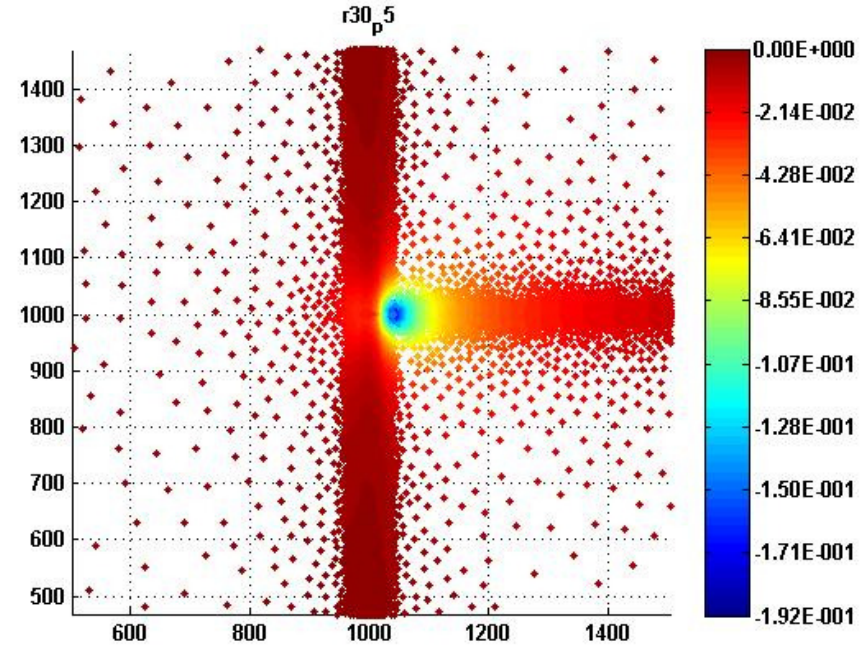

Figure 36: Contour View of $\phi = 5x10^{-6}$ m/s

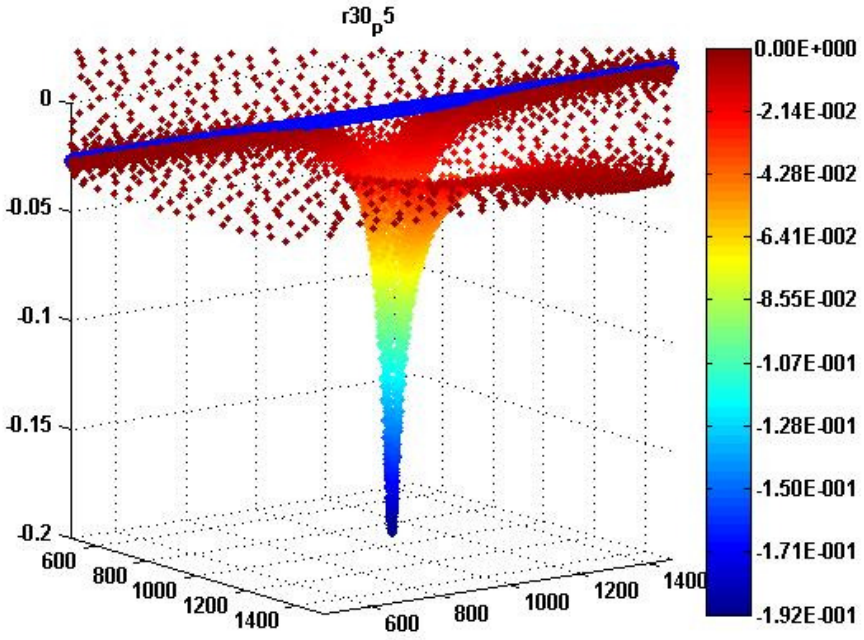

Figure 37: 3d view of $\phi = 5x10^{-6}$ m/s

5.3 Forward Particle Tracer

5.3.1 Comparison of Hydraulic Conductivity

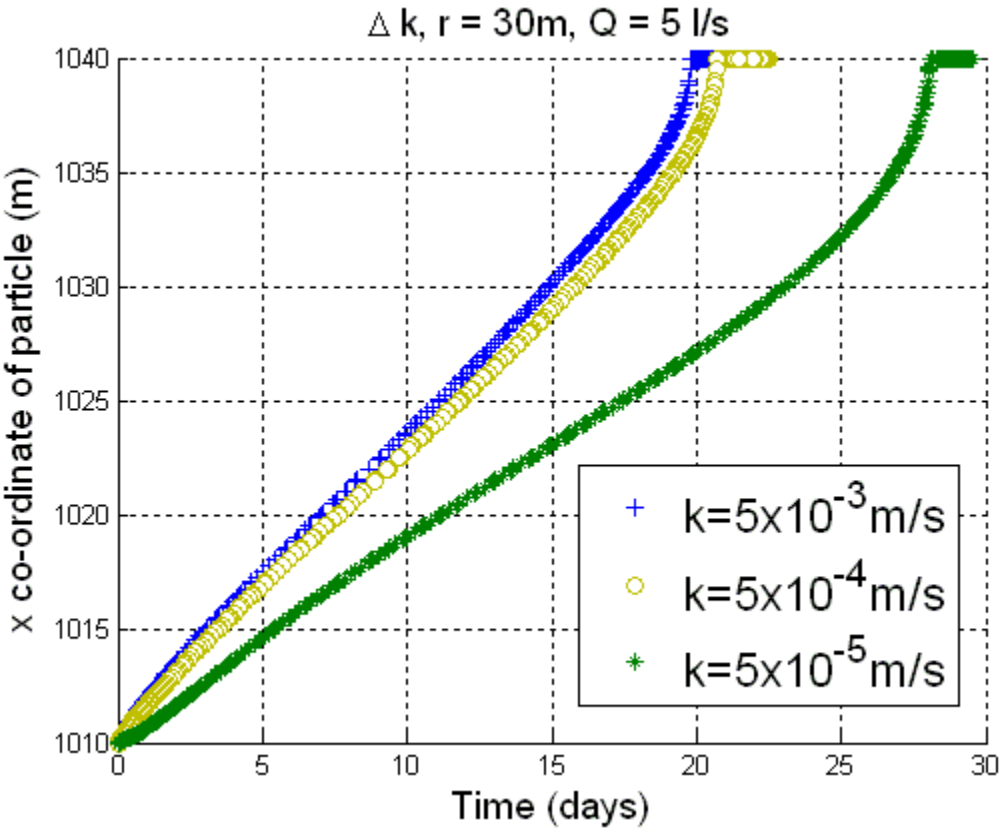

Figure 38: Backwards Particle Tracing - Change in Hydraulic Conductivity

As the hydraulic conductivity decreased, the time for the particle to reach the pumping bore increased. There seemed to be a disproportionate amount of variation, as the favourable case ($k = 5 \times 10^{-3}$ m/s) and base case had similar termination times. However another decrease in magnitude of hydraulic conductivity ($k = 5 \times 10^{-5}$ m/s) greatly lengthened the time by over a week.

5.3.2 Comparison of Pumping Rate

As the pumping rate increased, the time taken to reach the pumping bore decreased. The results indicated a linear proportionality to the pumping rate.

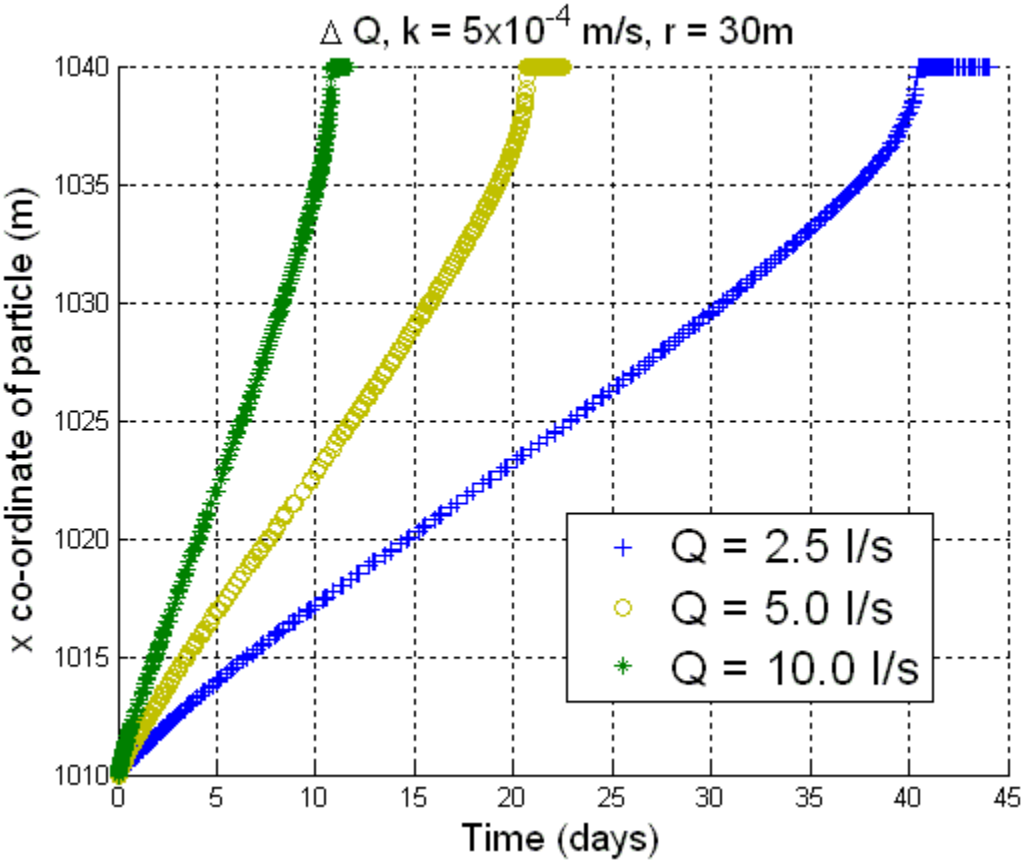

Figure 39: Backwards Particle Tracing - Comparison of Pumping Rate

5.3.3 Comparison of Pumping Location

The variation of pumping location in the sensitivity analysis had an effect on the time taken for the particle to terminate, as shown in Figure 40. The longer the distance the further it took the particle to travel. This result gives a time frame on what could be expected if the distances are varied.

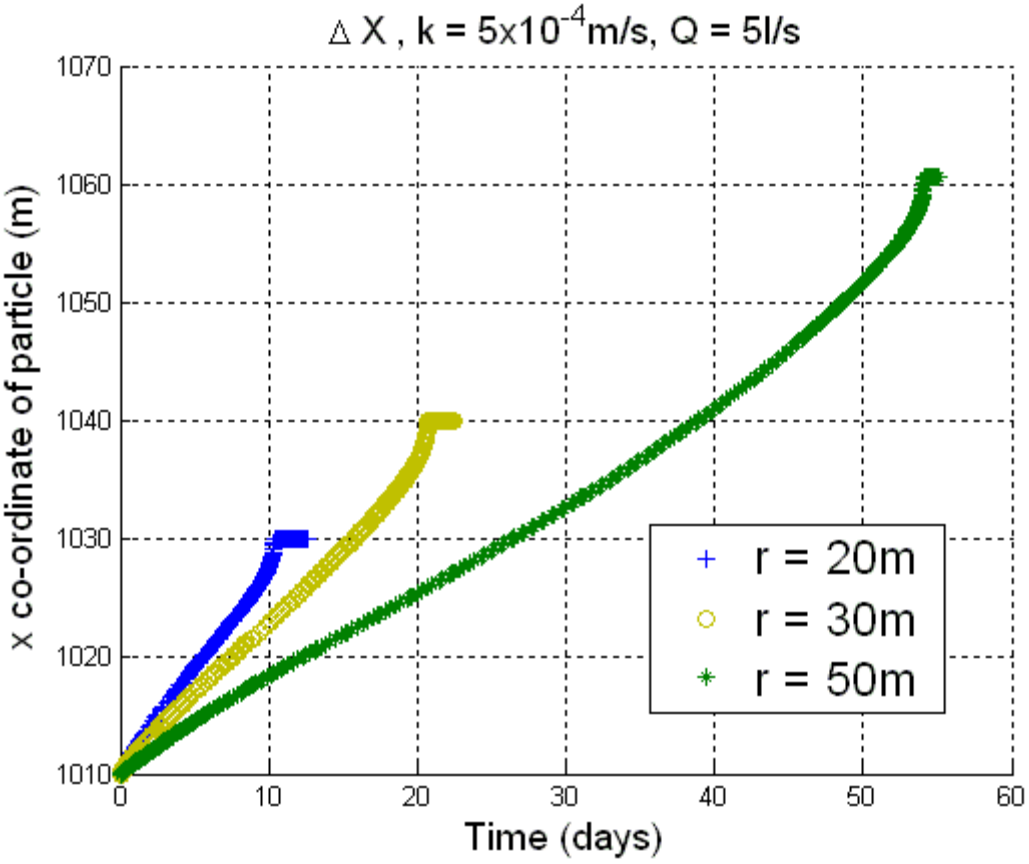

Figure 40: Backwards Particle Tracing - Comparison of pumping location

5.3.4 Comparison of Clogging Layer

Figure 41 is a comparison of the extreme cases for backwards particle tracing. This graph has a similar distribution to Figure 38. The geometry of the path remained the same as the magnitude of the clogging layer decreased, appearing to shift in correspondence to the change in the clogging layer.

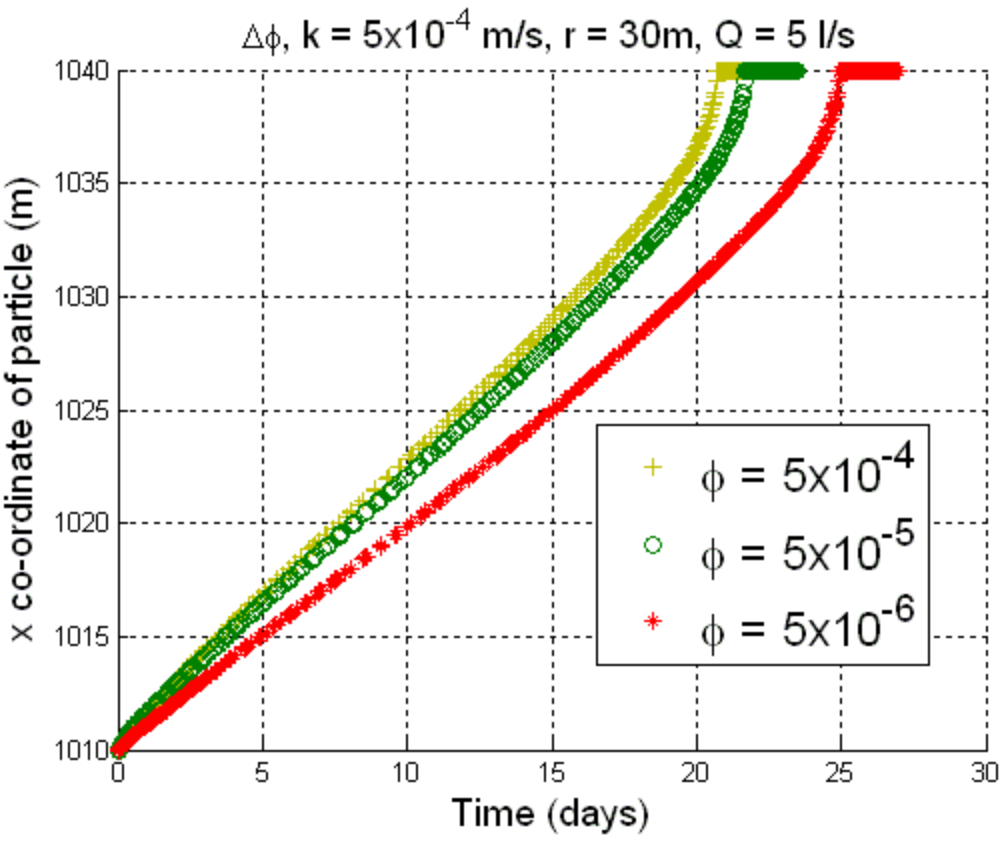

Figure 41: Backwards Particle Tracing - Comparison of clogging layers

5.3.5 Comparison of Extreme Cases

The extreme cases for backwards particle tracing are shown in Figure 42. There is a large spread in the graphs between cases ranging from less than 10 days to more than 120 days. In the worst case scenario there seems to be large scattering of distance data. This could indicate that the rate of change of the particle (velocity) rapidly increased between 50 and 80 days.

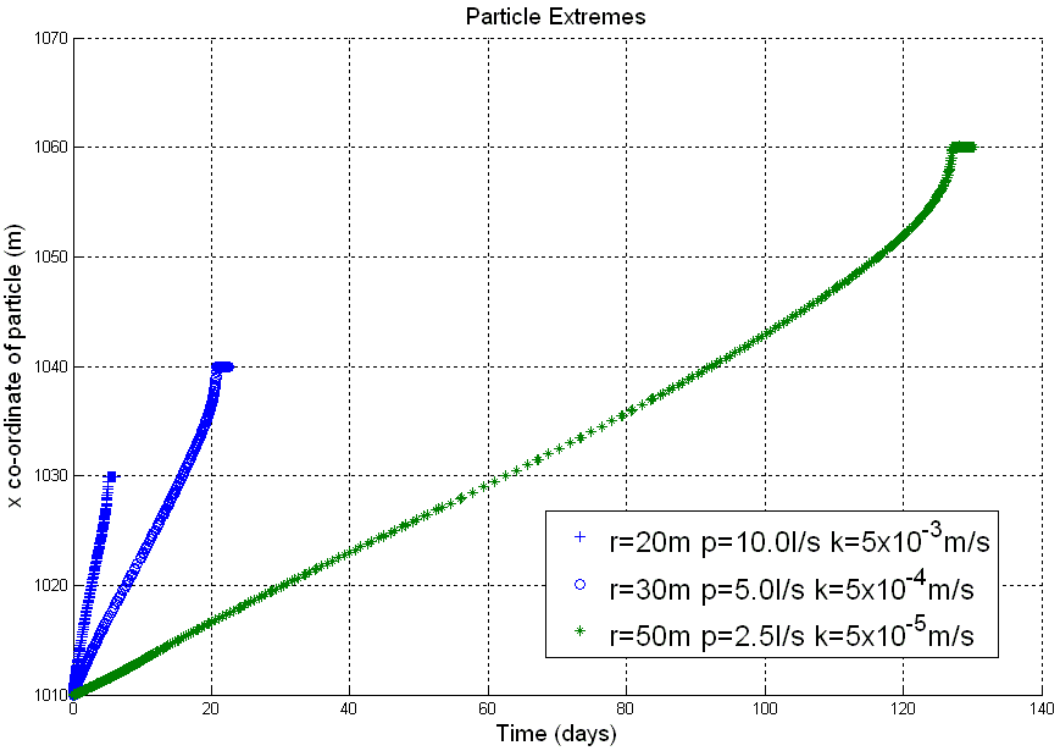

Figure 42: Backwards Particle Tracing - Comparison of extreme cases

5.3.6 Table of results

Table 7 contains values of the terminating particles as shown in the previous sections. The difference in days between favourable and unfavourable cases was ranked for each model scenario (Figure 7). The parameter with the largest variation in the results had the highest rank and the parameter with the lowest rank had the smallest variation in results. The rank indicates which parameter is most likely to influence the drawdown in a field experiment configured in a similar manner to the model domain.

Table 7: Backwards Particle Tracing – Tabulated summary of results

Parameter Change	Favourable (days)	Base (days)	Unfavourable (days)	Rank
Hydraulic Conductivity	19	21	27	3
Pumping Rate	11	21	41	2
Distance	11	21	55	1
Clogging Layer	21	21	25	4
Extreme	5	21	127	-

Table 7 indicates the time that each particle took to reach the pumping bore. This can give an indication of the velocity of the particle, as in most forms of comparison the distance that the pumping bore was placed from the river remained constant. In this form of comparison the hydraulic conductivity had little variation from the base case compared to the other parameters as indicated by the rank. This is in contrast to the drawdown near the river where the hydraulic conductivity had more variation providing further evidence that the hydraulic conductivity affects the geometry of the drawdown cone causing water to be sourced elsewhere in the aquifer. The distance has the largest variation according to the rank. This is attributed to the fact that the pumping rate did not change causing the particle to travel the same speed for a difference distance; the effects of time and distance are directly related and have more correlation than the hydraulic conductivity and clogging layer. The same remains true for the pumping rate; a larger pumping rate for the same distance will directly increase the velocity of the particle.

5.4 Plume Evolution

5.4.1 Comparison of Hydraulic Conductivity

Figure 43 shows the effect of hydraulic conductivity on the water being drawn from the top of the river. The higher the hydraulic conductivity the shorter the time of impact but taking into consideration the magnitudes of the hydraulic conductivities, the range of the time of impact was small. The bandwidth increased as the hydraulic conductivity decreased but for the lowest hydraulic conductivity, the contour lines of the plume became coarser because; the particles were harder to interpolate since they were located closer to each other.

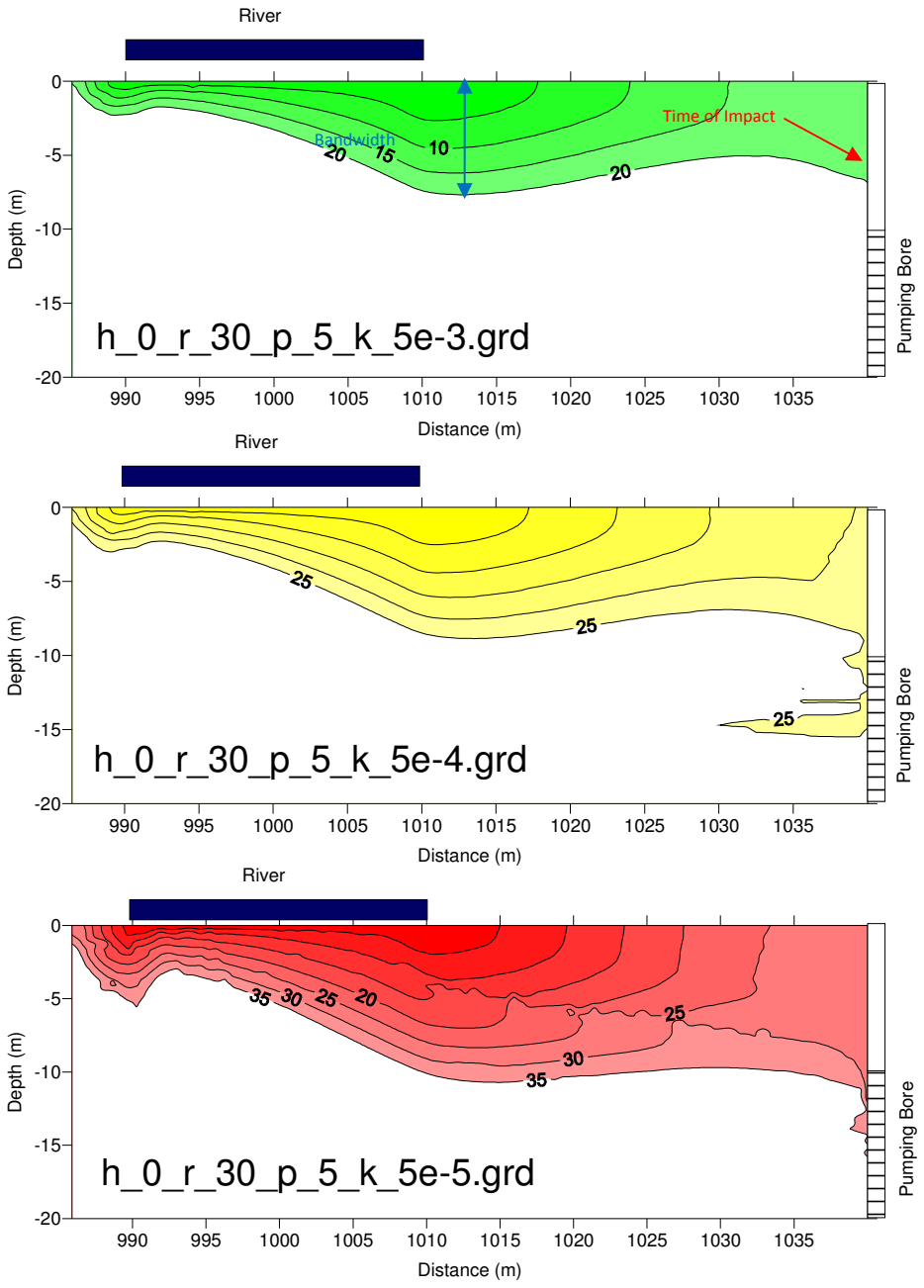

Figure 43: Plume Evolution - Comparison of Hydraulic Conductivity

5.4.2 Comparison of Pumping Rate

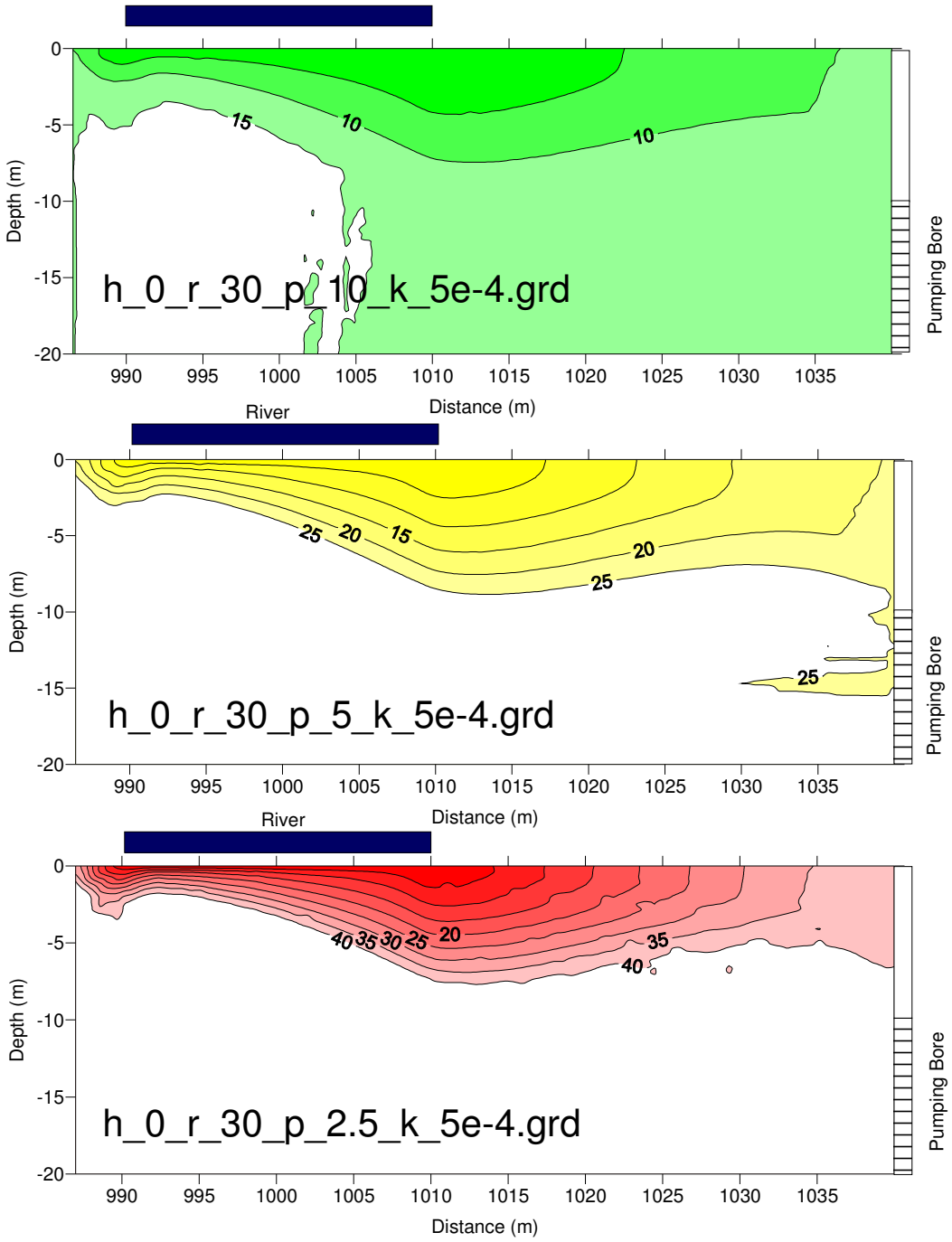

Figure 44: Plume Evolution - Comparison of Pumping Rate

Figure 44 shows that the rate of pumping influenced the time of impact when the water from the river reached the pumping bore. The rate of pumping however did not have much impact

on the bandwidth. This suggests that the direction of the path lines across the river is similar but travel much faster according to the rate of pumping.

5.4.3 Comparison of Pumping Location

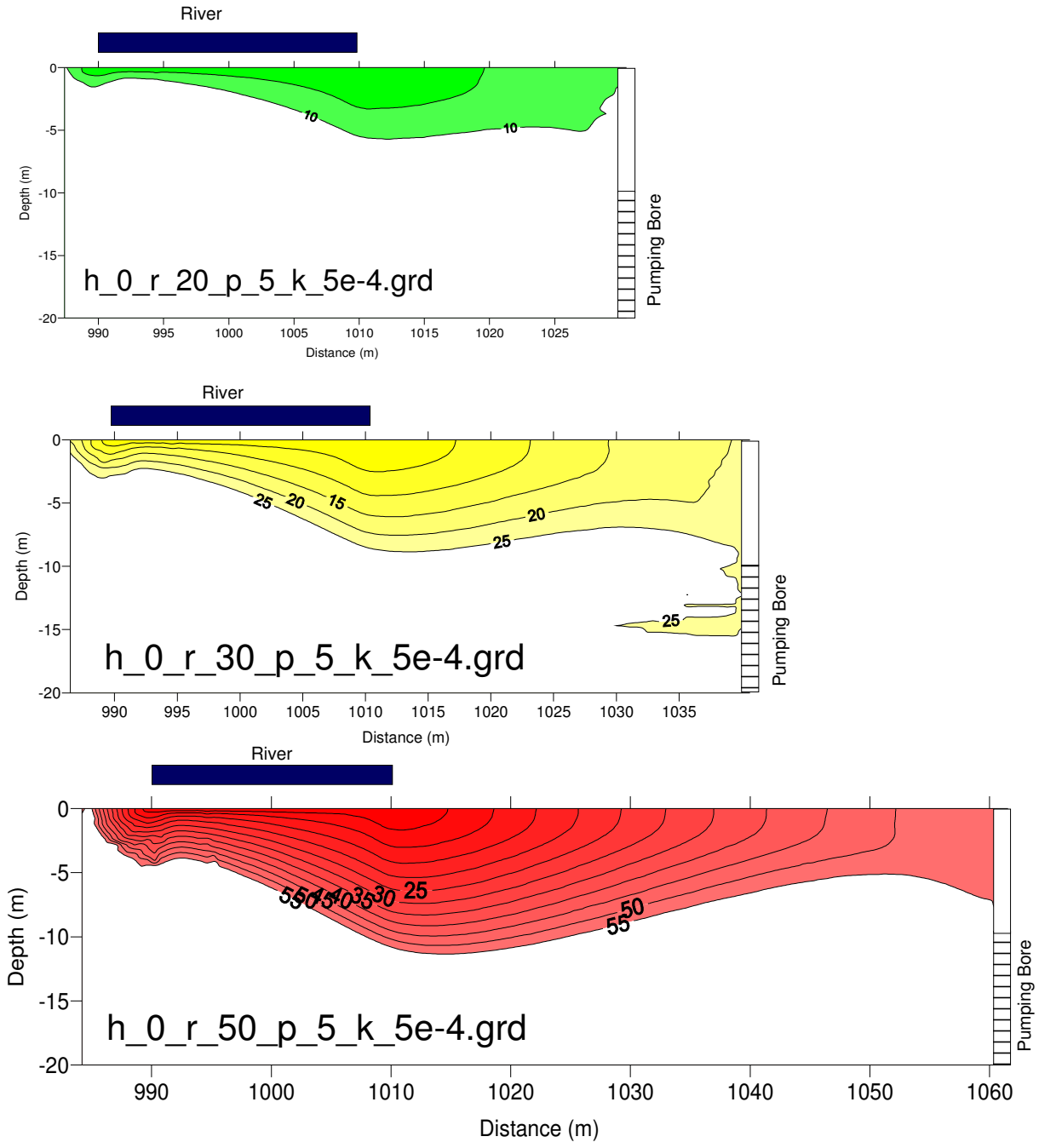

Figure 45: Plume Evolution - Comparison of Pumping Distance

Figure 45 shows that time of impact increases as distance increases, this shows the water from the river taking longer to reach the pumping bore when placed further away. The bandwidth of the plume also increases as the distance increases, allowing for more spread of the plume with distance. Consequently more water from the river will spread in the aquifer.

5.4.4 Comparison of Clogging Layer

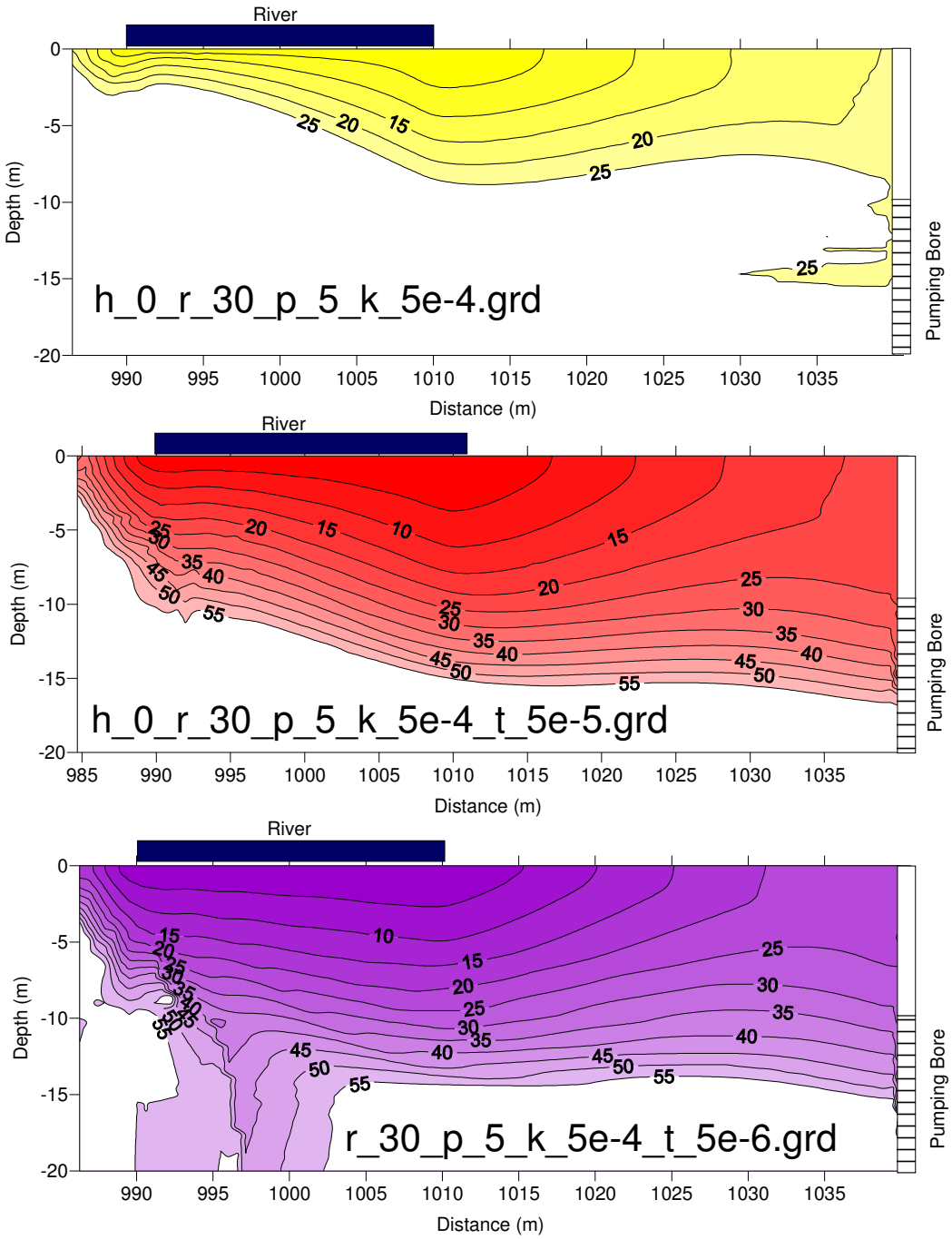

Figure 46: Plume Evolution - Comparison of clogging layers

Figure 46 shows the effects on clogging layers on the plume. It is clear that the clogging layers had an impact of the flow of the water in the aquifer. The water being sourced in the river

further away from the pumping bore was slowed down by the lower conductivity in the aquifer, while the water closer to the pumping bore was affected less.

5.4.5 Comparison of Extreme Cases

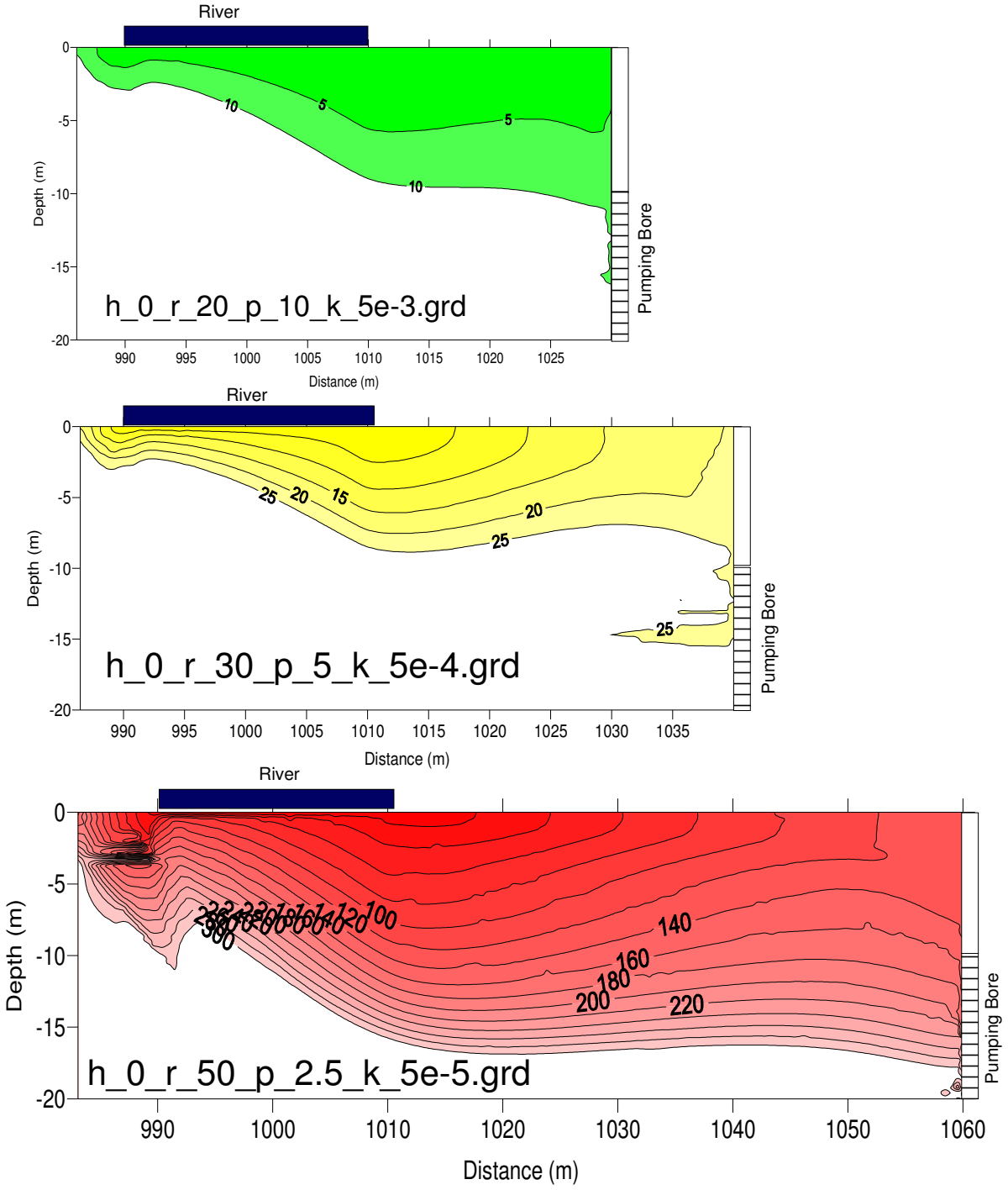

Figure 47: Plume Evolution - Comparison of extreme events

Figure 47 shows the change in the plume from the most favourable case to the least favourable case. The time of impact and bandwidth both increase as the case becomes less favourable. In the worst case scenario there appeared to be an issue with water being sourced from beyond the river as the contour lines seem much undefined. Refer to Appendix C Figure 73.

5.4.6 Table of results

Table 8 and Table 9 contain values of the time of impact and bandwidth as pictured in the previous sections. A rank was placed based on the difference in days between the favourable and unfavourable cases for each mode scenario (Figure 7). The parameter with the largest variation in the results had the highest rank and vice versa. The rank indicates which parameter is most likely to influence the drawdown for a field experiment configured in a similar manner to the model domain.

Table 8: Plume Evolution - Time of impact table

Parameter Change	Favorable (days)	Base (days)	Unfavorable (days)	Rank (days)
Conductivity	20	25	30	3
Pumping Rate	12	25	40	2
Distance	10	25	60	1
Clogging Layer	25	25	25	4
Extreme	6	25	140	-

Table 8 indicates that the greatest influence on the time of impact was the distance the pumping bore is positioned from the river followed by pumping rate, conductivity, and finally clogging layer. The clogging layer appears to have little effect on the time evolution of the plume, as water was being sourced for the pump from other areas in the aquifer.

Table 9: Plume Evolution - Table of Bandwidth values

Parameter Change	Favorable (m)	Base (m)	Unfavorable (m)	Rank (days)
Conductivity	8	9	10	2
Pumping Rate	8	9	7	3
Distance	6	9	11	1
Clogging Layer	9	9	9	4
Extreme	11	9	11	-

Table 9 indicates that the greatest influence on the Bandwidth of the plume was distance followed by conductivity and clogging layer. The favourable and unfavourable case for the pumping rated was lower than the base case.

5.5 Percent Sourced from River

5.5.1 Comparison of Hydraulic Conductivity

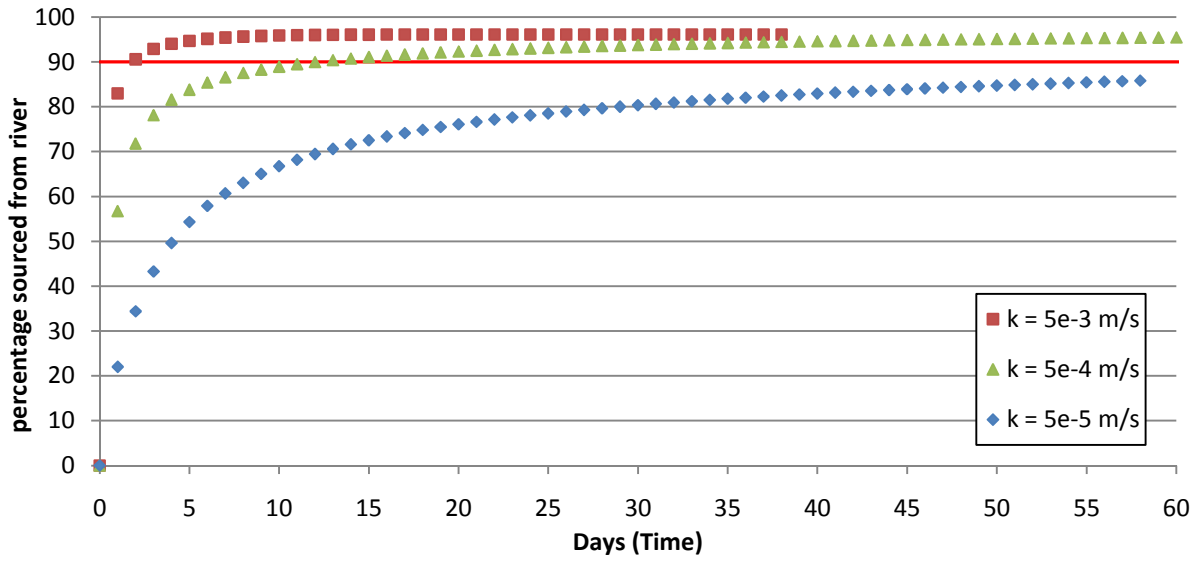

Figure 48: Precent sourced from river - Comparison of Hydraulic Conductivity

The hydraulic conductivity had a large influence on the time the pump took to source water 90% of the water from the river; the higher the hydraulic conductivity the shorter the time. For the unfavourable case (k = $5x10^{-5}$ m/s) the time taken to reach 90% was estimated as insignificant time was allocated to this case.

5.5.2 Comparison of Pumping Rate

The pumping rate did not appear to have any impact on the water being sourced from the river. As the results were normalised (amount of water being sourced from the river/ the pumping rate), the graph would indicate that the amount being sourced from the river is directly proportional to the amount being pumped from the river.

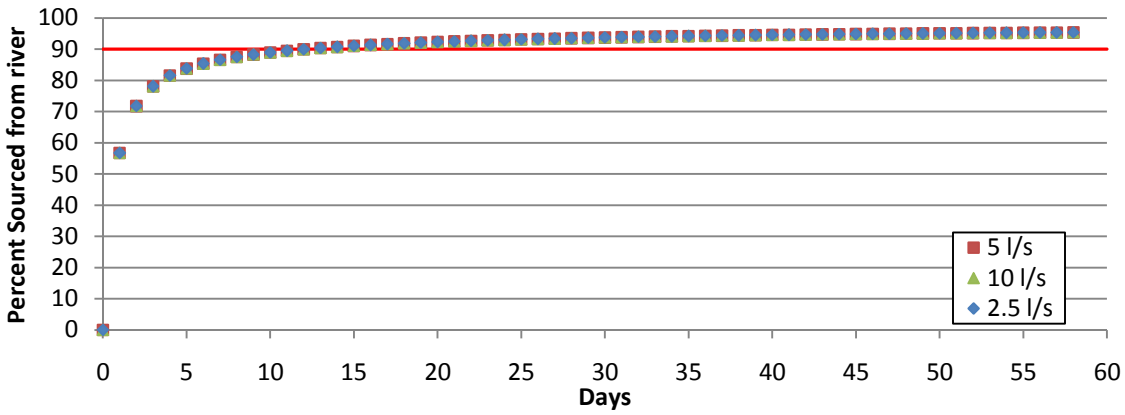

Figure 49: Precent Sourced from River - Comparison in Pumping Rates

5.5.3 Comparison of Pumping Location

The further the distance of the pump from the river, the longer it took for the pump to source 90% of water from the river. At 50 m from the river, the rate at which 90% was reached was slower compared to all cases.

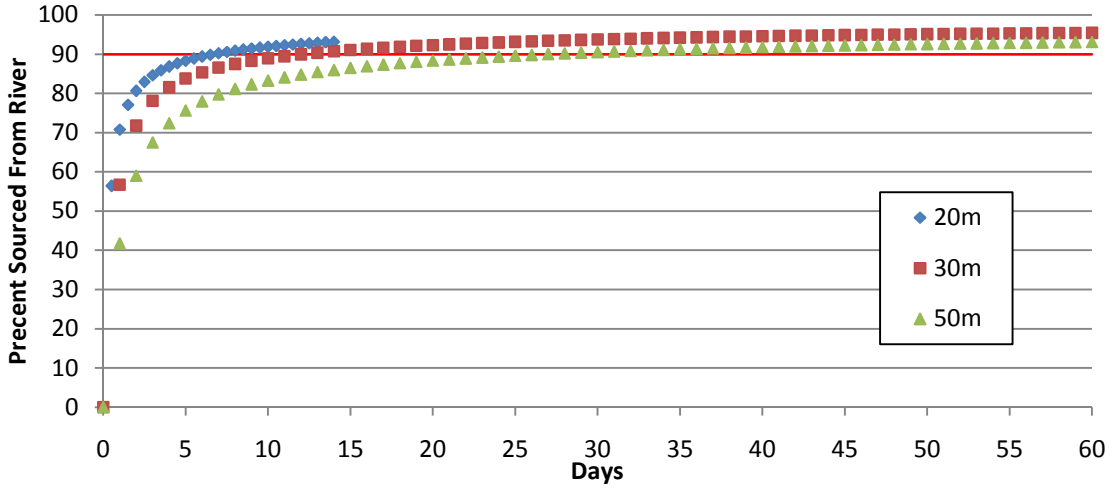

Figure 50: Precent Sourced from River - Comparison of pumping location

5.5.4 Comparison of Clogging Layers

The clogging layer with one magnitude lower than the hydraulic conductivity (ϕ = 5x10^{-5} m/s) has little impact on the time taken to pump 90% of the water from the river. However in the case where the clogging layer was two magnitudes lower (ϕ = 5x10^{-6} m/s), there was a significant difference in the time taken to source 90% of the water.

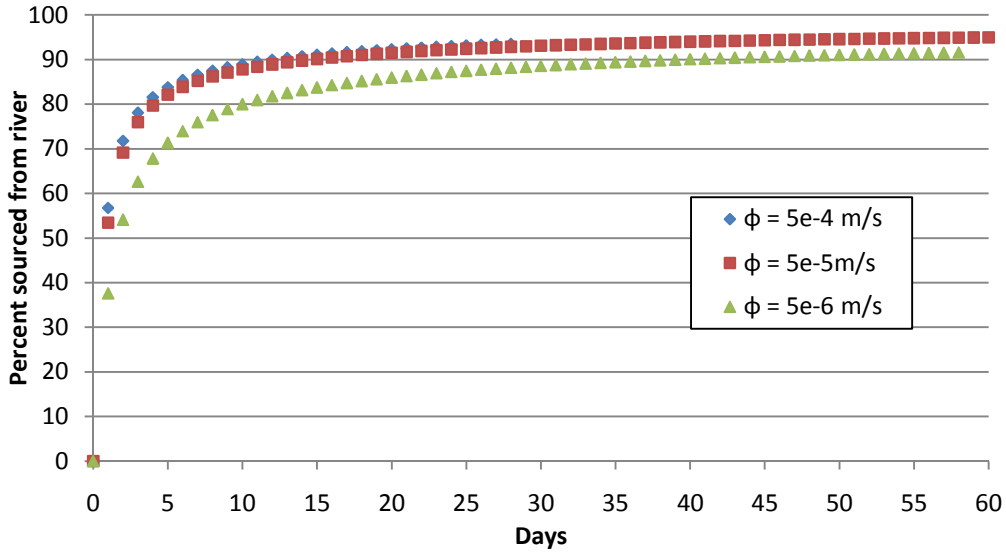

Figure 51: Percentage Sourced from river - Comparison of Clogging Layers

5.5.5 Comparison of Extreme Cases

The best and worst case scenario has provided a good upper and lower range of expectations for each parameter.

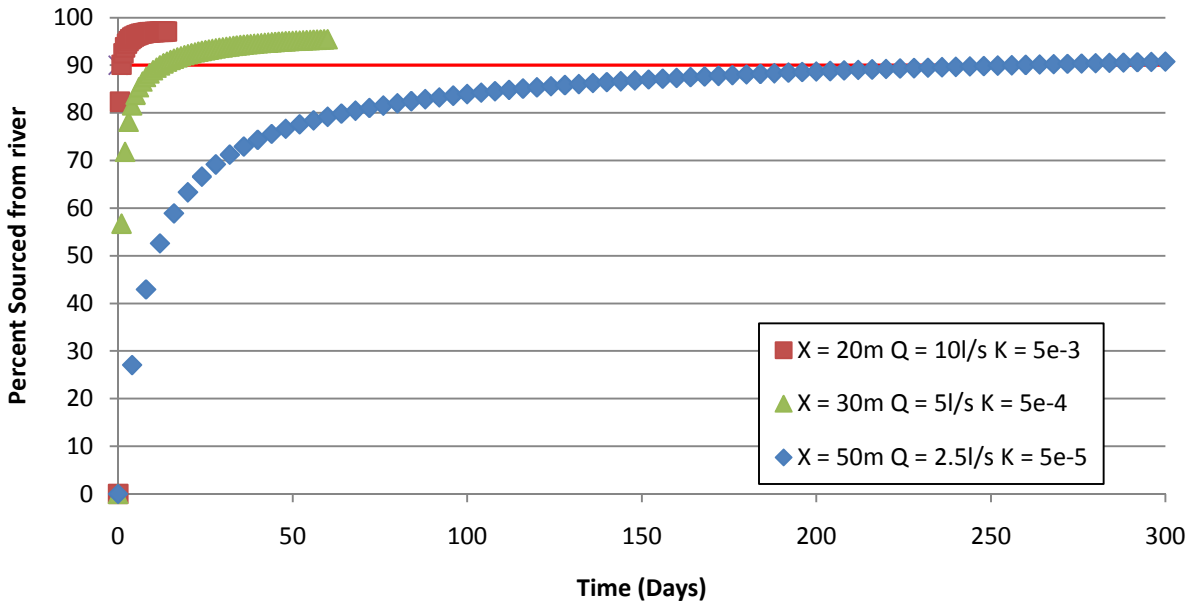

Figure 52: Precent Sourced from River - Comparison of extreme cases

5.5.6 Table of results

Table 10 tabulates the results for Section 5.5. The column labelled *Favourable* refers to the model scenario with the more favourable conditions, for example with the comparison of hydraulic conductivity; the *Favourable* scenario refers to the scenario with a hydraulic conductivity of $5x10^{-3}$ m/s. The *Unfavourable* situation refers to the opposite scenario. For values refer to the conceptual diagram in Figure 16.

Table 10: Percentage Sourced from River - Tabulated summary of results

Parameter Change	Favorable (days)	Base (days)	Unfavorable (days)	Rank
Conductivity	2.5	12	65	1
Pumping Rate	12	12	12	4
Distance	7	12	27.5	3
Clogging Layer	12	15	40	2
Extreme	1	12	252	-

Table 10 tabulates the variation that each parameter had on the water being sourced from the river. For this set of comparisons the hydraulic conductivity had the greatest variation followed by the clogging layer, distance from river and the pumping rate.

5.6 Stream Depletion

5.6.1 Hydraulic Conductivity

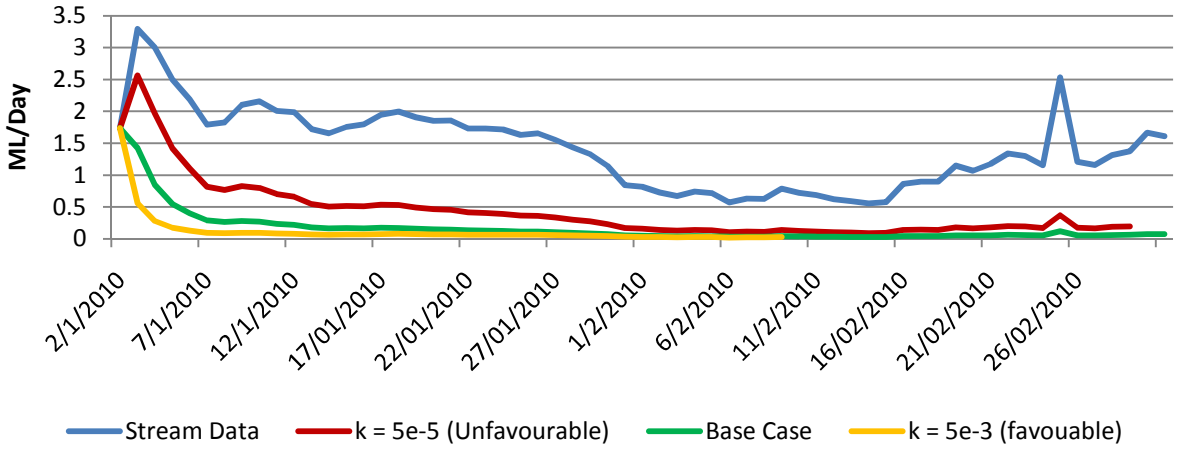

Figure 53: Stream Depletion Comparisons - Hydraulic Conductivity

Figure 53 shows the hydraulic conductivity had a varied effect on stream flow; the first few days the varying hydraulic conductivities had different values flow. However during the period of low flow the flow in the stream came close to a period of no flow regardless of the model run.

5.6.2 Pumping Rate

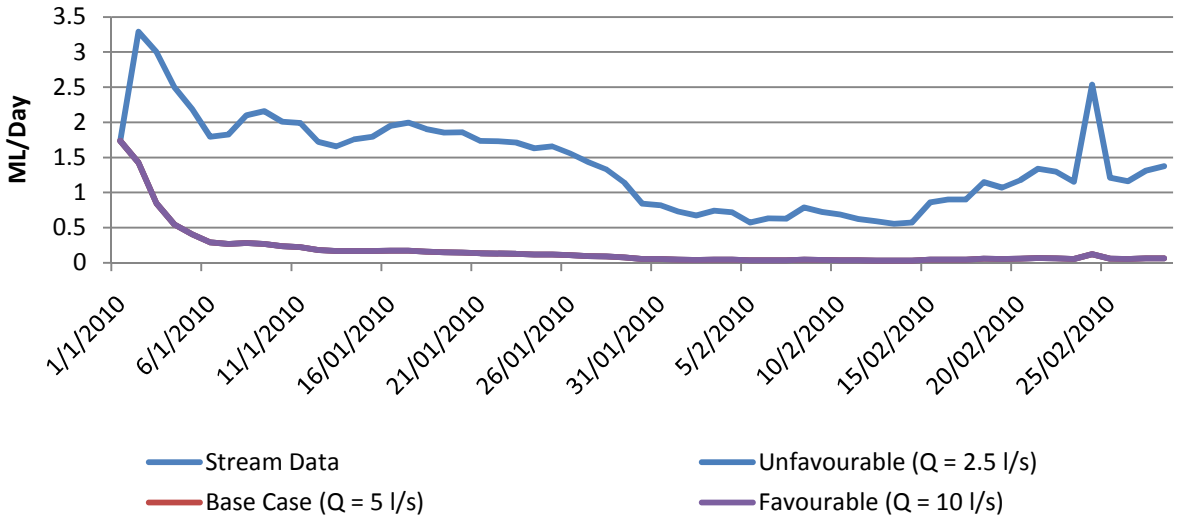

Figure 54: Stream Depletion Comparisons – Pumping Rate

Due to the percentage sourced from the river being the same for all cases the stream depletion didn't vary as shown in Figure 54.

5.6.3 Pumping Location

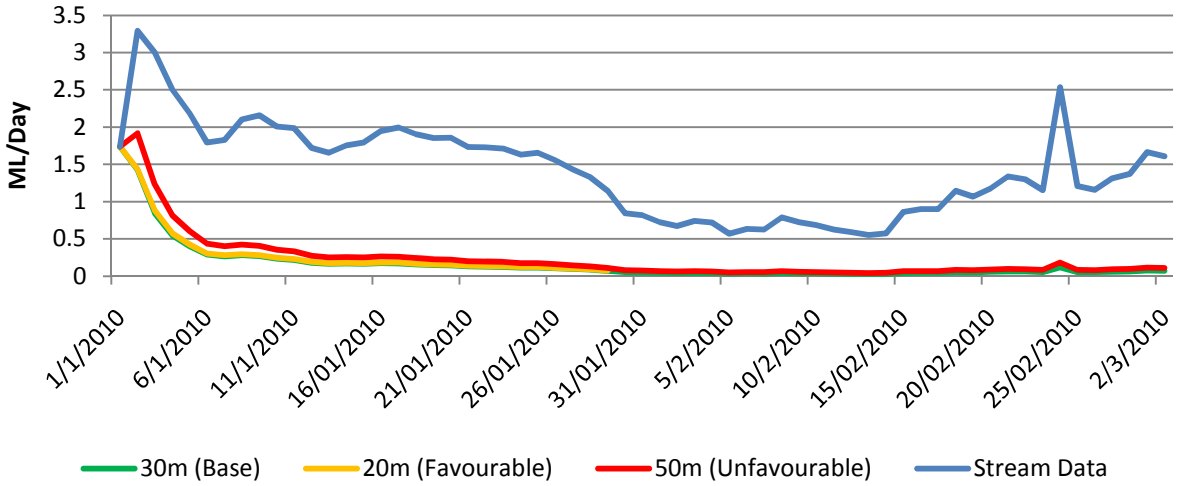

Figure 55: Stream Depletion Comparisons – Location of pump

The variation in stream depletion for the pumping location was not large as shown in Figure 55. This indicates that distances between 20m to 50m have similar effects on the flow of the river.

There is a slight lag in effects on the stream depletion due to varied distances. However during low flow periods of 0.5 ML/Day all the pumping locations had similar values of river flow.

5.6.4 Clogging Layers

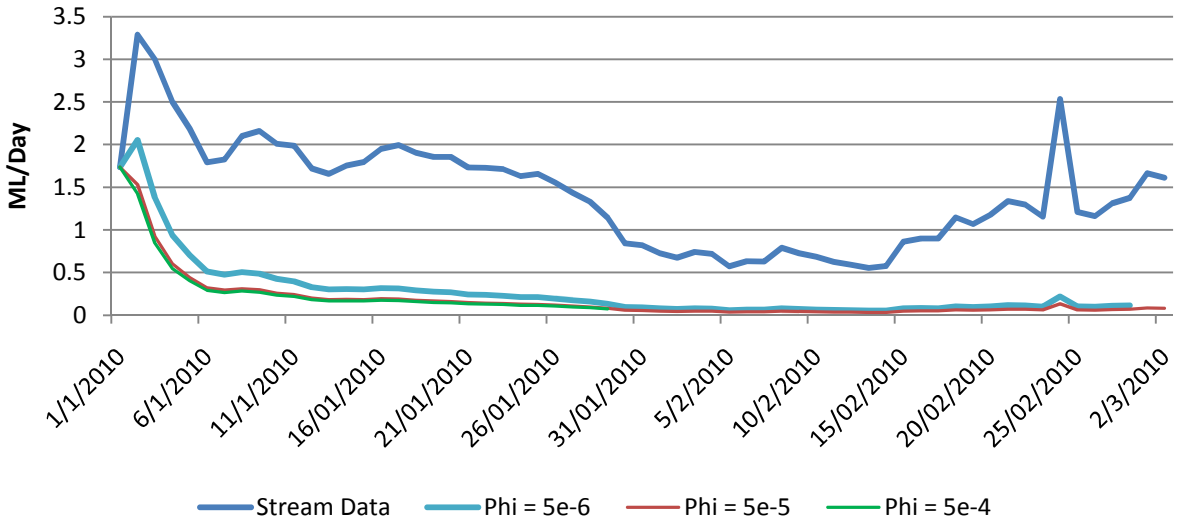

Figure 56: Stream Depletion Comparisons - Clogging Layers

The variation in stream depletion due to clogging layers varied dramatically when the worst case scenario was run as shown in Figure 56. The clogging layers acted to slow down stream depletion rates, however during low flow the stream depletion rates converged to a similar value.

5.6.5 Extreme Cases

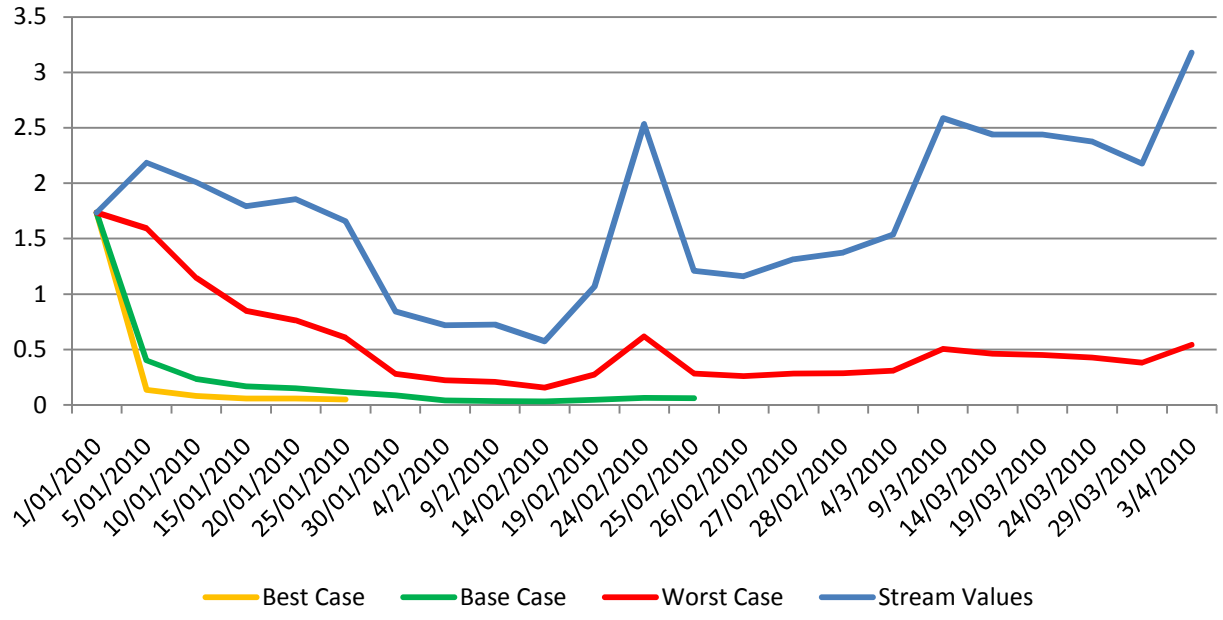

Figure 57: Stream Depletion Comparisons - Extreme Cases

The comparison of the extreme cases was placed in Figure 57. The worst case had the least impact on the stream depletion as the low hydraulic conductivity caused water to be sourced from other areas in the aquifer. In the best case the majority of the water was being sourced from the aquifer causing very low levels of flow in the river.

6 Discussion

6.1 Parameters

This thesis examined the effects that chosen parameters has on a river-aquifer system when a pumping bore is placed in near a river. The effects were shown by using different forms of comparison. Fetter 1994 provided an analytical solution to solving the governing equations for the drawdown of a pumping bore in an unconfined aquifer:

$$h_o - h = \frac{Q}{4\pi bk} W(u, \Gamma) \quad 6.1$$

Where $W(u, \Gamma)$ is the well function:

$$u = \frac{r^2 S}{4bkt} \quad 6.2$$

$$\Gamma = \frac{r^2}{b^2} \quad 6.3$$

Where:

$h_0 - h$ the drawdown (m)

b breath of aquifer (m)

r radial distance from the pumping well (m)

k hydraulic conductivity (m/s)

S specific yield

t time (s)

The hydraulic conductivity was the parameter with the greatest variation as it varied across several magnitudes. The unfavourable case (k = $5x10^{-5}$ m/s) consistently showed a abnormal results with a large drawdown in water levels near the aquifer (Figure 23), a large time lag in the terminating particle (Figure 38) and a similar large time lag in the percentage sourced from the river (Figure 48). A possible explanation for the large variation in parameters can be

illustrated by Equation 6.1 and Equation 6.2. Since the hydraulic conductivity has an inverse effect on the drawdown if all other parameters remained constant that is, $(h_o - h) \to \infty$ as $k \to 0$, the fact that the hydraulic conductivity was decreased by a magnitude of 10 caused the drawdown to increase significantly. This explained why for Figure 23 the drawdown for the unfavourable case was larger than the worst case in the extreme comparisons (Figure 27). Despite the large geometry of the drawdown cone the stream depletion for the unfavourable case (Figure 53) has the least amount of impact on the river. To investigate the drawdown cone of the base case and unfavourable case was plotted in Figure 74 in Appendix D. Figure 74 showed that due the water was being sourced from the aquifer rather than the river, as indicated by the low hydraulic conductivity rate. This was because the low hydraulic conductivity forced a bottle neck of flow near the aquifer so to compensate for the lack of water being sourced from the river; the water was being sourced from other areas in the aquifer.

The pumping rate yielded a direct effect on the drawdown in general. In water levels near the aquifer (Figure 24) appeared to have a linear relationship with pumping rate; as the pumping increased the water levels decreased linearly. This effect was observed in the perpendicular particle comparison (Figure 39) as the increase of the velocity linearly increased with pumping rate. The plume height and time of impact also had a linear increase (Figure 43). This constant increase could be attributed to Equation 6.1. When rearranged to place the constant parameters on the right hand side:

$$\frac{h_o - h}{Q} = \frac{W(u, \Gamma)}{4\pi bk} \qquad 6.4$$

A direct relationship between the drawdown and the pumping rate will be governed by a constant rate of the other parameters. Figure 75 is a velocity plot of Figure 39 and it shows the constant rate that Equation 6.4 describes. The lack of variation in percentage sourced from river (Figure 48), can be explained by Sophocleous et al. 1995; when pumping rates were changed from Q = 0.5m^3/s to Q = 0.005m^3/s the stream depletion rates remained identical. The lack of hydraulic gradient could have further attributed to the lack of variation.

As the distance from the river increased the drawdown of the river decreased (Figure 25). This was consistent with other forms of comparison, the depth of the plume decreased as the distance increased (Figure 45). The time taken for the perpendicular particle to reach the pumping bore increased (Figure 40) as the velocity of the particle remained constant the distance to travel was longer. Equation 6.1 offers a mathematical explanation; as r increases in Equation 6.2 and Equation 6.3 increases Γ and u. Γ and u are both included in the well function and as these parameters increase the well function decreases. This in turn decreases the drawdown in Equation 6.1.

The clogging layers were compared in a different format to the other parameters; the base case was considered a favourable case where there was no clogging layer present. These set of model runs highlighted the fact that clogging layers in numerical models and in general is not well understood (Brunner et al. 2009). In both scenarios for the varying clogging layers the condition for disconnection (Equation 3.19) was satisfied (see Appendix D) but under the results of the models indicated there was no disconnection. However the clogging layer caused the water to be sourced from the other side of the river as shown in Figure 35. As mentioned previously, the low hydraulic conductivity of the clogging layer forces the water to be sourced from other areas in the aquifer as this is reflected in the comparison of stream depletion levels in clogging layers (Section 5.6.4). The difference between Figure 74 is that more water was being sourced from the river rather than the surrounding aquifer; the higher hydraulic conductivity in the aquifer allowed more leakage from the river to flow to the pumping bore.

The numerical experiment in pumping was designed to determine the effects that certain parameters will have. The values were chosen based on the conditions of the field experiment. Because of this the configuration of the sensitivity analysis was biased towards the conditions in the field experiment. For example comparing the effects of moving the pumping bore to the effects that hydraulic conductivity is difficult; the distances of the pumping bore was relatively small than to the difference in magnitudes for the hydraulic conductivity. This becomes apparent in most of the comparisons; the hydraulic conductivity has been identified as having the largest variation in the parameters.

However in aiding the decisions of the field experiment this study has merit. The hydraulic conductivity has great variation in the numerical experiment; it might cause great variation in field results however this cannot be controlled. The distance of the pumping bore will also affect the time of results; the closer the bore is placed to the river the faster the results inducing abstraction will occur. The pumping rate which can be controlled in the field should be allowed to reach the maximum pumping capacity. Clogging layers should not be a big concern as the results of the sensitivity analysis showed time delay with varying cases.

6.2 Limitations

The modeling involved in this thesis did not address a few issues; the drawdown expected at the in the pumping bore, recharge of the aquifer, unsaturated elements and possibly a correct method of determining a realistic stream depletion. The head values at the location of the pumping bore are not the true drawdown and further analytical methods would be required to calculate the true drawdown at the bore.

The hydraulic gradient should have been given more considering. Chen et al. 2001 makes the point that for a stream aquifer system with no hydraulic gradient there is no baseflow giving the implication that this thesis is focused entirely around induced stream infiltration i.e. all results in this thesis have immediate impacts on stream depletion. Depending if the stream is gaining or loosing there will be a time difference in the results; a gaining stream will induce a time lag in the results while a losing aquifer will accelerate time of the results. The addition of the hydraulic gradient as an extra parameter in the methods of comparison should have been included, the loosing and gaining as the favourable and unfavourable cases would have provided a better time frame of the results.

The section on stream depletion (Section 5.6) was a crude attempt to simulate the effects of stream depletion. As mentioned previously all results in this thesis make the assumption of no hydraulic gradient, the water table is initially flat. By lowering the water table with pumping the stream has become a gaining stream, so the results of stream depletion have been exaggerated. Another assumption was the river would flow the same regardless of if pumping

was induced or not. This assumption may not be correct as pumping would have influenced the flow of the river.

6.3 New approaches

Traditionally the approach on simulating stream-aquifer interactions used variations of Equation 3.15 to quantify the effects of pumping has on the river-aquifer system. This method provides an often abstract view on the process involved in stream depletion. In this thesis new methods were provided to quantify these effects such as contouring the particle tracers and visualising the drawdown cone, making the process more intuitive. In conjunction with the traditional methods the process of stream depletion can be placed in a new context.

Sophocleous et al. 1995 and Chen et al. 2002 both address the river-aquifer interactions on a long term scope with pumping seasons of at least a year and large values of distance between the river and pumping bore. This thesis however addresses the interactions on a more micro scale with a reduction in time and distances between the river and the pumping bore. There are few papers which address the issue of a single borehole and its effects on stream depletion and none focus on smaller distances near the river. Work done through the sensitivity analysis provides a study of the macro scale of river-aquifer interactions.

6.4 Impacts on stream-aquifer interactions

As a secondary objective the physical effects that abstraction near a river was investigated. Sections 5.1 to Section 5.4 showed the physical processes involved in river-aquifer interactions. Section 5.5 and Section 5.6 illustrated the effects that pumping could have on river system.

During low stream flows as shown in Section 5.6 all the parameters eventually caused flow to be reduced to extremely low levels with the possibility of 97% of the water from the river to be extracted. Flows that are lower than normal levels have possible impacts on the environment. A commissioned report by the Food and Organisation of the United Nations (Dougherty 1995) provided guidelines on the Environmental Impact Assessment of irrigation and drainage projects. Several major social-economical issues with low flow were highlighted; the quality and

amount of water will decrease denying downstream users of usable river water. Excessive pumping would also affect the ecosystem; biological communities established in flow water conditions are well adapted to their environment (Statzner et al. 1988). Inducing unnaturally low flows caused by water abstraction would have damaging impacts on these biological communities and their associated biota (McKay et al. 2006).

Another effect induced by pumping near a river was the affect of hydraulic conductivity on the geometry of the drawdown cone, as Figure 74 demonstrated that a change in the magnitude of the hydraulic conductivity caused the drawdown cone to widen and deepen. Hydraulic conductivity is a function of temperature and can vary in the same location with a change of temperature (Cox et al. 2007). In areas such as Maules Creek temperatures can range dramatically from 15^{o} to 36^{o} during the year; this will have an effect on the hydraulic conductivity which will change the reach of the drawdown cone. An increased drawdown cone will lower the water table which could affect the surrounding ecosystem near the river.

7 Conclusion

A generic model of a river-aquifer system was created and the effects of groundwater pumping on the river-aquifer interactions were investigated. An extensive literature search found four parameters which dictated the governing equations describing the processes of river-aquifer interactions induced by pumping; the hydraulic conductivity of the aquifer, the flow rate of the pump, the distance the pump was placed from the river and the influence of the clogging layer. Of these parameters it was found that the hydraulic conductivity and clogging layer had the greatest influence on the geometry of the drawdown cone caused by the pumping. The pumping rate and the position of the pumping bore had the greatest impact on velocity of the water travelling to the river.

This study was based on the short term pumping of a field experiment located at Elfin Crossing. As the model was a generic model it can be applied to any aquifer river system and as a secondary objective the physical effects pumping has on the river was examined. It was found that within a few days of pumping flow in the river the flow levels were extremely low. This has implications on pumping near a river in general as a larger irrigation projects if unregulated can cause social-economical and environmental impacts.

8 References

Acworth, I. (2010). Short Course notes – Groundwater Resource Investigation. Kensington, Sydney, University of New South Wales.

Alley, W. M., Reilly, T.E., Franke, L. (1999). Sustainability of ground-water resources., US Geological Survey Circular 1186.

Andersen, M. and R. Acworth (2009). "Stream-aquifer interactions in the Maules Creek catchment, Namoi Valley, New South Wales, Australia." Hydrogeology Journal **17**(8): 2005-2021.

Anderson, M. P. and W. W. Woessner (1992). Applied groundwater modelling simulation of flow and advective transport., New York: Academic Press.

Bouwer, H. (2002). "Artificial recharge of groundwater: hydrogeology and engineering." Hydrogeology Journal **10**(1): 121-142.

Brunner, P., P. Cook and C. Simmons (2009). "Hydrogeologic controls on disconnection between surface water and groundwater." Water Resources Research **45**(1): W01422.

Burchi, S. (1999). National Regulations for Groundwater: Options, Issues and Best Practices, Legal Office, FAO.

Chen, X. and L. Shu (2002). "Stream-Aquifer Interactions: Evaluation of Depletion Volume and Residual Effects from Ground Water Pumping." Ground Water **40**(3): 284-290.

Chen, X. and Y. Yin (2001). "STREAMFLOW DEPLETION: MODELING OF REDUCED BASEFLOW ANI INDUCED STREAM INFILTRATION FROM SEASONALLY PUMPED WELLS1." JAWRA Journal of the American Water Resources Association **37**(1): 185-195.

Chen, X. and Y. Yin (2001). "Streamflow depletion: Modelling of reduced baseflow and induced stream infiltration from seasonally pumped wells." JAWRA Journal of the American Water Resources Association **37**(1): 185-195.

Chen, X. and Y. Yin (2004). "Semianalytical Solutions for Stream Depletion in Partially Penetrating Streams." Ground Water **42**(1): 92-96.

Cox, M. H., G. W. Su and J. Constantz (2007). "Heat, Chloride, and Specific Conductance as Ground Water Tracers near Streams." Ground Water **45**(2): 187-195.

Dougherty, T. C. (1995). Environmental impact assessment of irrigation and drainage projects / by T.C. Dougherty, A.W. Hall. Rome :, Food and Agriculture Organization of the United Nations.

Fetter, C. W. (1994). Applied Hydrogeology, Prentice-Hall.

Glover, R. E. (1974). Transient ground water hydraulics. Fort Collins, Dept. of Civil Engineering, College of Engineering, Colorado State University.

Glover, R. E. B., C. G. (1954). "River depletion resulting from pumping a well near a river." American Geophysical Union Transactions **35**(3): 468-470.

Hantush, M. S. (1965). "Wells near Streams with Semipervious Beds." J. Geophys. Res. **70**(12): 2829-2838.

Hunt, B. (1999). "Unsteady Stream Depletion from Ground Water Pumping." Ground Water **37**(1): 98-102.

Information, N. W. (2011). Waterinfo, NSW Water Information. Lasted Accessed May 2011 <http://waterinfo.nsw.gov.au/water.shtml?ppbm=SURFACE_WATER&rs&3&rskm_url>

Jacob, C. E. (1950). Flow of groundwater, John Wiley.

Kim, G.-B. (2010). "Application of analytical solution for stream depletion due to groundwater pumping in Gapcheon watershed, South Korea." Hydrological Processes **24**(24): 3535-3546.

Knochenmus, L. A. R., James L. (1996). Descriptions of anisotropy and heterogeneity and their effect on ground-water flow and areas of contribution to public supply wells in a karst carbonate aquifer system, U.S. G.P.O. .

Konikow, L. F. and J. D. Bredehoeft (1992). "Ground-water models cannot be validated." Advances in Water Resources **15**(1): 75-83.

Madison, P. (2011). Surfer, Goldern Software.

McDonald, M. G. and A. W. Harbaugh (1988). A modular three-dimensional finite-difference ground-water flow model.

McKay, S. F. and A. J. King (2006). "Potential ecological effects of water extraction in small, unregulated streams." River Research and Applications **22**(9): 1023-1037.

Morris, B. L., A. R. L. Lawrence, P. J. C. Chilton, B. Adams, R. C. Calow and B. A. Klinck (2003). Groundwater and its Susceptibility to Degradation: A Global Assessment of the Problem and Options for Management. Early Warning and Assessment Report Series, United Nations Environment Programme. **03-3**.

Parkin, G., S. J. Birkinshaw, P. L. Younger, Z. Rao and S. Kirk (2007). "A numerical modelling and neural network approach to estimate the impact of groundwater abstractions on river flows." Journal of Hydrology **339**(1-2): 15-28.

Rau, G., M. Andersen, A. McCallum and R. Acworth (2010). "Analytical methods that use natural heat as a tracer to quantify surface water–groundwater exchange, evaluated using field temperature records." Hydrogeology Journal **18**(5): 1093-1110.

Rushton, K. R. and L. M. Tomlinson (1979). "Possible mechanisms for leakage between aquifers and rivers." Journal of Hydrology **40**(1-2): 49-65.

Sinclair, P., C. Barrett and R. M. Williams (2005). Impact of groundwater Extraction on Maules Creek – Upper Namoi River, NSW, Australia, Department of Infrastructure and Natural Resources NSW.

Sophocleous, M. (2002). "Interactions between groundwater and surface water: the state of the science." Hydrogeology Journal **10**(1): 52-67.

Sophocleous, M., A. Koussis, J. L. Martin and S. P. Perkins (1995). "Evaluation of Simplified Stream-Aquifer Depletion Models for Water Rights Administration." Ground Water **33**(4): 579-588.

Spalding, C. P. and R. Khaleel (1991). "An evaluation of analytical solutions to estimate drawdowns and stream depletions by wells." Water Resour. Res. **27**(4): 597-609.

Statzner, B., J. A. Gore and V. H. Resh (1988). "Hydraulic Stream Ecology: Observed Patterns and Potential Applications." Journal of the North American Benthological Society **7**(4): 307-360.

Theis, C. V. (1941). "The effect of a well on the flow of a nearby stream." American geophysical Union Transactions **3**: 764-738.

Treese, S., T. Meixner and J. F. Hogan (2009). "Clogging of an Effluent Dominated Semiarid River: A Conceptual Model of Stream-Aquifer Interactions1." JAWRA Journal of the American Water Resources Association **45**(4): 1047-1062.

Trefry, M. G. and C. Muffels (2007). "FEFLOW: A Finite-Element Ground Water Flow and Transport Modeling Tool." Ground Water **45**(5): 525-528.

Walton, W. C. (1970). Groundwater Resources Evaluation. New York, McGraw-Hill.

Zlotnik, V. A. (2004). "A concept of maximum stream depletion rate for leaky aquifers in alluvial valleys." Water Resour. Res. **40**(6): W06507.

Zume, J. and A. Tarhule (2008). "Simulating the impacts of groundwater pumping on stream–aquifer dynamics in semiarid northwestern Oklahoma, USA." Hydrogeology Journal **16**(4): 797-810.

Appendix A

Table 11: Model Parameter comparison

X (m)	Q l/s	K_v m/s	K_v/K_h -	I -	ϕ m/d	Peak %	Source
152	32	9.6E-04	1.00	0.15	-	85	Chen et. al. 2001, Fig 3
152	32	9.6E-04	1.00	0.30	-	85	Chen et. al. 2001, fig 3
152	32	9.6E-04	1.00	0.60	-	85	Chen et. al. 2001, fig 3
152	32	9.5E-06	0.01	0.15	-	67	Chen et. al. 2001,fig 4
152	32	9.5E-05	0.10	0.15	-	85	Chen et. al. 2001, fig 4
305	32	9.5E-05	0.10	0.15	-	85	Chen et. al. 2001, fig 5
710	32	9.5E-05	0.10	0.15	-	59	Chen et. al. 2001, fig 5
1525	32	9.5E-05	0.10	0.15	-	29	Chen et. al. 2001, fig 5
600	52	1.2E-04	0.10	0.30	0.50	12	Chen et. al 2002, table 2
600	52	1.2E-04	0.10	0.30	1.25	20	Chen et. al 2002, table 2
600	52	1.2E-04	0.10	0.30	2.50	43	Chen et. al 2002, table 2
600	52	1.2E-04	0.10	0.30	5.00	57	Chen et. al 2002, table 2
600	52	1.2E-04	0.10	0.30	10.00	69	Chen et. al 2002, table 2
600	52	1.2E-04	0.10	0.30	20.00	76	Chen et. al 2002, table 2
600	52	1.2E-04	0.10	0.30	50.00	77	Chen et. al 2002, table 2
300	52	1.2E-03	1.00	0.06	5.00	47	Chen et. al 2004, fig 4(a)
300	52	1.2E-03	1.00	0.09	5.00	45	Chen et. al 2004, fig 4(b)
80	500	1.0E-03	1.00	1.00	-	95	Sophcelous et. Al. 1995 fig 4
80	500	6.0E-04	1.00	1.00	-	95	Sophcelous et. Al. 1995 fig 5
80	500	6.0E-04	1.00	1.00	5.18	38	Sophcelous et. Al. 1995 fig 6
80	500	6.0E-04	1.00	1.00	0.52	90	Sophcelous et. Al. 1995 fig 6

Figure 12: Comparison of variables

Best Subsets Regression: Peak versus X, Q, Kv, I, ϕ

Response is Peak

Vars	R-Sq	R-Sq(adj)	Mallows C-p	S	K	X	Q	v	I	ϕ
1	32.3	28.7	-0.7	21.407		X				
1	10.5	5.8	4.5	24.603				X		
2	36.0	28.9	0.4	21.380		X		X		
2	32.9	25.4	1.1	21.896		X				
3	36.6	25.4	2.2	21.891		X		X	X	
3	36.2	24.9	2.3	21.974		X	X			
4	37.4	21.8	4.0	22.423		X	X		X	
4	36.7	20.9	4.2	22.544		X		X	X	
5	37.5	16.6	6.0	23.147		X	X	X	X	

Figure 58: Mintab output - Best Subsets Regression

Regression Analysis: Peak versus X, Q, Kv, I, ϕ

The regression equation is
Peak = 75.0 - 0.0432 X - 0.0346 Q - 1743 Kv + 24.9 I + 0.410 ϕ

Predictor	Coef	SE Coef	T	P
Constant	75.00	17.16	4.37	0.001
X	-0.04318	0.01922	-2.25	0.040
Q	-0.03459	0.08208	-0.42	0.679
Kv	-1743	14345	-0.12	0.905
I	24.86	46.00	0.54	0.597
ϕ	0.4098	0.4700	0.87	0.397

S = 23.1471 R-Sq = 37.5% R-Sq(adj) = 16.6%

Analysis of Variance

Source	DF	SS	MS	F	P
Regression	5	4819.2	963.8	1.80	0.174
Residual Error	15	8036.8	535.8		
Total	20	12856.0			

Source	DF	Seq SS
X	1	4149.1
Q	1	10.4
Kv	1	43.8
I	1	208.5
ϕ	1	407.4

Unusual Observations

Obs	X	Peak	Fit	SE Fit	Residual	St Resid
20	80	38.00	80.18	11.73	-42.18	-2.11R

R denotes an observation with a large standardized residual.

Figure 59: Mintab output - Regression on all variables

Regression Analysis: Peak versus X, Q, ϕ

The regression equation is
Peak = 78.2 - 0.0430 X + 0.0060 Q + 0.443 ϕ

Predictor	Coef	SE Coef	T	P
Constant	78.25	10.18	7.69	0.000
X	-0.04300	0.01613	-2.67	0.016
Q	0.00602	0.02995	0.20	0.843
ϕ	0.4432	0.4408	1.01	0.329

S = 21.9739 R-Sq = 36.2% R-Sq(adj) = 24.9%

Analysis of Variance

Source	DF	SS	MS	F	P
Regression	3	4647.5	1549.2	3.21	0.049
Residual Error	17	8208.5	482.9		
Total	20	12856.0			

Source	DF	Seq SS
X	1	4149.1
Q	1	10.4
ϕ	1	488.0

Unusual Observations

Obs	X	Peak	Fit	SE Fit	Residual	St Resid
8	1525	29.00	12.86	18.19	16.14	1.31 X
15	600	77.00	74.92	20.05	2.08	0.23 X
20	80	38.00	80.11	11.07	-42.11	-2.22R

R denotes an observation with a large standardized residual.
X denotes an observation whose X value gives it large influence.

Figure 60: Minitab output - Regression for Q,X,Phi

Regression Analysis: Peak versus X, I, Q

The regression equation is
Peak = 74.3 - 0.0398 X + 29.6 I - 0.0441 Q

Predictor	Coef	SE Coef	T	P
Constant	74.32	13.00	5.72	0.000
X	-0.03975	0.01626	-2.45	0.026

I 29.57 43.96 0.67 0.510
Q -0.04409 0.07821 -0.56 0.580

S = 22.3227 R-Sq = 34.1% R-Sq(adj) = 22.5%

Analysis of Variance

Source DF SS MS F P
Regression 3 4384.9 1461.6 2.93 0.063
Residual Error 17 8471.1 498.3
Total 20 12856.0

Source DF Seq SS
X 1 4149.1
I 1 77.4
Q 1 158.4

Unusual Observations

Obs X Peak Fit SE Fit Residual St Resid
3 152 85.00 84.61 17.99 0.39 0.03 X
8 1525 29.00 16.73 17.84 12.27 0.92 X
9 600 12.00 57.05 6.13 -45.05 -2.10R
20 80 38.00 78.67 11.15 -40.67 -2.10R

R denotes an observation with a large standardized residual.
X denotes an observation whose X value gives it large influence.

Figure 61: Minitab output - Regression for Q,X,I

Appendix B

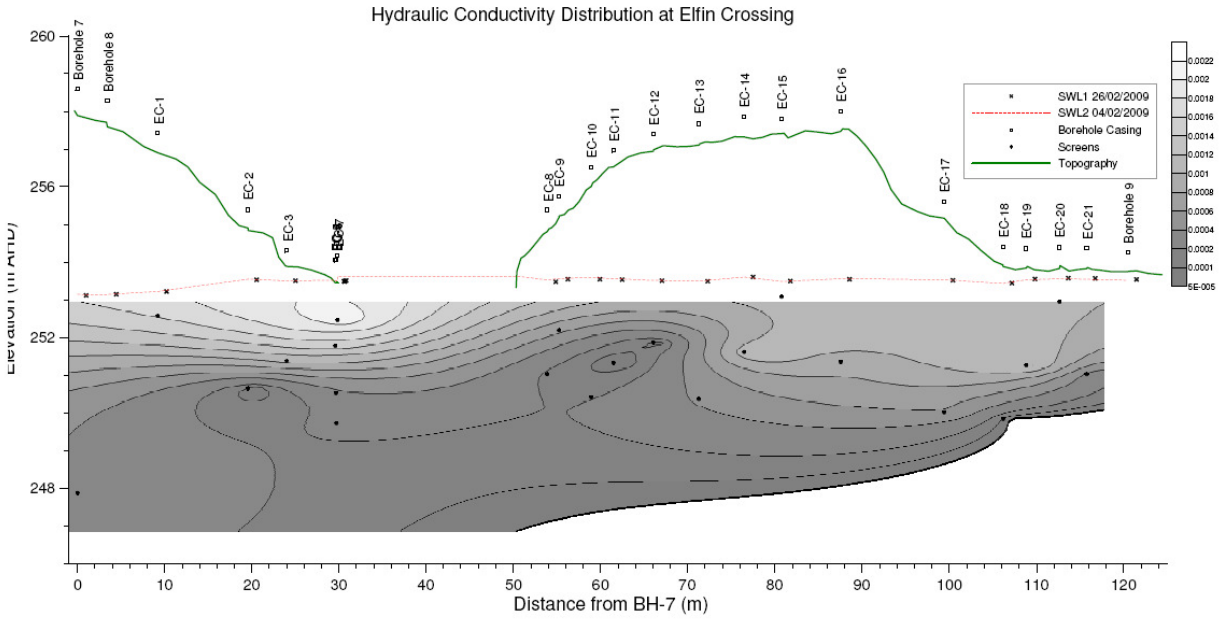

Figure 62: Slug Test of Elfin Crossing

Combination	1	2	3	4	5	6
Pumping Rate - Q (l/s)	2.5	5	10	5	5	5
Hydraulic Conductivity - K (m/s)	5.E-04	5.E-04	5.E-04	5.E-04	5.E-04	5.E-04
Pumping Distance - X (m)	30	30	30	20	30	50

Combination	7	8	9	10	11
Pumping Rate - Q (l/s)	5	5	5	2.5	10
Hydraulic Conductivity - K (m/s)	5.E-05	5.E-04	5.E-03	5.E-05	5.E-03
Pumping Distance - X (m)	30	30	30	50	20

Combination	12	13	14
Pumping Rate - Q (l/s)	5	5	5
Hydraulic Conductivity - K (m/s)	5.E-04	5.E-04	5.E-04
Clogging Layer - ϕ (m/s)	5.E-04	5.E-05	5.E-06
Pumping Distance - X (m)	30	30	30

Table 13: Sensitivity Analysis Parameters

Appendix C

Drawdown

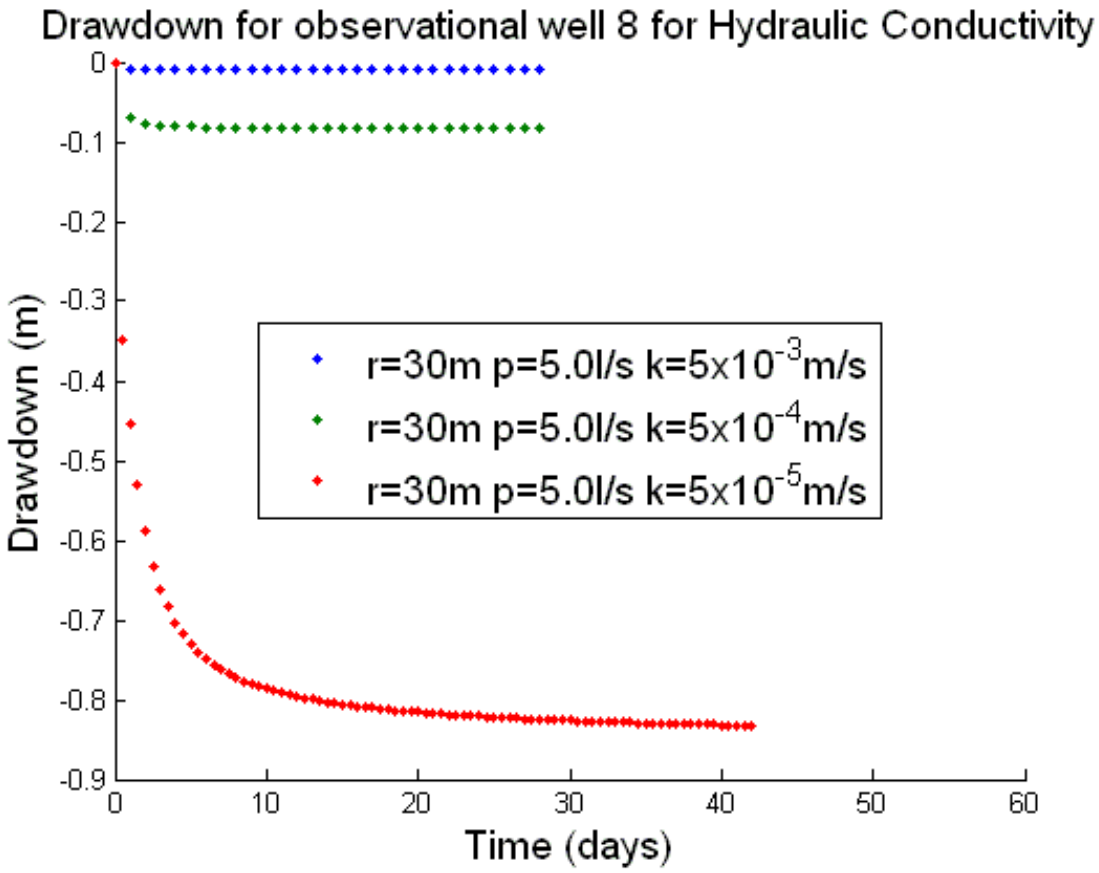

Figure 63: Hydraulic Conductivity - drawdown for observational well 8

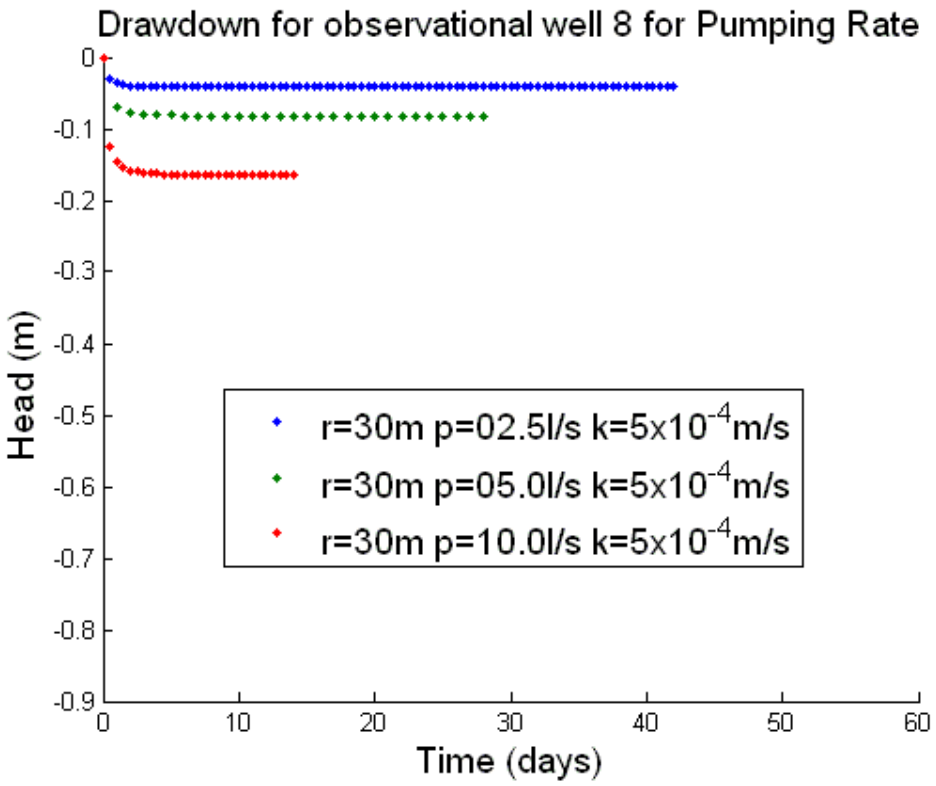

Figure 64: Pumping Rate - drawdown for observational well 8

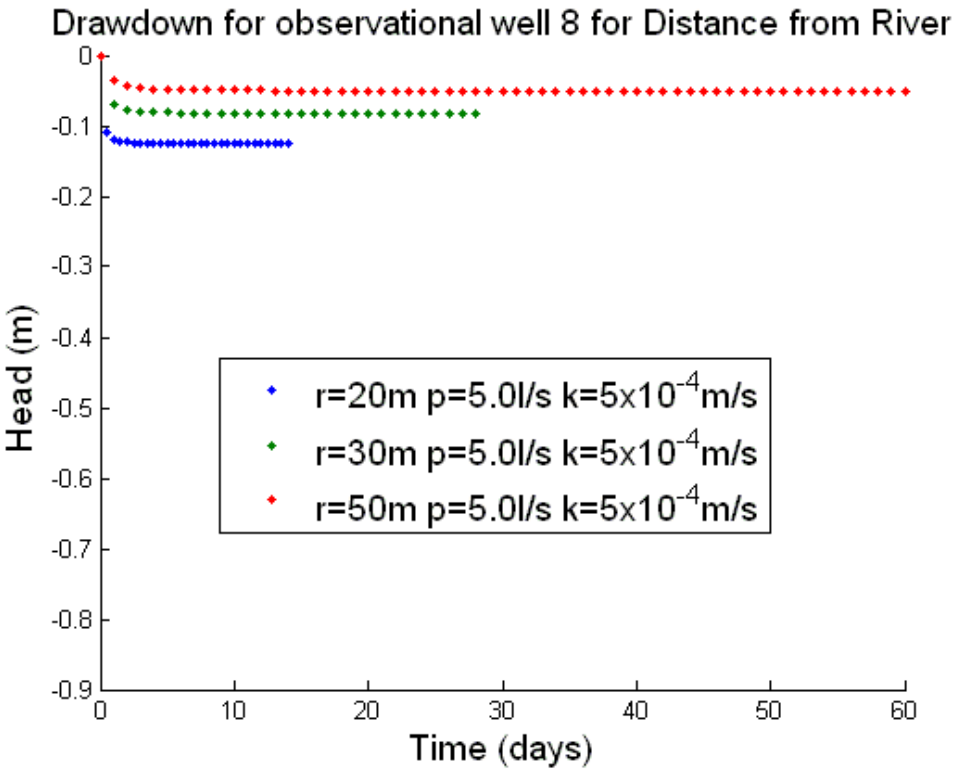

Figure 65: Distance from river - drawdown for observational well 8

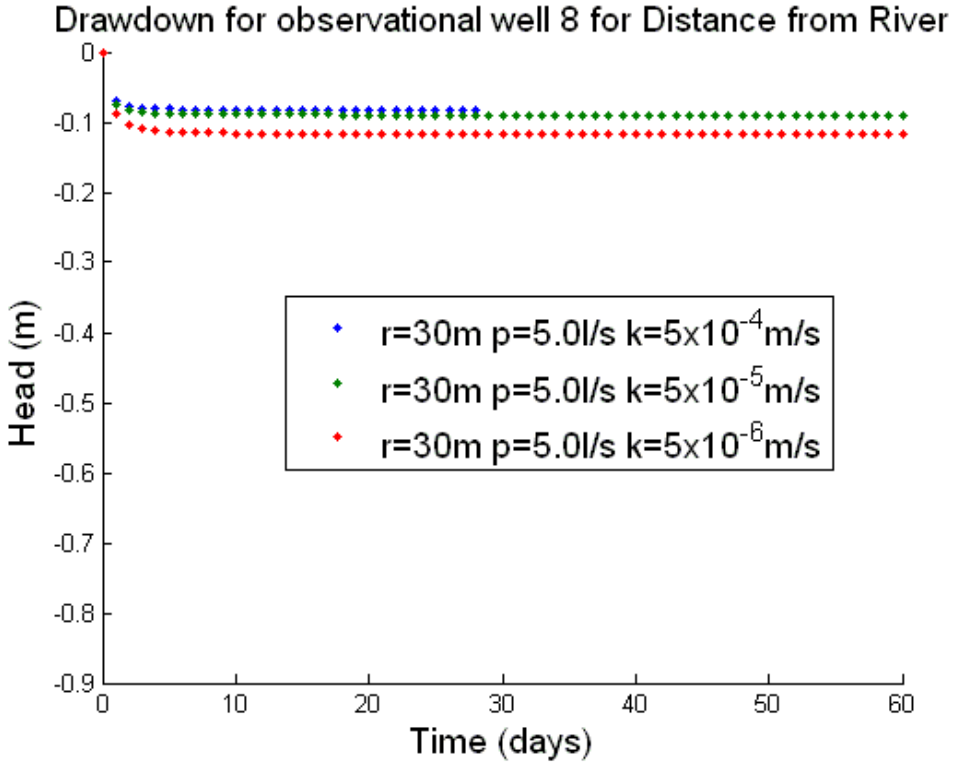

Figure 66: Clogging Layer - drawdown for observational well 8

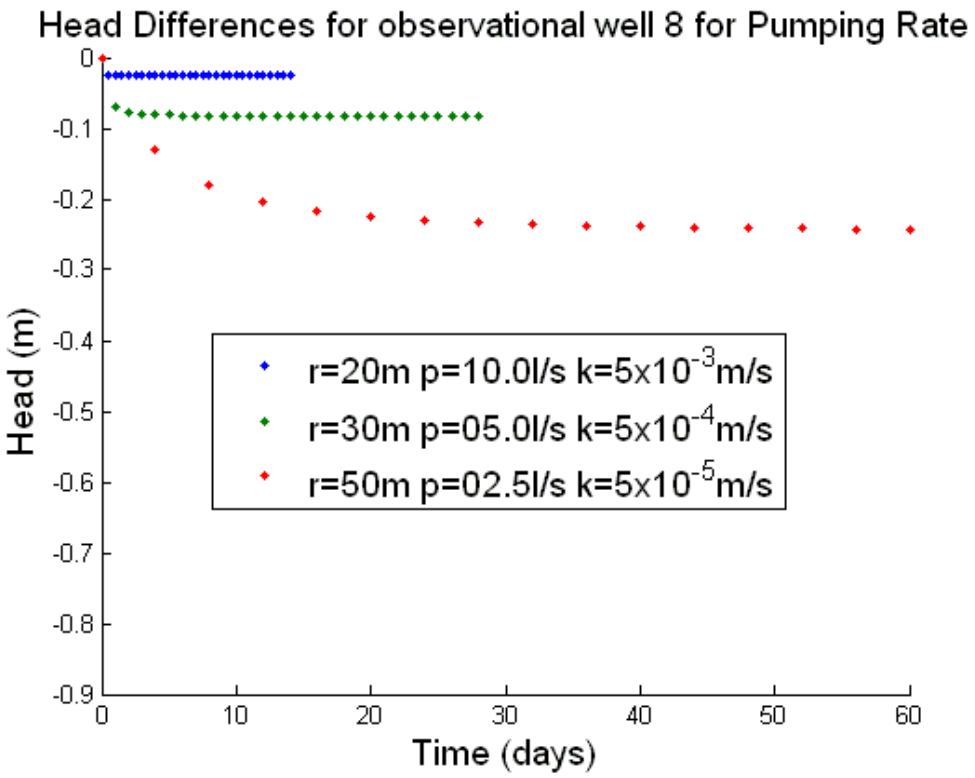

Figure 67: Extremes - drawdown for observational well 8

Drawdown Cone

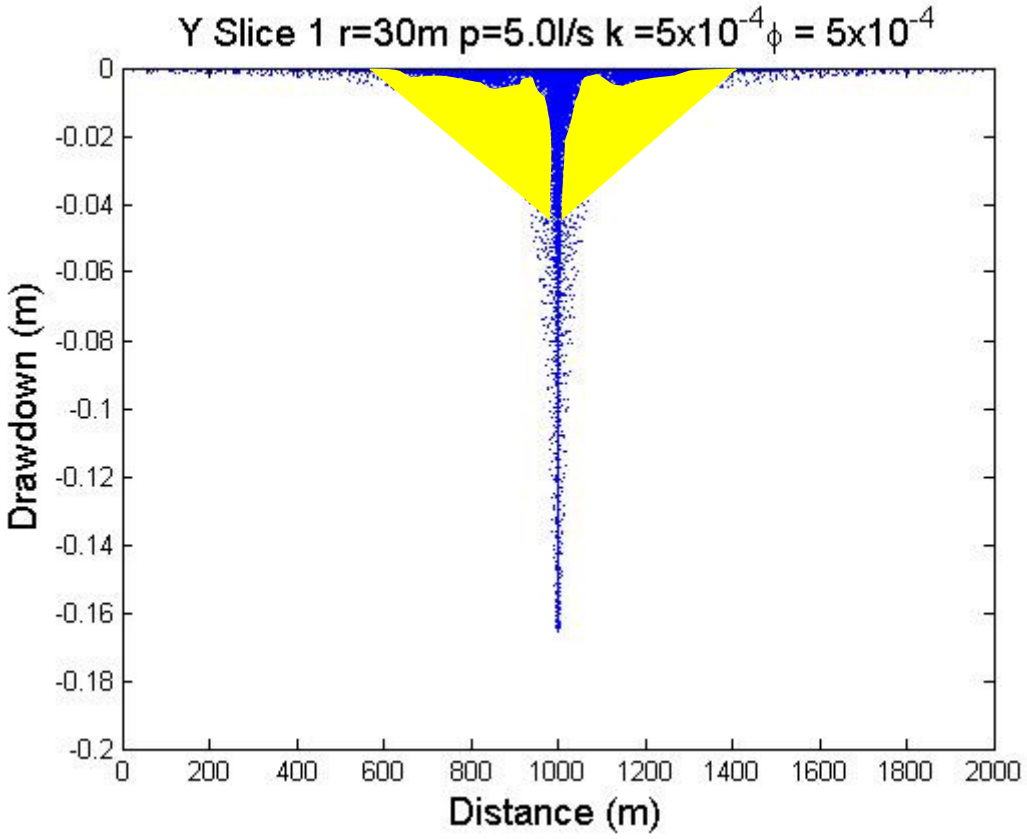

Figure 68: Highlighted density of the drawdown cone of Y-axis

X

Clogging Layers

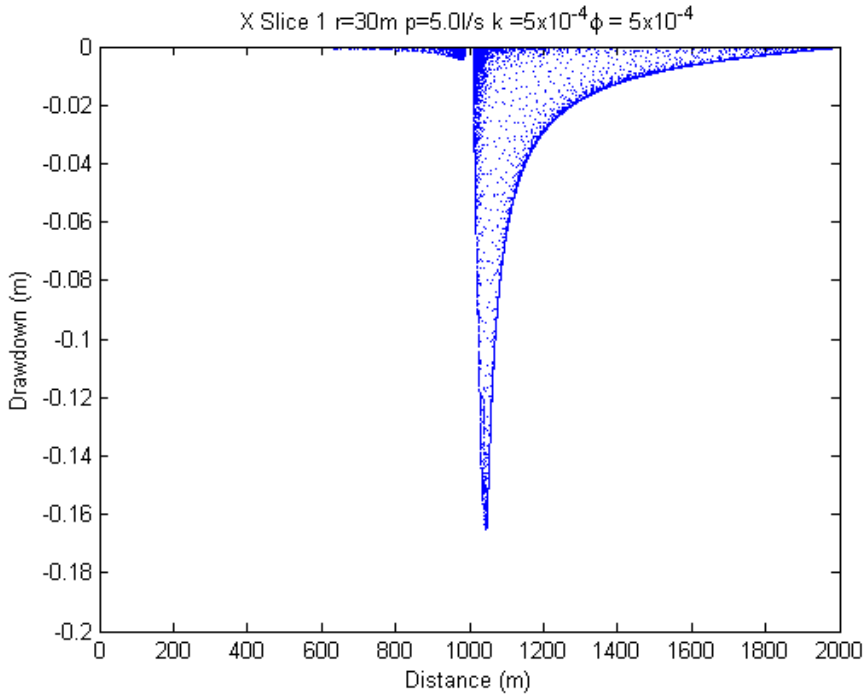

Figure 69: Base Case (No Clogging Layer)

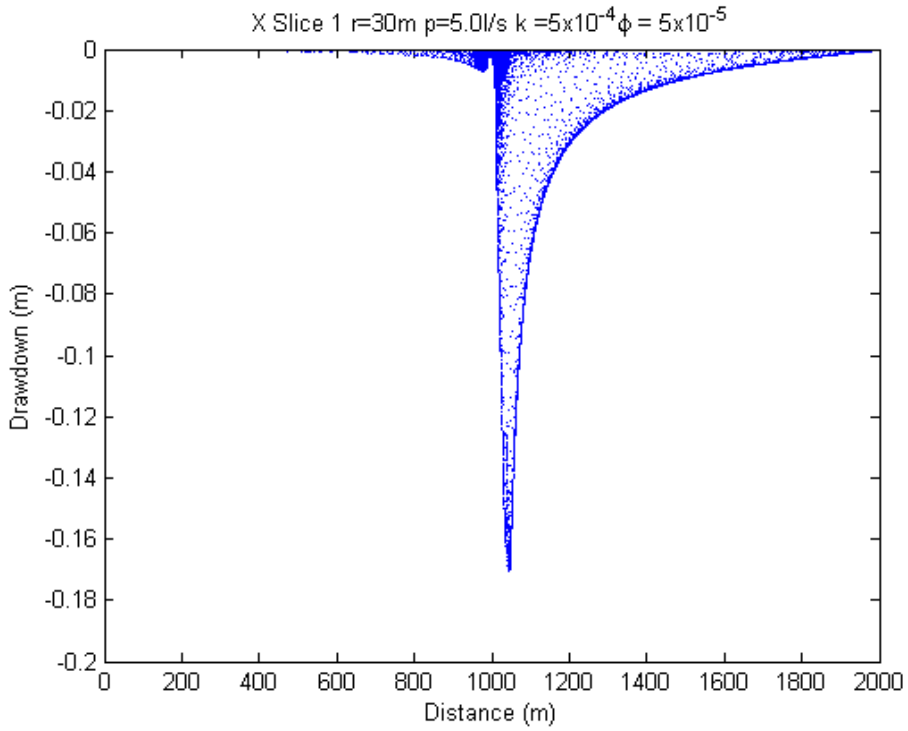

Figure 70: Drawdown Cone of Clogging Layer

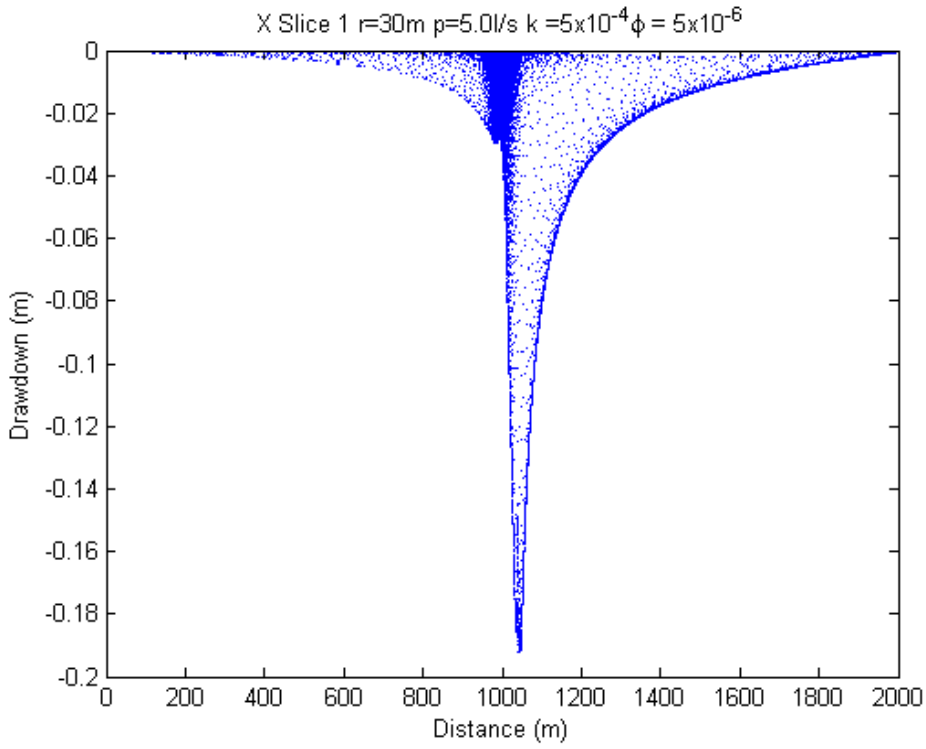

Figure 71: Drawdown cone of worst case Clogging Layer

Perpendicular Particle

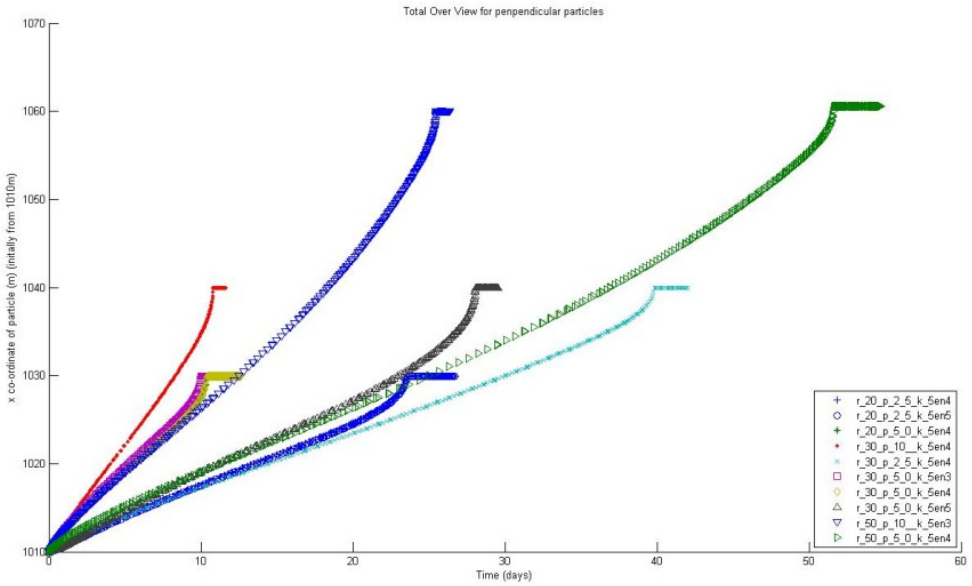

Figure 72: Backwards Particle Analysis - Plot of all model scenarios

Plume Evolution

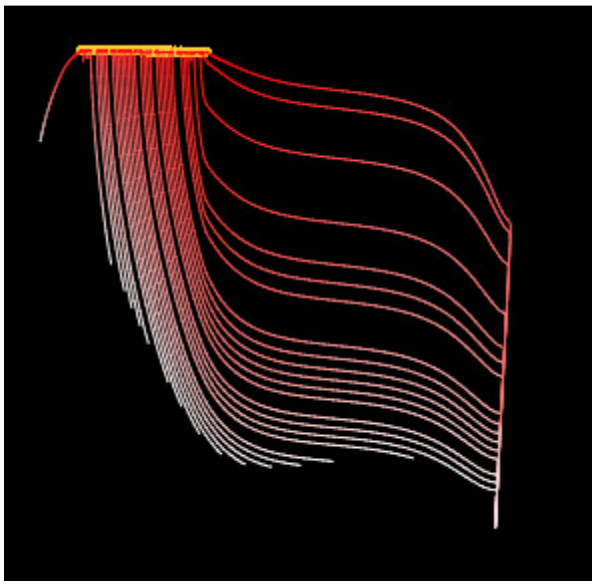

Figure 73: Plume Evolution - Worst case scenario

Appendix D

Disconnection Calculation

From Equation 3.19 for $\phi = 5 \times 10^{-5}\text{m/s}$:

$$\frac{k_c}{k_a} \leq \frac{h_c}{d + h_c}$$

Where:

k_c Hydraulic conductivity of the clogging layer (m/s)

k_a Hydraulic conductivity of the aquifer (m/s)

h_c Thickness of the clogging layer (m)

d Depth of ponded water

$$h_c = \frac{k}{\phi} = \frac{5 \times 10^{-4}}{5 \times 10^{-5}} = 10$$

$$\frac{5 \times 10^{-5}}{5 \times 10^{-4}} \leq \frac{10}{1 + 10}$$

$$0.1 \leq 0.91$$

From Equation 3.19 for $\phi = 5 \times 10^{-6}\text{m/s}$:

$$\frac{k_c}{k_a} \leq \frac{h_c}{d + h_c}$$

$$h_c = \frac{k}{\phi} = \frac{5 \times 10^{-4}}{5 \times 10^{-6}} = 100$$

$$\frac{5 \times 10^{-6}}{5 \times 10^{-4}} \leq \frac{100}{1 + 100}$$

$$0.01 \leq 0.99$$

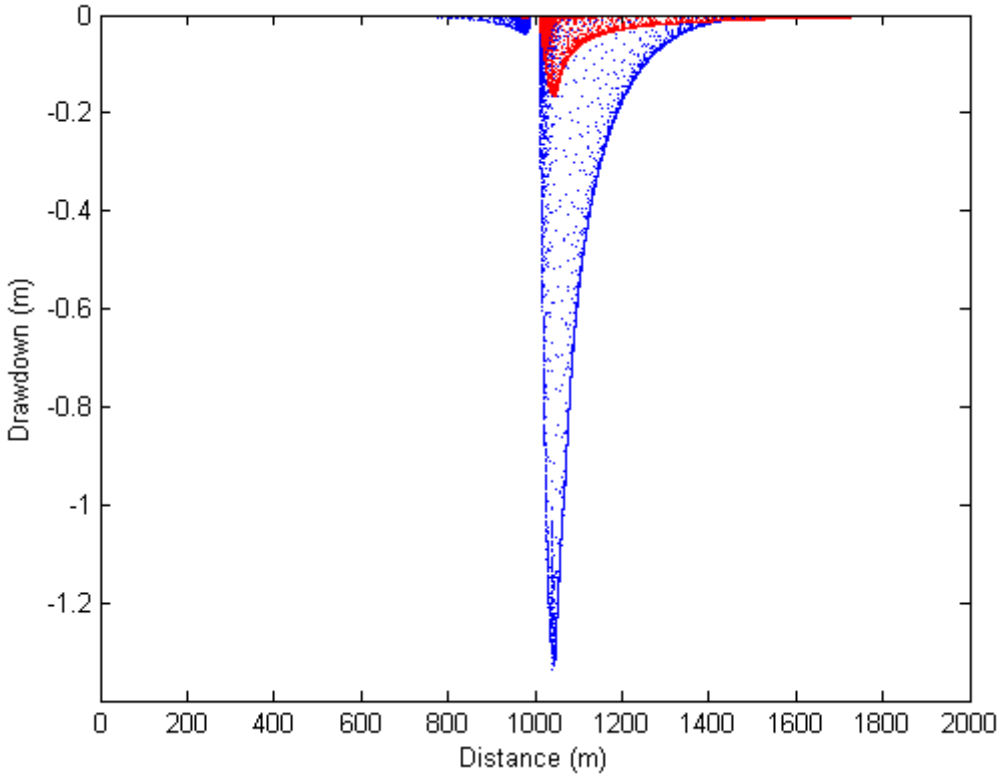

Figure 74: Comparison of drawdown cone between basecase and unfavourable hydraulic conductivity

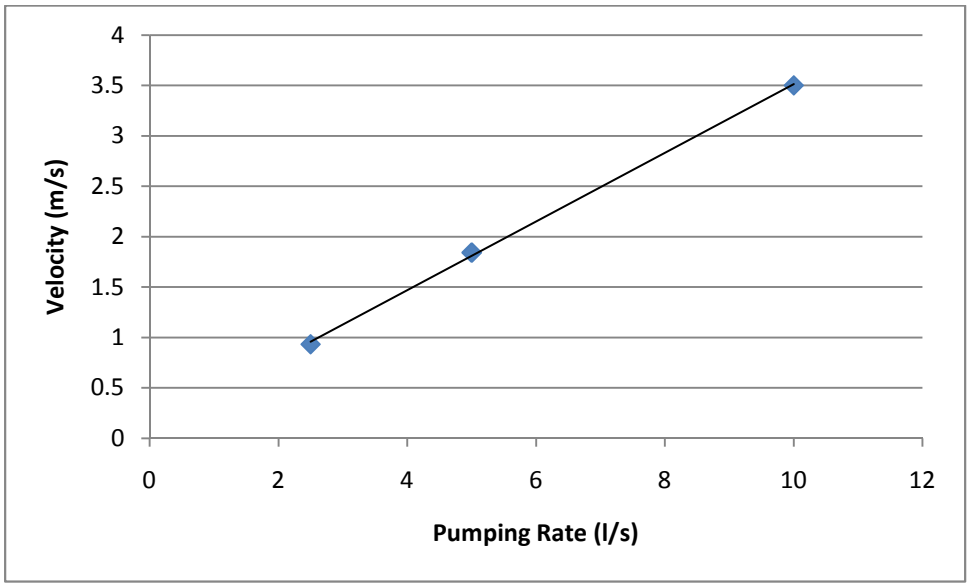

Figure 75: Velocity vs pumping rate

Table 14: Data from BOM stating average temperatures of all years from 2010 to 2011

Statistic	Jan	Feb	Mar	Apr	May	Jun
Lowest	31.8	29.9	29.5	24	21.9	15.3
Highest	36.3	34.9	32.4	30	23.7	19.8
Statistic	**Jul**	**Aug**	**Sep**	**Oct**	**Nov**	**Dec**
Lowest	16.4	17.2	22	25.1	27.4	30.4
Highest	19.4	23.1	25.5	30.9	35.4	34.8